Artificial Intelligence in Agriculture 2 (2019) 38–84

Contents lists available at ScienceDirect

Artificial Intelligence in Agriculture

journal homepage: http://www.keaipublishing.com/en/journals/artificial-intelligence-in-agriculture/

Reliable execution of a robust soft computing workplace found on multiple neuro-fuzzy inference systems coupled with multiple nonlinear equations for exhaustive perception of tractor-implement performance in plowing process

S.M. Shafaei, M. Loghavi, S. Kamgar *

Department of Biosystems Engineering, School of Agriculture, Shiraz University, Shiraz 71441-65186, Iran

ARTICLE INFO

Article history:
Received 7 May 2019
Received in revised form 21 June 2019
Accepted 21 June 2019
Available online 16 July 2019

Keywords:
Draft force
Wheel slip
Fuel consumption
Neuro-fuzzy strategies
Intelligent simulation

ABSTRACT

Tendency towards computer simulations linked to agricultural machinery has enormously increased in recent years. In this regard, the principal contribution of current research was to develop soft computing simulation workplaces for performance prognostication of tractor-implement system in plowing process. Two neuro-fuzzy strategies based on multiple adaptive neuro-fuzzy inference systems (MANFIS) scenario and the MANFIS coupled with multiple nonlinear equations (MNE) scenario were executed in the workplace. Additionally, neural strategy based on artificial neural network (ANN) scenario was also fulfilled in the workplace. Operational variables of plowing depth (10–30 cm), forward speed (2–6 km/h), and tillage implement type (moldboard, disk, and chisel plow) were considered as the workplace inputs and ten performance parameters were taken as the workplace outputs. According to the obtained prognostication accuracy, simulation time, and user-friendly configuration of three scenarios (ANN, MANFIS, and MANFIS+MNE), the MANFIS+MNE was recognized as the prominent simulation scenario. According to the MANFIS+MNE workplace results, for each tillage implement, the compound effect of plowing depth and forward speed on some performance parameters (required draft force of implement, tractor rear wheel slip, fuel consumption per working hour, specific volumetric fuel consumption, tractor drawbar power, energy requirement for tillage implement, overall energy efficiency, and tractor tractive efficiency) was nonlinearly synergetic. However, it was nonlinearly antagonism in case of specific draft force and fuel consumption per tilled area. The MANFIS+MNE workplace simulation results provide opportunity for technical farmer associations involved in the decision-making of agricultural machinery management in order to gain exhaustive fundamental insights into the compound effect of plowing depth and forward speed on performance of tractor-implement systems in plowing process.

1. Introduction

Studying performance of tractor-implement system in plowing process could be advantageous to gain accurate view about how the system performs in the process. The performance realization provides the possibility of upgrading the system mechanisms without performing refabrication process. Moreover, the obtained view would be assistive to devise proper management strategies for inventory of tillage systems and thereby, it could remarkably reduce total cost of crop production systems, repair, maintenance, fuel, ownership, and other involved operational issues. On the other hand, performance results of tractor-implement system in plowing process could be applied to develop exhaustive information bank for multivariate analysis through partitioned graphical descriptions.

In this realm, modeling strategies help to comprehend performance of tractor-implement system in plowing process on the basis of extension of discrete operational results towards integral interpretable results. The discrete operational data are gained by performing limited experiments. The integral interpretable results provide an opportunity to ascertain general trend of variations of dependent performance parameters when independent operational variables change. These determinations lead to presentation of physical meaning of phenomena occurring in the process and showing what happens along different working states of the process. Therefore, it can be indicated that a

Abbreviations: ANFIS, adaptive neuro-fuzzy inference system; ANN, artificial neural network; ASABE, American Society of Agricultural and Biological Engineers; FIS, fuzzy inference system; MANFIS, multiple adaptive neuro-fuzzy inference systems; MRDM, mean relative deviation modulus; MAVSRE, mean of absolute values of simulation residual errors; MANOVA, multivariate analysis of variance; MFWD, mechanical front wheel drive; MLR, multiple linear regression; MNE, multiple nonlinear equation; MNR, multiple nonlinear regression; RMSE, root mean square error; RNAM, Regional Network for Agricultural Machinery; SD, standard deviation; CV, coefficient of variation; CNU, coefficient of non-uniformity; SLR, simple linear regression; 2WD, two-wheel drive; 4WD, four-wheel drive; R^2, coefficient of determination.

* Corresponding author at: Department of Biosystems Engineering, School of Agriculture, Shiraz University, Shiraz, Iran.

E-mail address: kamgar@shirazu.ac.ir (S. Kamgar).

https://doi.org/10.1016/j.aiia.2019.06.003

Nomenclature

CNU	coefficient of non-uniformity (%)
CV	coefficient of variation (%)
E_f	implement field efficiency (%)
ERTI	energy requirement for tillage implement (MJ/ha)
FCTA	fuel consumption per tilled area (L/ha)
FS	forward speed (km/h)
GTF	gross traction force (kN)
h	working hour (h)
IFC	implement field capacity (ha/h)
M	mean of used data
MAVSRE	mean of absolute values of simulation residual errors
MRDM	mean relative deviation modulus (%)
N	number of used data
NTF	net traction force (kN)
OEE	overall energy efficiency (%)
PD	plowing depth (m)
PP_i	ith performance parameter
PP_{max}	maximum value of performance parameter
PP_{min}	minimum value of performance parameter
PP_{obtave}	average of obtained performance parameter
$PP_{obt,i}$	ith obtained performance parameter
$PP_{sim,i}$	ith simulated performance parameter
R^2	coefficient of determination
RMSE	root mean square error
S	driving wheel slip (%)
SD	standard deviation
SDF	specific draft force (kN/m^2)
SVFC	specific volumetric fuel consumption (L/kW h)
TDP	tractor drawbar power (kW)
TFC	tractor fuel consumption (L)
TTE	tractor tractive efficiency (%)
V_f	forward speed of outer radius of the fifth wheel (km/h)
V_d	forward speed of outer radius of rear driving wheel of the tractor (km/h)
w	implement working width (m)
X	dry weight of stubble per unit surface area (Lb/acre)
Y	percentage of stubble cover (%)

well-developed model is able to guarantee presentation of exhaustive perception of the phenomena in a wide ranges of conditions. Hence, a well-developed model is a supportive tool for researchers, engineers, and managements in solving problems associated with performance of tractor-implement system and thereby, optimization of the mechanized plowing process can be performed without conducting expensive and time-consuming field tests.

The modeling strategies frequently employed by the researchers can be classified into two main branches of mathematical and soft computing models. In general term, mathematical models (SLR, MLR, one variable nonlinear regression, MNR, dimensional analysis, etc.) are linear or nonlinear equations with specific constants and coefficients. However, soft computing models (ANN, FIS, ANFIS, support vector machines, etc.) are computer simulation workplaces which are originally worked through predetermined consecutive calculations.

Among soft computing models, the ANN performs regarding intelligent computational scenario with self-learning algorithm. The FIS works on the basis of predetermined linguistic transparency in form of IF and THEN rules. The ANFIS includes advantages of both the ANN and the FIS. Therefore, the ANN and ANFIS soft computing scenarios are generally known as intelligent powerful modeling tools for dynamic, uncertain, and multidimensional and highly nonlinear interrelations, especially when physical relationships between input and output data are not fully understood.

The main body of this paper is organized in four parts. The first part is review and analysis of literature for relevant published attempts previously completed in domain of model development for prognostication of performance parameters of tractor-implement system in plowing process. In this part, existing deficits of several sequential attempts documented by earlier researchers are discussed and ultimately, aims and questions of the research are described. The second part is dedicated to execute simulation workplaces based on intelligent soft computing scenarios. The third part is devoted to extensively validate outstanding simulation workplace. The forth part presents exhaustive perception of performance parameters of tractor-implement system in plowing process on the basis of remarkable results obtained from prominent simulation workplace.

1.1. Review and analysis of literature

Modeling performance parameters of tractor-implement system in plowing process have been of great interest to researchers over the past five decades in stationery tests and field operations. The stationery tests have been commonly performed in indoor soil bin facility or asphalt test track with load car. Meanwhile, field operations have been generally accomplished utilizing tillage implements in farm conditions. Table 1 presents tendency of the researchers to apply mathematical models for prognostication of the performance parameters. As it can be seen in the Table 1, the SLR, MLR, ASABE equations, MNR, one variable nonlinear regression, and dimensional analysis methodologies have been frequently employed by the researchers to model variations in some performance parameters based on some input variables of plowing depth, forward speed, static load, tractor engine speed, and implement type in conditions of field operations or stationery tests. For each case, results of these attempts have led to fit several equations to desired performance parameters which are applicable for a specific condition. Although some equations have been satisfactorily fitted to actual data, constants and coefficients of the equations varied as tested conditions changed. Moreover, inherent drawback of these parametric models confines them to prognosticate one output variable. Therefore, to prognosticate whole tractor performance parameters, there is a need to develop several equations with different constants, coefficients, and assumptions. This fact prevents the widest applicability of acceptable prognostications for set of input and output variables within tested ranges. Hence, the researchers focused their efforts to apply another methodology with taking multiple input and output variables into account. This scheme motivated the researchers to release user-friendly software and programs with multiple objects. The software and programs are great outreach potential tools for prognostication of some performance parameters on the basis of several input variables. Table 2 summarizes details of the software and programs. According to the information manifested in the Table 2, it can be pointed out that the software and programs suffer from wide range applications owing to dependency to equations defined based on the mathematical relationships documented in the ASABE standards or classical soil mechanics theory. Therefore, these software and programs, similar to mathematical models, could be only applied for certain conditions of stationery tests or field operations.

Recent progressive advancements in applications of soft computing models in engineering based simulation practices extend range of possibilities in prognostication of some performance parameters of tractor-implement system in plowing process based on multiple operational input variables. In this context, much interest has been focused on the ANN, FIS, and ANFIS soft computing scenarios by some researchers, in case of field operations and stationery tests. The overall descriptions concerning these employments are briefed in Table 3. Reviewing the results of cited papers in the Table 3 demonstrated that these soft computing scenarios are adaptable computer simulation environments. It means that model structure established based on these soft computing scenarios is trained with inventory data sets and it can be possible to be

Table 1
Mathematical models applied for prognostication of performance parameters of tractor-implement systems in plowing process.

Experimental conditions	Performance parameter	Modeling strategy	Authors
Field operations	Draft force, drawbar power	SLR	Harrison and Reed (1962)
	Draft force	Dimensional analysis	Gee-Clough et al. (1978)
	Draft force	MNR	Upadhyaya et al. (1984)
	Draft force	One variable nonlinear regression	Summers et al. (1986)
	Specific draft force, fuel consumption per tilled area	ASABE equation, SLR	Cullum et al. (1989)
	Specific draft force	MLR	Bashford et al. (1991)
	Draft force, fuel consumption per working hour	ASABE equation, SLR	Ismail and Burkhardt (1993)
	Draft force, specific draft force	One variable nonlinear regression	Smith (1993)
	Draft force	MNR	Glancey and Upadhyaya (1995)
	Draft force	ASABE equation	Harrigan and Rotz (1995)
	Draft force	Dimensional analysis	Glancey et al. (1996)
	Draft force	MNR	Grisso et al. (1996)
	Specific draft force	MNR	Al-Janobi and Al-Suhaibani (1998)
	Draft force, tractor rear wheel slip, fuel consumption per working hour	SLR	Manian and Kathirvel (2001)
	Draft force, tractor rear wheel slip, specific volumetric fuel consumption	MNR	Thomas and Singh (2002)
	Specific draft force, fuel consumption per working hour, specific volumetric fuel consumption	ASABE equation, MNR	Kheiralla et al. (2004)
	Draft force, fuel consumption per working hour, specific volumetric fuel consumption	SLR, MNR	Serrano et al. (2007)
	Fuel consumption per working hour, specific volumetric fuel consumption	ASABE equation, SLR, MNR	Tafesse et al. (2007)
	Fuel consumption per working hour, fuel consumption per tilled area, draft force, drawbar power	ASABE equation	Grisso et al. (2007)
	Draft force	One variable nonlinear regression	Godwin et al. (2007)
	Tractor tractive efficiency	Dimensional analysis	Fakhraei and Karparvarfard (2008)
	Draft force, fuel consumption per working hour, tractor rear wheel slip	One variable nonlinear regression	Juostas and Janulevicius (2008)
	Energy requirement for tillage implement	SLR, one variable nonlinear regression	Khadr (2008)
	Specific draft force	SLR	Serrano and Peca (2008)
	Draft force	One variable nonlinear regression	Sahay et al. (2009)
	Fuel consumption per working hour	SLR	Fathollahzadeh et al. (2009)
	Fuel consumption per tilled area	SLR	Fathollahzadeh et al. (2010)
	Specific draft force	MNR	Al-Suhaibani et al. (2010)
	Fuel consumption per working hour	MNR	Udompetaikul et al. (2011)
	Fuel consumption per tilled area	SLR, MNR	Ajav and Adewoyin (2012)
	Draft force	Dimensional analysis	Nkakini and Akor (2012)
	Fuel consumption per tilled area	SLR, MNR	Adewoyin (2013)
	Fuel consumption per tilled area	SLR, MNR	Adewoyin and Ajav (2013)
	Draft force	ASABE equation	Askari and Khalifahamzehghasem (2013)
	Draft force	MNR	Ranjbar et al. (2013)
	Fuel consumption per working hour, fuel consumption per tilled area	SLR, one variable nonlinear regression	Moitzi et al. (2014)
	Specific volumetric fuel consumption, draft force	ASABE equations	Pitla et al. (2014)
	Draft force	Dimensional analysis	Moeenifar et al. (2014)
	Specific volumetric fuel consumption	Dimensional analysis, ASABE equation	Karparvarfard and Rahmanian-Koushkaki (2015)
	Draft force	Dimensional analysis	Nkakini (2015a)
	Draft force	SLR	Nkakini (2015b)
	Draft force	MLR	Al-Suhaibani et al. (2015)
	Draft force	ASABE equation	Askari et al. (2016)
	Fuel consumption per working hour, fuel consumption per tilled area, specific volumetric fuel consumption	MNR	Almaliki et al. (2016a)
	Specific draft force	SLR	Ndisya et al. (2016)
	Draft force, specific draft force, drawbar power	ASABE equation, classical soil mechanics based equations	Ahmadi (2016a)
	Draft force, specific draft force, drawbar power	Classical soil mechanics based equations	Ahmadi (2016b)
	Draft force, drawbar power	ASABE equation, classical soil mechanics based equations	Ahmadi (2016c)
	Draft force, fuel consumption per working hour, fuel consumption per tilled area, tractor rear wheel slip, drawbar power, overall energy efficiency, tractor tractive efficiency	ASABE equation, SLR	Ranjbarian et al. (2017)
	Draft force	SLR	Askari et al. (2017)
	Drawbar power	Classical soil mechanics based	Ahmadi (2017a)

Table 1 (*continued*)

Experimental conditions	Performance parameter	Modeling strategy	Authors
		equations	
	Draft force, drawbar power	Classical soil mechanics based equations	Ahmadi (2017b)
	Draft force	Classical soil mechanics based equations	Ahmadi (2018)
	Draft force, drawbar power	One variable nonlinear regression, MNR	Okoko et al. (2018)
	Tractor tractive efficiency	Dimensional analysis	Moinfar and Shahgholi (2018)
	Drawbar power	SLR, one variable nonlinear regression	Alele et al. (2018)
Stationary tests	Fuel consumption per working hour	MNR	Hansson et al. (2003)
	Fuel consumption per working hour, specific volumetric fuel consumption	ASABE equation, SLR	Grisso et al. (2004)
	Draft force	MNR	Mamman and Oni (2005)
	Draft force	MNR	Sahu and Raheman (2006)
	Fuel consumption per working hour, specific volumetric fuel consumption	MNR	Grisso et al. (2008)
	Fuel consumption per working hour, specific volumetric fuel consumption	MNR	Coffman et al. (2010)
	Fuel consumption per working hour	SLR, MNR	Kim et al. (2011)
	Draft force	Dimensional analysis	Moeenifar et al. (2013)
	Draft force	MNR	Machindra and Raheman (2017)
	Fuel consumption per working hour	MLR	Kocher et al. (2017)
	Specific draft force	MNR, ASABE equation	Upadhyay and Raheman (2019b)

extended with the same structure for other future conditions. This eminent ability encourages the investigators to follow the previous researches in order to complement the knowledge in this realm.

Careful inspection of available literature which are chronologically reported in the Table 3 indicated that, although some partial attempts have been accomplished by the investigators to apply soft computing scenarios for individual or component prognostication of some performance parameters of tractor-implement system in field operations, deficiency of an exhaustive attempt to simulate whole performance parameters is tedious.

Table 2
Software and program developed for prognostication of performance parameters of tractor-implement systems in plowing process.

Experimental conditions	Performance parameter	Modeling strategy	Authors
Field operations	Fuel consumption per tilled area	ASABE equations based program	Colvin et al. (1989)
	Fuel consumption per working hour, tractor rear wheel slip	ASABE equations based program	Alimardani et al. (1989)
	Tractor rear wheel slip, draft force, tractor tractive efficiency	ASABE equations based program	Al-Hamed et al. (1994)
	Tractor tractive efficiency, tractor rear wheel slip, draft force, drawbar power	ASABE equations based software	Al-Hamed and Al-Janobi (2001)
	Draft force, tractor rear wheel slip	ASABE equations based software	Sahu and Raheman (2008)
	Draft force, fuel consumption per working hour	ASABE equations based software	Pranav and Pandey (2008)
	Draft force, tractor rear wheel slip, fuel consumption per working hour, drawbar power	ASABE equations based software	Kumar and Pandey (2009)
	Drawbar power, draft force	ASABE equations based software	Ishola et al. (2010)
	Drawbar power, tractor tractive efficiency	ASABE equations based software	Al-Hamed et al. (2010)
	Draft force, tractor tractive efficiency, tractor rear wheel slip, specific volumetric fuel consumption, fuel consumption per tilled area	Classical tractor mechanics based program	Kolator and Bialobrzewski (2011)
	Drawbar power	ASABE equations based software	Mehta et al. (2011)
	Draft force, tractor tractive efficiency, tractor rear wheel slip, fuel consumption per working hour	ASABE equations based software	Pranav et al. (2012)
	Fuel consumption per working hour, specific volumetric fuel consumption, draft force, tractor rear wheel slip	ASABE equations and nonlinear regression based software	Kumar and Pandey (2015)
	Fuel consumption per working hour, drawbar power	ASABE equations based program	Dahab et al. (2016)
	Fuel consumption per working hour, fuel consumption per tilled area, specific volumetric fuel consumption	MLR, ASABE equations based program	Lee et al. (2016)
	Draft force, tractor rear wheel slip, tractor tractive efficiency, fuel consumption per working hour	ASABE equations based software	Kumar et al. (2017a)
	Draft force	ASABE equations based program	Battiato and Diserens (2017)
Stationary tests	Tractor rear wheel slip	ASABE equations based software	Catalan et al. (2008)
	Tractor tractive efficiency	ASABE equations based software	Santos and Queiroz (2016)

Table 3
Soft computing scenarios employed for prognostication of performance parameters of tractor-implement systems in plowing process.

Experimental conditions	Performance parameter	Soft computing scenario and modeling strategy	Authors
Field operations	Specific draft force	ANN	Al-Janobi et al. (2001)
	Draft force	ANN	Aboukarima and Saad (2006)
	Draft force	ANN, one variable nonlinear regression	Aboukarima (2007)
	Draft force	ANN	Alimardani et al. (2009)
	Fuel consumption per tilled area	ANN	Al-Janobi et al. (2010)
	Draft force, specific draft force	ANN	Al-Hamed et al. (2013)
	Draft force	ANN	Saleh and Aly (2013)
	Fuel consumption per working hour, fuel consumption per tilled area, specific volumetric fuel consumption, drawbar power, tractor tractive efficiency	ANN	Almaliki et al. (2016b)
	Draft force	ANFIS, ASABE equation	Shafaei et al. (2017a)
	Fuel consumption per working hour, fuel consumption per tilled area, specific volumetric fuel consumption	ANN, ANFIS	Shafaei et al. (2018a)
	Draft force	ANN, MLR, ASABE equation	Shafaei et al. (2018b)
	Draft force, specific draft force	ANFIS, ASABE equation	Shafaei et al. (2018c)
	Energy requirement for tillage implement, overall energy efficiency	ANN, ANFIS	Shafaei et al. (2019c)
	Tractor tractive efficiency	ANN, ANFIS	Shafaei et al. (2018d)
	Tractor rear wheel slip	ANN, ANFIS	Shafaei et al. (2019e)
Stationary tests	Draft force	ANN	Choi et al. (2000)
	Draft force	ANN	Roul et al. (2009)
	Specific draft force	FIS	Marakoglu and Carman (2010)
	Fuel consumption per working hour	ANN, MLR	Rahimi-Ajdadi and Abbaspour-Gilandeh (2011)
	Draft force	FIS	Mohammadi et al. (2012)
	Draft force	ANN	Akbarnia et al. (2014)

In a remarkable attempt, some performance parameters (fuel consumption per working hour, fuel consumption per tilled area, specific volumetric fuel consumption, tractor drawbar power, tractor tractive efficiency) in plowing process with moldboard implement were intelligently simulated by means of the ANN scenario (Almaliki et al., 2016b). The ANN simulation workplace was trained well in accordance with input operational data sets of plowing depth and forward speed. However, the effects of plowing depth and forward speed on required draft force of the implement, tractor rear wheel slip, specific draft force, energy requirement for tillage implement, and overall energy efficiency were not simulated in the research. Additionally, further interpretations for presentation of clear physical perceptions of the effect of the operational variables on the desired performance parameters have not been expressed by the researchers. Hence, it is still indispensable to take drastic efforts for extension of the ANN simulation workplace and employment of another intelligent simulation workplace (ANFIS) of soft computing scenario for exhaustive prognostication of whole performance parameters of tractor-implement system in plowing process.

1.2. Hypotheses and problematic challenge of research

The ANFIS soft computing scenario includes unique properties integrating advantages of the ANN and FIS soft computing scenarios. The FIS provide a strong mechanism for knowledge representation when expert knowledge is available. However, it does not possess the capabilities for automated learning. The ANN do not possess knowledge representation capability, but it has powerful mechanism of learning from sample data when expert knowledge is limited. The ANFIS overcomes the limitations of both soft computing scenarios of the ANN and FIS. It means that the ANFIS offers particularly strong simulation workplace with identification techniques when relationship between input and output data is not trivial. Therefore, it is understandable that the ANFIS is able to build a fuzzy rule based on the structure of the FIS (IF and THEN) and tune the parameters of the FIS membership functions from a given set of input/output data by training itself, like the ANN. Hence, between two intelligent soft computing scenarios of the ANN and ANFIS, it is anticipated that the ANFIS better performs than the ANN in simulation

Table 4
Key technical specifications of 4WD tractor used in the research.

Specification	Value	Unit
Manufacture	ITM-Iran	–
Model	MF-399	–
Front tires	37.85–60.96	cm
Rear tires	46.74/38.10–86.36	cm
Wheel base	264	cm
Total weight	39.34	kN
Drawbar height	43.3	cm
Rear axle width	151.8–242.8	cm
Front axle width	172.6–209.4	cm
Weight of rear axle	24.52	kN
Weight of front axle	14.82	kN
Maximum power at 2200 rpm	81	kW
Inflation pressure of front tire	204	kPa
Inflation pressure of rear tire	136	kPa

Table 5
Major technical characteristics of the transducers used in the digital instrumentation system.

Transducer	Model	Manufacture	Country	Specification	Accuracy
Rotary shaft encoders	E50S8-500-3-T-24	Autonics	Korea	500 (pulse/revolution)	1 (pulse)
Flow meters	FS300A G3/4	Meinte	China	0–60 (L/min)	0.2 (L)
Load cell	NS4-5t	Mavin	China	0–50 (kN)	2.5 (N)

practices. This hypotheses was approved by the authors in their previous researches, especially in case of the component effect of nominal and numeral variables on desired target (Shafaei et al., 2015; Shafaei et al., 2018d; Shafaei et al., 2019b; Shafaei et al., 2019e). Accordingly, it is desired to validate the hypotheses in case of simulation of the component effect of plowing depth, forward speed, and tillage implement type on whole performance parameters (required draft force of implement, tractor rear wheel slip, fuel consumption per working hour, specific volumetric fuel consumption, tractor drawbar power, energy requirement for tillage implement, overall energy efficiency, tractor tractive efficiency, specific draft force, and fuel consumption per tilled area). To accomplish this, there is need to develop the ANFIS computer simulation workplace with three input variables and ten output parameters. In this regard, a challenging problem exists in the ANFIS computer simulation workplace, when the number of output parameters is more than one. Practically, in the ANFIS computer simulation workplace, to link several input and output data, definition of fuzzy rules based on the structure of IF and THEN is very complex and impossible. Thus, to avoid this problem, the overall ANFIS structure has been established based on consideration of one output parameter in accordance with several input variables.

Literature review concerning application of the ANFIS computer simulation workplace for prognostication of several output parameters indicated that the investigators completed desired simulations by means of development of a simulation workplace including several ANFIS sub-environments, each for one output parameter, based on the same multiple input variables (Shafaei et al., 2016a; Shafaei et al., 2018a; Shafaei et al., 2018c; Shafaei et al., 2019c). Although, this simulation scenario obviated inherent drawback of structure of the ANFIS computer simulation workplace for prognostication of several output parameters, more simulation time required to develop several sub-environments were reported by the investigators. Besides, user-friendly configuration of the simulation workplace was diminished with development of several sub-environments.

1.3. New simulation scenario

According to aggregation of outcome results of some previous published papers of the same authors (Shafaei et al., 2018a; Shafaei et al., 2018c; Shafaei et al., 2018d; Shafaei et al., 2019c), it was found that master performance parameters of tractor-implement system in plowing process are required draft force of implement, tractor rear wheel slip, and fuel consumption per working hour. Other seven slave performance parameters (specific draft force, fuel consumption per tilled area, specific volumetric fuel consumption, tractor drawbar power, tractor tractive efficiency, energy requirement for tillage implement, and overall energy efficiency) can be mathematically obtained utilizing the three master performance parameters. Hence, to achieve higher prognostication accuracy and user-friendly configuration of the workplace as well as lower simulation time, a new simulation scenario is presented in this research for the first time. The scenario is based on developing simulation workplace for stepwise prognostication of ten performance parameters with respect to three input variables of plowing depth, forward speed, and tillage implement type. The simulation procedure is performed in two main stages. In the first stage, the MANFIS configuration consisting of the ANFIS environments is developed to prognosticate three master performance parameters. In the second stage, the obtained simulation values of three master performance parameters

Fig. 1. An instrumented tractor at base station, a) flow meters, b) rotary shaft encoder mounted on non-driving fifth wheel, c) data acquisition unit, and d) rotary shaft encoder mounted on driving rear wheel.

Table 6
Principal technical specifications of the mounted implements used in the research.

Implement	Model	Manufacture	Country	Main components	Working width (cm)
Chisel plow	CPP	Rau	Germany	Nine spring curved shanks	225
Disk plow	TAKA 165	TAKA	Iran	Three disk bottoms	120
Moldboard plow	3000IP65	Moradi	Iran	Three bottoms	90

are employed for stepwise prognostication of the other seven slave performance parameters. This task is performed by utilization of two MNE configurations. Therefore, it can be deduced that new simulation scenario is established based on development of the MANFIS coupled with the MNE. However, efficiency of new simulation scenario (MANFIS+MNE) is ascertainable in comparison with the two known simulation scenarios (ANN and MANFIS).

1.4. Aims and questions of research

The systematic literature survey concludes that there is an inevitable demand to obviate the aforementioned problematic challenge and investigate the hypothesis through development of robust soft computing workplace operated based on the new introduced simulation scenario (MANFIS+MNE) for exhaustive prognostication of whole performance parameters (required draft force of implement, tractor rear wheel slip, fuel consumption per working hour, specific draft force, fuel consumption per tilled area, specific volumetric fuel consumption, tractor drawbar power, tractor tractive efficiency, energy requirement for tillage implement, and overall energy efficiency) of tractor-implement system regarding three independent input variables of plowing depth, forward speed, and tillage implement type. The novelty of this research can be addressed not only to validate the new simulation scenario, but also to follow to respond the main questions outlined below:

- Is efficiency of neuro-fuzzy strategy higher than neural strategy in prognostication of desired output targets based on the compound effect of nominal and numeral input variables?
- Are prognostication accuracy and simulation time of the MANFIS +MNE simulation workplace better rated than that of the ANN and MANFIS simulation workplaces?
- Is user-friendly configuration of MANFIS+MNE simulation workplace simple enough to be considered as applicable neuro-fuzzy calculator?
- Do physical perceptions obtained from results of prominent simulation workplace enrich state of the art in the domain of comprehending behavior of the performance parameters?

2. Research methodology

2.1. Tillage site layout

Three experimental zones in an arable land of Bajgah Agricultural Research Station of Shiraz University (29°32′ N 52°35′ E, North West of Shiraz city, Iran) were considered as tillage site. The site had clay loam soil texture (35% sand, 30% silt, and 35% clay) and flat topography. Each site was partitioned into 27 separated plots (30 m long by 5 m wide) resulting in a total of 81 plots. To measure moisture content of plot soils, in five random locations of the plots, a sampling procedure in 30 cm topsoil layer was carried out utilizing a cylindrical core sampler. The collected soil samples were immediately packed in separate polyethylene bags and transferred to research laboratory. The samples were dried in a convection oven at 105 ± 1 °C until constant weight was obtained (SAA, 1977). To avoid experimental error, the drying process was triplicated for each soil sample and mean value was used. The moisture content of the site soil was found to be 8.84% (g water/g dry sample).

One of the tillage sites employed for chiseling process was covered with uniform wheat stubble. The percentage of wheat stubble coverage was calculated 22% based on Eq.(1) (Papendick, 2002).

$$Y = \left(1 - e^{-0.000644X}\right) \times 100 \tag{1}$$

2.2. Specifications of tractor-implement systems

A popular 4WD tractor with MFWD system, with its front wheels smaller than rear wheels, was used in this research. The key technical specifications of the tractor are provided in Table 4. To measure principal performance parameters in plowing process, the tractor was fully equipped with a digital instrumentation system. The system was developed and validated by the same authors in the previous work (Shafaei et al., 2019a). The instrumentation system composed of a data acquisition unit and three groups of transducer assembly (two flow meters, three rotary shaft encoders, and one load cell). The major engineering details of the transducers are completely reported in Table 5. The instrumented tractor at base station is shown in Fig. 1.

The two flow meters were utilized for measuring tractor fuel consumption. The first one was embedded between the injector pump and fuel filter of the tractor. The second one was also embedded in the line between injection pump and fuel tank and thereby, excess fuel returned to the tank was measured. The difference between two measured values obtained from the flow meters was considered as the tractor fuel consumption value.

The load cell was used to measure required draft force of implement in accordance with the method standardized by the RNAM institute (RNAM, 1995). This method has been frequently used in previous works by the researchers (Zhang et al., 2001; Shah et al., 2015; Rahmanian-Koushkaki et al., 2015; Shafaei et al., 2019d).

Driving wheel slip can be continuously measured using the method suggested by Pranav et al. (2010). In this method, to measure forward speed of outer radius of the wheels (ground speed), two encoders were

Table 7
Independent and dependent variables considered in the field operations.

Independent variables			Dependent variables	
Forward speed (km/h)	Plowing depth (cm)	Implement	Master	Slave
2	10	Chisel plow	Required draft force of implement	Specific draft force
4	20	Disk plow	Tractor rear wheel slip	Fuel consumption per tilled area
6	30	Moldboard plow	Fuel consumption per working hour	Specific volumetric fuel consumption
				Tractor drawbar power
				Tractor tractive efficiency
				Energy requirement for tillage implement
				Overall energy efficiency

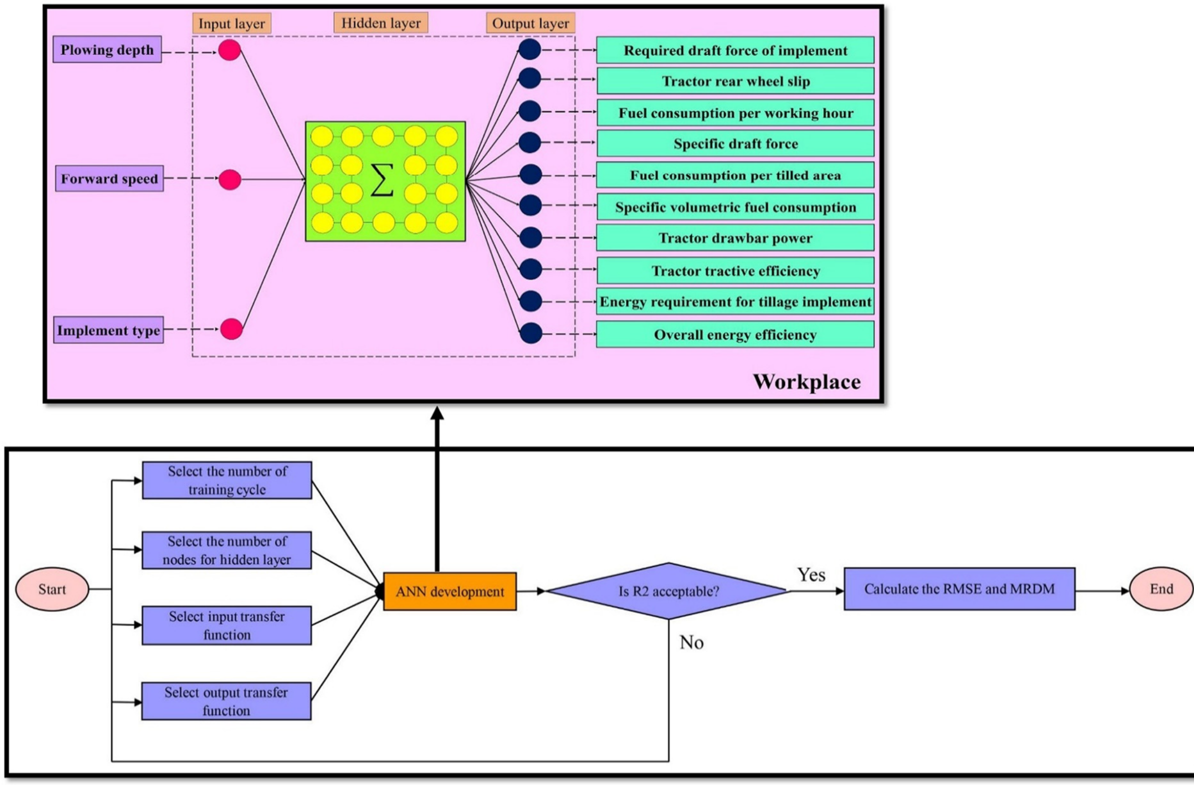

Fig. 2. Flowchart for selection of the best structure of the ANN simulation workplace in accordance with schematic of simulation scenario.

fitted into the wheel hubs of the rear wheels and one on a fifth wheel employing some mechanical joints. The fifth wheel was hinged to the tractor chassis between rear and front wheels as a non-driving wheel. It was reasonable to assume that slip of left and right driving wheels of the rear axle might not be equal at the same time, owing to existence of different soil conditions in the field. Hence, average values of obtained ground speed of left and right driving wheels were considered as theoretical forward speed. Meanwhile, measured ground speed of the fifth wheel was considered as actual forward speed. To calculate slip percentage of rear driving wheel of the tractor, Eq.(2) was applied in data acquisition unit of the digital instrumentation system (ASAE, 2003).

$$S = \left(1 - \frac{V_f}{V_d}\right) \times 100 \tag{2}$$

Three mounted implements of disk, chisel, and moldboard plow commonly used by farmers in southern area of the country were employed in this research. Principal technical specifications of the implements are tabulated in Table 6. To restrict redundant and lateral forces acting on the implement in plowing process, the implement attached to the tractor was leveled utilizing three-point hitch links of the tractor. Prior to field operations, initial inspection of the tractor-implement system was also performed at base station.

2.3. Field operations

The field operations were conducted in a half day (10 AM to 4 PM) on January 16, 2017 in predetermined plots. For each implement type, arrangement of the plots was randomized and blocked based on split plot design with three replications. In this design, plowing depth and forward speed were considered as major and minor treatments, respectively.

Before entering the plots, three-point linkage height lever was activated to lower the implement corresponding to the desired plowing depth. The tractor, in 2WD mode, was also operated at respective gear and throttle settings (rated speed of engine) to achieve desired forward speed at selected plowing depth in a practice area. These settings of the tractor were remained invariable along each test plot. Before each plot, a practice area was considered to adjust operational treatments (plowing depth and forward speed) until a steady state reached. For each combination of the treatments, three runs were performed to ensure repeatability and reliability of collected data. Arithmetic average of the collected data was then used for next step (data processing). The considered levels of the treatments (independent variables) applied in field operations and the master performance parameters of tractor-implement systems measured in field operations in accordance with the slave calculated performance parameters (dependent variables) are reported in Table 7.

In the plots, as the tractor-implement system reached the first installed flag marking, data collection for the master performance parameters was started utilizing the digital instrumentation system. The data collection process continued until end of the plot, and it was stopped as the tractor-implement system passed the second installed flag marking. At end of each plot, a headland area was allocated for turning the tractor-implement system in order to enter into the next plot.

In each plot, required draft force of the implement was measured based on the RNAM method. According to the method, the main tractor-implement system was pulled by an auxiliary tractor (model: 4450, Company: John Deere, Country: USA), while the load cell transducer of the digital instrumentation system was horizontally connected between the two tractors. During applying the RNAM method, it was ensured that the main tractor-implement system and the auxiliary tractor were placed on level ground in both lateral and longitudinal directions and the connection line of the transducer was parallel to ground surface. The operations were carried out with the mounted implement at desired plowing depth and forward speed. Obtained data from the transducer were considered as gross traction forces. The operations were also conducted at desired forward speed with the implement in transport position and the collected data from the transducer were considered as rolling resistance force of the tractor wheels. Finally, required

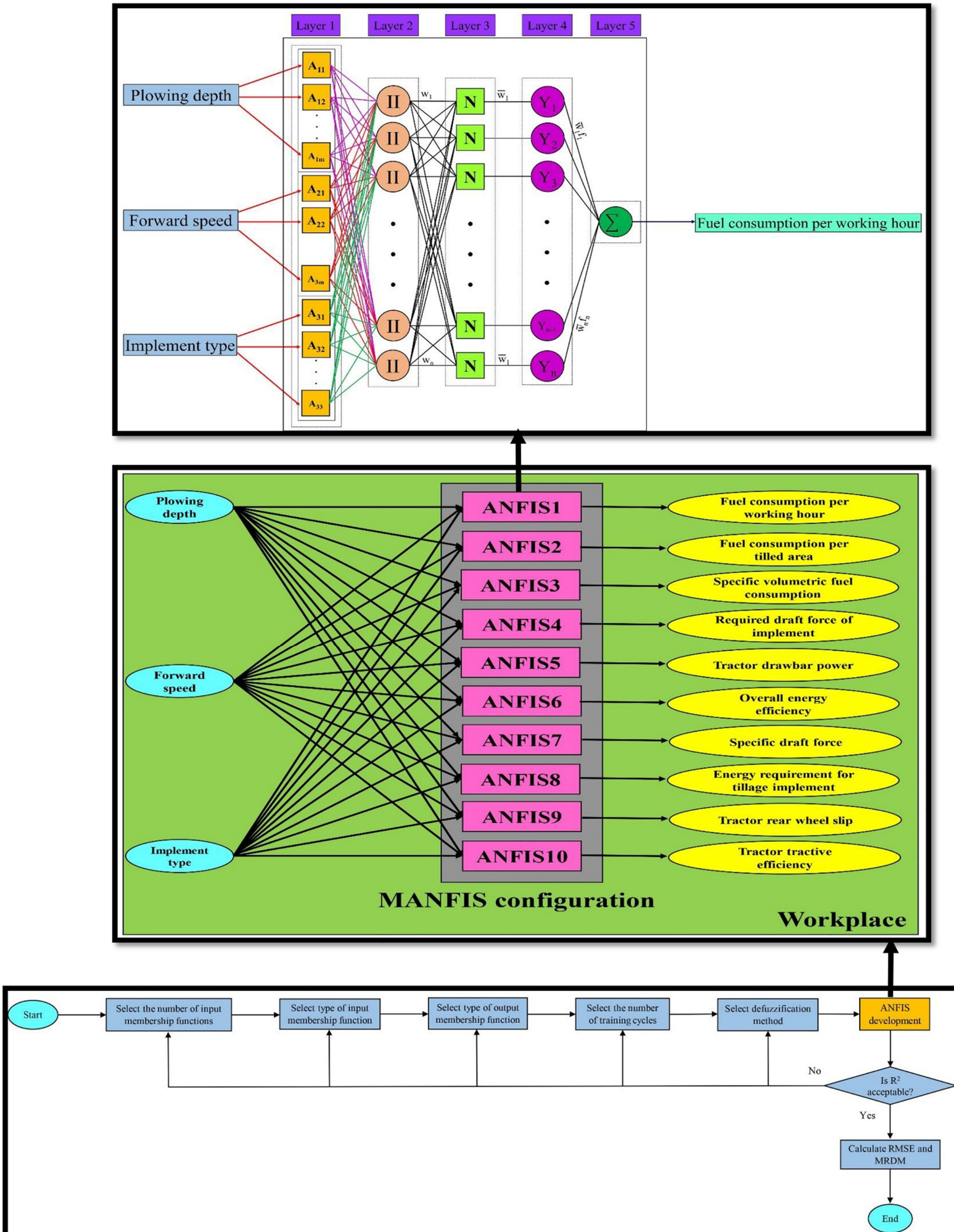

Fig. 3. Flowchart for selection of the best structure of the MANFIS simulation workplace in accordance with schematic of simulation scenario and five-layered structure of the ANFIS.

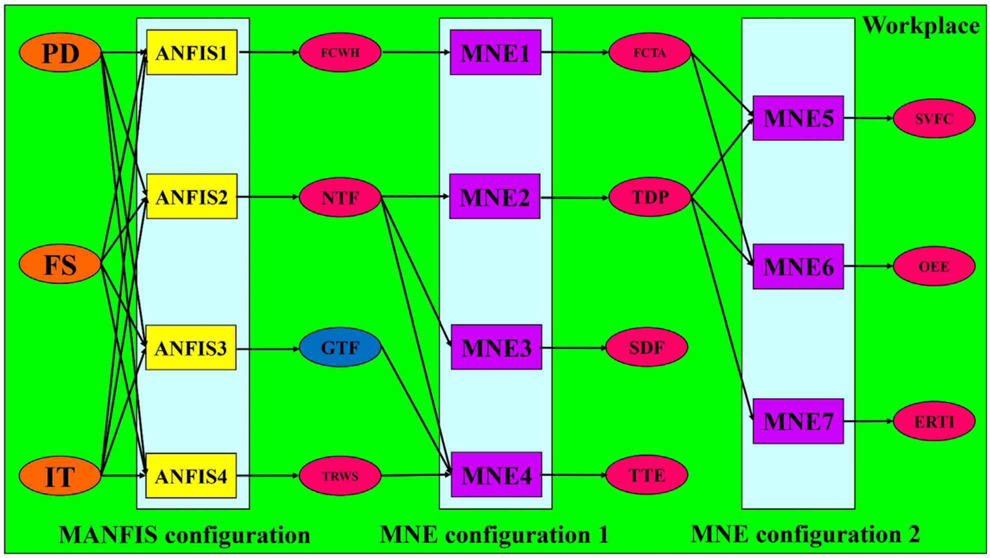

Fig. 4. Schematic of new simulation scenario of the MANFIS+MNE (FS: forward speed, PD: plowing depth, IT: implement type, FCWH: fuel consumption per working hour, NTF: net traction force (required draft force of implement), GTF: gross traction force, TRWS: tractor rear wheel slip, FCTA: fuel consumption per tilled area, TDP: tractor drawbar power, SDF: specific draft force, TTE: tractor tractive efficiency, SVFC: specific volumetric fuel consumption; OEE: overall energy efficiency, ERTI: energy requirement for tillage implement).

draft force of the implement (net traction force) was calculated once rolling resistance force of the main tractor was deducted from the gross traction force. It should be noted that the operations were conducted, while transmission system of the main tractor was set to neutral position.

2.4. Data processing

Collected data for the master performance parameters (required draft force of implement, tractor rear wheel slip, fuel consumption per working hour) make it possible to calculate the slave performance parameters (specific volumetric fuel consumption, tractor drawbar power, energy requirement for tillage implement, overall energy efficiency, tractor tractive efficiency, specific draft force, and fuel consumption per tilled area) by means of the following equations (Jr, 1989; ASAE, 2011; Ahmadi, 2016a).

$$\mathrm{SVFC} = \frac{3.6 \times \mathrm{TFC}}{\mathrm{NTF} \times \mathrm{FS} \times \mathrm{h}} \tag{3}$$

$$\mathrm{TDP} = \frac{\mathrm{NTF} \times \mathrm{FS}}{3.6} \tag{4}$$

$$\mathrm{ERTI} = \frac{\mathrm{TDP}}{\mathrm{IFC}} \tag{5}$$

$$\mathrm{OEE} = \frac{3.6 \times \mathrm{TDP}}{38.7 \times \mathrm{FCTA} \times \mathrm{IFC}} \times 100 \tag{6}$$

$$\mathrm{TTE} = (1-\mathrm{S})\frac{\mathrm{NTF}}{\mathrm{GTF}} \times 100 \tag{7}$$

$$\mathrm{SDF} = \frac{\mathrm{NTF}}{\mathrm{PD} \times \mathrm{w}} \tag{8}$$

$$\mathrm{FCTA} = \frac{\mathrm{TFC}}{\mathrm{IFC} \times \mathrm{h}} \tag{9}$$

To calculate implement field capacity in order to substitute in the Eqs.(5), (6) and (9), the following Eq.(10) was used (ASAE, 2011).

$$\mathrm{IFC} = \frac{\mathrm{w} \times \mathrm{FS} \times \mathrm{E_f}}{10} \tag{10}$$

2.4.1. Statistical descriptions

Statistical descriptions for obtained performance parameters of the tractor-implement system in plowing process were performed by utilization of some statistical descriptor parameters (mean, standard deviation, coefficient of variation, and coefficient of non-uniformity) based on the following equations (Shafaei and Kamgar, 2017).

$$\mathrm{M} = \frac{\sum_{i=1}^{i=N} \mathrm{PP_i}}{\mathrm{N}} \tag{11}$$

$$\mathrm{SD} = \frac{\sqrt{\sum_{i=1}^{i=N} (\mathrm{PP_i} - \mathrm{M})^2}}{\mathrm{N}} \tag{12}$$

$$\mathrm{CV} = \left(\frac{\mathrm{SD}}{\mathrm{M}}\right) \times 100 \tag{13}$$

$$\mathrm{CNU} = \left(\frac{\mathrm{PP_{max}} - \mathrm{PP_{min}}}{\mathrm{M}}\right) \times 100 \tag{14}$$

2.5. Execution of soft computing simulation workplace

2.5.1. ANN

The multi-layer perceptron architecture of the ANN scenario was employed in the simulation workplace. The architecture comprises three main layers: an input layer, hidden layer, and an output layer. Each layer includes several nodes. The number of nodes in the input and output layer is equal to the number of input and output variables in the simulation workplace. The connections among the nodes in the hidden layer significantly influence prognostication accuracy. The ANN

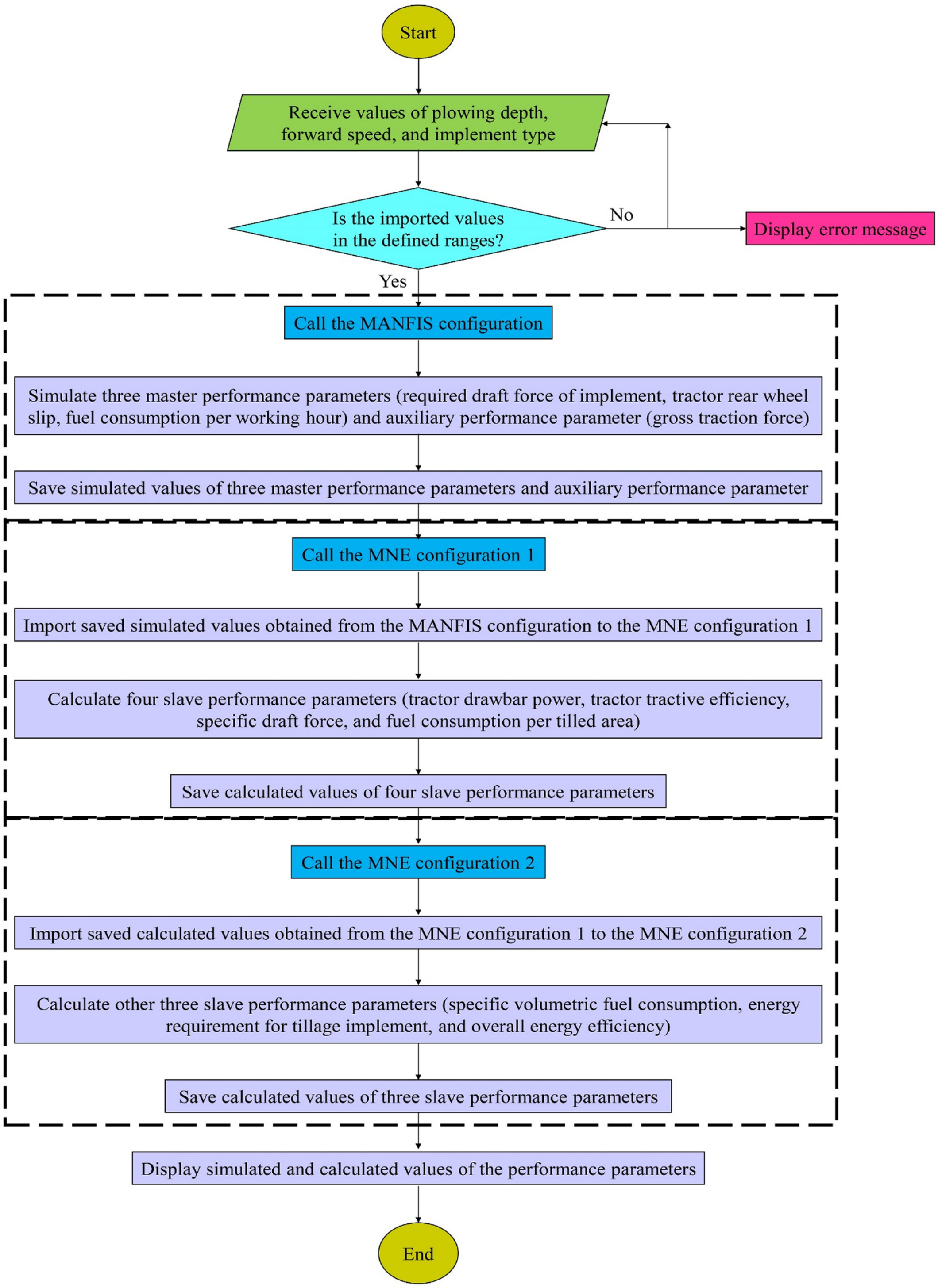

Fig. 5. Operational flowchart of the program algorithm written for running the new simulation scenario of the MANFIS+MNE.

scenario repeatedly decreases overall error of prognostication through modification of its connections among hidden nodes in predetermined training algorithm. In this scenario, prognostication process is automatically completed by means of neural computing through the layers. The data sets in input layer are intelligently mapped to hidden layer and consequently mapped to output layer by means of input and output transfer functions, respectively.

In the simulation workplace, the ANN scenario was developed based on three layers. The values of three input variables of plowing depth (10, 20 and 30 cm), forward speed (2, 4 and 6), and implement type (moldboard, disk, and chisel plow) were imported into the input layer and the values of ten performance parameters of tractor-implement systems in plowing process were imported into output layer, too. Therefore, the ANN scenario was established with three and ten nodes in input and output layers, respectively. In input layer of the simulation workplace, to have possibility of arbitrary selection of the implement, the integers 1, 2 and 3 were assigned for moldboard, disk, and chisel plow implement, respectively.

To import data sets into the ANN simulation workplace, data sets were randomly classified into three categories of training, testing and validation sets by 70:15:15 ratios. During training the ANN simulation workplace, the ANN scenario is tested in contradiction of the test data

Table 8
The values of statistical descriptor parameters determined for required draft force of the implements in plowing process.

Implement	Minimum (kN)	Maximum (kN)	Mean (kN)	SD (kN)	CV (%)	CNU (%)
Chisel plow	7.88	37.81	21.87	10.55	48.24	136.85
Disk plow	5.55	21.06	13.52	4.70	34.76	114.72
Moldboard plow	3.85	23.04	11.52	5.99	52.00	166.58

set to control correctness, and training process is stopped when the mean average error remained constant for a specific number of training cycles. This task is considered to avoid over fitting.

According to the ANN structure, several structural arrangements were tried to obtain the best structure with the highest prognostication accuracy. Various structural parameters of the scenario (the number of training cycles, input and output transfer functions, and the number of nodes in hidden layer) were run through frequent simulation tests in the ANN toolbox of STATISTICA 12 software (StatSoft Inc., Tulsa, OK, USA). During development process of the ANN scenario, the number of nodes in the hidden layer was set to a range from 2 to 10. The transfer functions of nodes were considered as follows: tangent, logistic, linear, Gaussian, sine, unit step, logarithm, and exponential. Fig. 2 illustrates the flowchart for selection of the best structure of the ANN simulation workplace in accordance with schematic of simulation scenario.

2.5.2. MANFIS

The first order Takagi-Sugeno-Kang type of the ANFIS scenario was used to prognosticate ten performance parameters of the tractor-implement systems in plowing process, on the basis of three independent input variables of plowing depth, forward speed, and implement type. The ANFIS is a five-layered structure including different nodes in each layer. The nodes in each layer connect with the nodes in the previous layer and receive input data coming from the previous nodes. These five layers are known as fuzzification, normalization, fuzzy rule, defuzzification, and output layer, respectively. The ANFIS simulation scenario is completed through passing data sets in these five layers. The scenario is described in the following paragraph.

When input data are assigned to the first layer nodes, they are graded between zero and one by input membership functions (constant, triangular, generalized bell (Gbell), gaussian, trapezium, and sigmoid). The graded data are shifted to the second layer nodes as input data. The numerical weights are allocated to the data in the second layer. Furthermore, the second layer normalizes the weighted input data. The weighted input data are transferred to the third layer nodes as input data of fuzzy rules. These rules are defined based on the IF and THEN structure. Output data obtained by the rules are gathered and aggregated to one output value in the fourth layer nodes. This value is converted to desired output variable by defuzzification method (weighted sum and weighted average) of the inference system. Output membership functions (constant and linear) are used for this job. The desired output variable is finally obtained in the fifth layer node.

The second layer of the ANFIS scenario normalizes the weighted input data by training itself. Training process is performed similar to that of the ANN scenario. The Hybrid algorithm is commonly used to train the simulation workplace. The algorithm is a combination of back-propagation and least square error algorithm. In the ANFIS scenario, the rules are also tuned automatically regarding relationships between input and output data. As it has been mentioned in Section 1.2, definition of fuzzy rules based on the structure of IF and THEN is very complex. The overall ANFIS structure has been established based on consideration of one output parameter in accordance with several input variables.

In the MANFIS simulation workplace of MATLAB R2016b software (The Mathworks, Inc., Natick, MA, USA), ten ANFIS sub-environments were individually developed for prognostication of ten performance parameters based on the same input variables of plowing depth (10, 20 and 30 cm), forward speed (2, 4 and 6 km/h), and implement type (moldboard, disk, and chisel plow implement). Similar to the ANN simulation workplace, to introduce implement type as input variable for the MANFIS simulation workplace, the integers 1, 2 and 3 were assigned for moldboard, disk, and chisel plow implement, respectively. Data sets obtained from the field operations were randomly shuffled and classified into three groups. The groups including 70, 15 and 15% of the data for training, validating and testing, respectively, of each developed ANFIS sub-environment. Calibration process was frequently performed until the best structure of the ANFIS scenario for each performance parameter with the highest prognostication accuracy was reached. The process was completed by trying different training cycles, the number of input membership functions, type of input membership functions, type of output membership functions, and defuzzification methods. Flowchart for selection of the best MANFIS scenario in accordance with schematic of simulation scenario and five-layered structure of the ANFIS are shown in Fig. 3.

2.5.3. MANFIS+MNE

The new simulation scenario of MANFIS+MNE was considered based on one MANFIS configuration coupled with two MNE configurations (Fig. 4). The MANFIS configuration consisted of four ANFIS sub-environments. Three ANFIS sub-environments were applied for prognostication of three master performance parameters (required draft force of implement, tractor rear wheel slip, fuel consumption per working hour) of tractor-implement systems in plowing process regarding three input variables of plowing depth (10, 20 and 30 cm), forward speed (2, 4 and 6 km/h), and implement type (moldboard, disk, and chisel plow). The forth ANFIS sub-environment was applied as auxiliary one for prognostication of gross traction force. The best finalized structures obtained for the ANFIS1, ANFIS4, and ANFIS9 in the previous Section 2.5.2 were employed in the workplace. Similarly, calibration process was frequently performed until the best structure (training cycles, the number of input membership functions, type of input membership function, type of output membership functions, and defuzzification methods) of the ANFIS4 was obtained for prognostication of gross traction force. The output prognostication values of the MANFIS configuration could be used in the MNE configuration1. The MNE configuration1 consisted of four MNE environments for prognostication of tractor drawbar power, tractor tractive efficiency, specific draft force, and fuel consumption per tilled area, based on the Eqs.(4), (7), (8) and (9), respectively. The values of four performance parameters calculated by the MNE configuration1 were delivered to the MNE configuration2 in

Table 9
The values of statistical descriptor parameters determined for tractor rear wheel slip in plowing process.

Implement	Minimum (%)	Maximum (%)	Mean (%)	SD (%)	CV (%)	CNU (%)
Chisel plow	8.98	49.02	27.24	12.24	44.93	146.99
Disk plow	5.11	38.65	22.60	10.30	45.58	148.41
Moldboard plow	6.54	46.23	23.07	11.52	49.93	172.04

Table 10
The values of statistical descriptor parameters determined for fuel consumption per working hour in plowing process.

Implement	Minimum (L/h)	Maximum (L/h)	Mean (L/h)	SD (L/h)	CV (%)	CNU (%)
Chisel plow	7.26	22.65	15.56	4.47	28.73	98.91
Disk plow	5.29	14.89	9.91	2.99	30.17	96.87
Moldboard plow	4.02	13.95	9.10	3.06	33.63	109.12

order to calculate other three performance parameters (specific volumetric fuel consumption, energy requirement for tillage implement, and overall energy efficiency) on the basis of the Eqs.(3), (5) and (6). Finally, obtained values of ten performance parameters were achievable in the simulation workplace output.

To run the MANFIS+MNE simulation scenario, a simple code was written in Command Window of MATLAB R2016b software. When the program (finalized code) was run, the prerequisite values of plowing depth in the range of 10–30 cm, forward speed in the range of 2–6 km/h, and tillage implement type (the integers 1, 2 and 3 for moldboard, disk, and chisel plow implement, respectively) were received and the MANFIS configuration, MNE configuration1, and MNE configuration2 were respectively called to simulate and calculate the ten performance parameters. The error message was displayed in Command Window, if the prerequisite values were not imported in desired ranges. It should be also noted that required specifications (working width and field efficiency) for each implement were defined for the program to be used in the MNE configuration1 and MNE configuration2. Finally, the prerequisite values in accordance with the ten obtained performance parameters were placed in predetermined appropriate columns of workspace in the MATLAB software. Therefore, it can be pointed out that the defined program for simulation workplace worked like a neuro-fuzzy calculator in workspace of the MATLAB software. It means that, values of the independent input variables were received and values of the ten performance parameters were tabulated. Operational flowchart of the program algorithm is shown in Fig. 5. As it can be seen in the Fig. 5, the algorithm consisted of three sub-programs for the MANFIS configuration, MNE configuration1, and MNE configuration2 which are called, respectively.

2.6. Prognostication appraisal of soft computing simulation workplaces

Goodness of prognostication accuracy of each performance parameter of tractor-implement systems in soft computing simulation workplaces for each scenario (the ANN, MANFIS, and MANFIS+MNE) was appraised by coefficient of determination of regression analysis utilizing Eq.(15) (Shafaei et al., 2016b). Moreover, absolute and relative error of prognostication were ascertained by Eqs.(16) and (17), respectively (Shafaei et al., 2017b). The highest values of coefficient of determination closed to one and the lowest values of the RMSE and MRDM indicate the best simulation workplace for each scenario. However, prognostication accuracy of prominent simulation workplace of each scenario must be compared with that of other ones.

$$R^2 = 1-\left(\frac{\sum_{i=1}^{i=N}\left(PP_{obt,i}-PP_{sim,i}\right)^2}{\sum_{i=1}^{i=N}\left(PP_{obt,i}-PP_{obtave}\right)^2}\right) \tag{15}$$

$$RMSE = \left[\frac{1}{N}\sum_{i=1}^{i=N}\left(PP_{sim,i}-PP_{obt,i}\right)^2\right]^{0.5} \tag{16}$$

$$MRDM = \frac{100}{N}\sum_{i=1}^{i=N}\left(\frac{\left|PP_{sim,i}-PP_{obt,i}\right|}{PP_{obt,i}}\right) \tag{17}$$

2.7. Performance benchmark of prominent soft computing simulation workplaces

Simulation residual errors for prominent simulation workplace of the ANN, MANFIS, and MANFIS+MNE scenario were plotted to apprise sensitivity of prognostication values to actual data. The MAVSRE was also calculated (Eq.(18)) for each prominent simulation workplace.

$$MAVSRE = \frac{1}{N}\sum_{i=1}^{i=N}\left|PP_{sim,i}-PP_{obt,i}\right| \tag{18}$$

To recognize prominent scenario for prognostication of performance parameters of tractor-implement systems, not only a comparative trend was performed between the values obtained from the Eqs.(15)–(18), but also simulation time and user-friendly configuration of three scenarios were benchmarked. The scenario with the highest prognostication accuracy, the lowest simulation time, and more user-friendly configuration was recognized as the prominent one.

3. Results and discussion

3.1. Statistical descriptions

3.1.1. Required draft force of implement

Table 8 reports values of statistical descriptor parameters obtained for required draft force of the implements in plowing process. According to the Table 8, it can be seen although the range of draft force variations of the implements has overlap, the range for chisel plow implement was higher than that of other two implements. This led to considerable higher mean value of the draft force of chisel plow implement than that of the other two implements. The possible explanation for this can be related to higher working width of chisel plow implement in comparison with that of the other ones (Table 6). Another reason for this fact might be corresponded to wheat stubble coverage of the tillage site for chiseling process. Because of wheat root concentration in 30 cm topsoil layer, resistance forces are higher and thereby, more draft forces are required to cut and break the soil.

The minimum and maximum values of draft force tabulated in the Table 8 were found in the lowest (forward speed = 2 km/h and plowing depth = 10 cm) and the highest (forward speed = 6 km/h and plowing depth = 30 cm) level of combination of the treatments, respectively, for all implements. The draft force variation ranges obtained in this

Table 11
The values of statistical descriptor parameters determined for fuel consumption per tilled area in plowing process.

Implement	Minimum (L/ha)	Maximum (L/ha)	Mean (L/ha)	SD (L/ha)	CV (%)	CNU (%)
Chisel plow	12.18	43.22	23.07	9.66	41.87	134.55
Disk plow	12.04	28.38	20.08	5.23	26.05	81.38
Moldboard plow	15.58	37.69	27.84	7.39	26.55	79.42

Table 12
The values of statistical descriptor parameters determined for specific volumetric fuel consumption in plowing process.

Implement	Minimum (L/kW h)	Maximum (L/kW h)	Mean (L/kW h)	SD (L/kW h)	CV (%)	CNU (%)
Chisel plow	0.36	1.66	0.88	0.43	48.86	147.73
Disk plow	0.47	2.05	1.07	0.48	44.86	147.66
Moldboard plow	0.36	1.87	0.97	0.50	51.55	155.67

research were within the similar ranges reported by Smith and Williford (1988) and Almaliki (2018).

3.1.2. Tractor rear wheel slip

The values of statistical descriptor parameters determined for tractor rear wheel slip in plowing process are tabulated in Table 9. As it can be seen in the Table 9, the wheel slip ranged from 5.11 to 49.02% for the implements. However, the wheel slip range for chisel plow implement was higher than that of moldboard plow followed by disk plow implement. This discrepancy might be attributable to the higher required draft force of chisel plow implement than that of other implements which is mentioned in the previous subset. Due to lack of proper traction force generated by the tractor wheels in some conditions, the wheel slip increases. Moreover, lower contact between the wheels and soil occurs, when the tillage site is covered with uniform wheat stubble. Therefore, higher wheel slip might be related to a condition that luges of the tires do not penetrate enough into the soil to make proper engagement needed for overcoming the higher implement draft.

Similar to the previous subset results, the minimum and maximum values of the wheel slip reported in the Table 9 were found in the lowest (forward speed = 2 km/h and plowing depth = 10 cm) and the highest (forward speed = 6 km/h and plowing depth = 30 cm) level of combination of the treatments, respectively, for the implements. The range of the wheel slip observed in this research overlaps with the range documented by previous authors in their research study reports (Kolahloo and Loghavi, 1994; Tayel et al., 2015; Taiwo and Owusu-Sekyere, 2015).

3.1.3. Fuel consumption per working hour

The values of statistical descriptor parameters determined for fuel consumption per working hour in plowing process are given in Table 10. With reference to the Table 10, it is clear that higher range of the fuel consumption per working hour for chisel plow implement than that of other implements led to higher associated mean value (approximately 1.6 times) of the fuel consumption for the chisel plow implement than that of the other implements. There are two potential causes for this observation. Higher required draft force of chisel plow implement than that of other implements and consequently, higher fuel energy requirements and fuel consumption per working hour. Additionally, higher wheel slip of tractor results in higher fuel consumption (Thansandote et al., 1977).

In parallel with two previously discussed performance parameters, the minimum and maximum values of fuel consumption per working hour noted in the Table 10 were found in the lowest (forward speed = 2 km/h and plowing depth = 10 cm) and the highest (forward speed = 6 km/h and plowing depth = 30 cm) level of combination of the treatments, respectively, for the implements. These results for variation of the fuel consumption are in compliance with the findings of previous researchers for strip tillage machine (Sarauskis et al., 2017).

3.1.4. Fuel consumption per tilled area

Table 11 presents values of statistical descriptor parameters determined for fuel consumption per tilled area in plowing process. It can be observed in the Table 11 that the fuel consumption ranged from 12.04 to 43.22 (L/ha) for the implements. However, the fuel consumption range for chisel plow implement is higher than that of other implements. According to Eq.(9), higher value of fuel consumption per working hour leads to calculation of higher value of fuel consumption per tilled area. Hence, higher values of fuel consumption per working hour of chisel plow implement than that of other implements resulted in the higher values of fuel consumption per tilled area of the chisel plow implement than that of other implements.

On the contrary with previously discussed performance parameters, the minimum and maximum values of the fuel consumption mentioned in the Table 11 were found in combination of the treatments of forward speed = 6 km/h and plowing depth = 10 cm, and forward speed = 2 km/h and plowing depth = 30 cm, respectively, for the implements. The variation range of the fuel consumption observed in the present research is consistent with the results published by previous researchers (Hughes and Baker, 1977; Hemmat and Khashoei, 1995; Stajnko et al., 2009).

3.1.5. Specific volumetric fuel consumption

The values of statistical descriptor parameters determined for specific volumetric fuel consumption in plowing process are organized in Table 12. As it can be found in the Table 12, the variation range of the fuel consumption for disk plow was higher than that of the other implements. One possible explanation for this is related to the Eq.(3). The Eq. (3) shows the inverse relation between specific volumetric fuel consumption and the draft force as well as direct relation between specific volumetric fuel consumption and fuel consumption per working hour. The combination of these two relations results in various values calculated for specific volumetric fuel consumption.

From analogical point of view, the minimum and maximum values of specific volumetric fuel consumption were obtained in different levels of combination of the treatments against those of fuel consumption per working hour and fuel consumption per tilled area. The minimum and maximum values of specific volumetric fuel consumption were obtained in the forward speed = 6 km/h and plowing depth = 30 cm, and the forward speed = 2 km/h and plowing depth = 10, respectively, for the implements. The variation range of the fuel consumption observed in the current research is consistent with the results of Parvanloo et al. (2015).

3.1.6. Specific draft force

The values of statistical descriptor parameters determined for specific draft force in plowing process are denoted in Table 13. With reference to the Table 13, the range of specific draft force for moldboard plow

Table 13
The values of statistical descriptor parameters determined for specific draft force in plowing process.

Implement	Minimum (kN/m^2)	Maximum (kN/m^2)	Mean (kN/m^2)	SD (kN/m^2)	CV (%)	CNU (%)
Chisel plow	35.02	70.09	47.33	10.25	21.66	74.10
Disk plow	46.21	77.27	59.82	15.32	25.61	51.92
Moldboard plow	34.44	109.66	64.29	21.72	33.78	117

Table 14
The values of statistical descriptor parameters determined for tractor drawbar power in plowing process.

Implement	Minimum (kW)	Maximum (kW)	Mean (kW)	SD (kW)	CV (%)	CNU (%)
Chisel plow	4.38	63.02	26	19.36	74.46	225.54
Disk plow	3.08	35.10	16.18	10.35	63.97	122.31
Moldboard plow	2.13	38.40	14.18	10.92	77.01	255.78

implement was higher than that of disk plow followed by chisel plow implement. This result is reasonable, since implement working width of moldboard plow was lower than that of other two implements. According to Eq.(8), the inverse relation between specific draft force and implement working width is observed. Therefore, lower implement working width leads to higher specific draft force in the same conditions. From another point of view, based on Eq.(8), the value of required draft force of implement is important in specific draft force calculation.

In case of chisel and moldboard plow implement, the minimum value of specific draft force was obtained in forward speed = 2 km/h and plowing depth = 20 cm, while in the case of disk plow implement, the minimum specific draft occurred in forward speed = 2 km/h and plowing depth = 30 cm. The maximum value of specific draft force for moldboard plow implement was obtained in forward speed = 6 km/h and plowing depth = 10 cm. Meanwhile, the maximum value of specific draft force for disk and chisel plow implement was obtained in forward speed = 6 km/h and plowing depth = 20 cm. These results are closely aligned with those reported by Plouffe et al. (1995) and Arvidsson et al. (2004).

3.1.7. Tractor drawbar power

The values of statistical descriptor parameters determined for tractor drawbar power in plowing process are classified in Table 14. In accordance with the values of the Table 14, it is clear that the range of the values of tractor drawbar power for chisel plow implement was considerably higher than that of other two implements. The reason behind this result is explained by the fact of direct relation between required draft force of implement and tractor drawbar power (Eq.(4)). Hence, based on the Eq.(4), higher required draft force of implement results in higher tractor drawbar power in the same tested conditions. Therefore, based on the Table 8, higher values of the draft force of chisel plow implement than those of other two implements lead to higher values of the drawbar power of chisel plow implement than those of other two implements.

Similar to the results of required draft force of implement, the minimum and maximum values of tractor drawbar power tabulated in the Table 14 were found in the lowest (forward speed = 2 km/h and plowing depth = 10 cm) and the highest (forward speed = 6 km/h and plowing depth = 30 cm) level of combination of the treatments, respectively, for the implements. The drawbar power results in this research are parallel to the results published by Chaplin et al. (1988), and Loghavi and Moradi (1996).

3.1.8. Tractor tractive efficiency

Table 15 reports the values of statistical descriptor parameters determined for tractor tractive efficiency in plowing process. According to the Table 15, tractor tractive efficiency is higher when disk plow implement was attached to the tractor. This might be attributed to lower tractor rear wheel slip (Table 9). Based on the Eq.(7), the tractive efficiency is direct function of the wheel slip and net traction force (required draft force of implement). Therefore, on the basis of the Table 9, lower tractor rear wheel slip, as disk plow implement attached to the tractor, than that of other two implement leads to higher tractor tractive efficiency.

The minimum and maximum values of tractor tractive efficiency reported in the Table 15 were found in the highest (forward speed = 6 km/h and plowing depth = 30 cm) and the lowest (forward speed = 2 km/h and plowing depth = 10 cm) level of combination of the treatments, respectively, for the implements. The observed results are in general agreement with the results of previous studies conducted by Inchebron et al. (2012) and Far et al. (2015a).

3.1.9. Energy requirement for tillage implement

Table 16 lists values of statistical descriptor parameters determined for energy requirement for tillage implements. The mean values of the energy requirement in the Table 16 tend to increase as implement varies from chisel to moldboard plow implement. A possible explanation for this result is related to implement working width (Eqs.(5) and (10)). Substitution of the Eq.(10) into the Eq.(5) shows that the energy requirements is an inverse function of implement working width. Accordingly, considering working width of the implements noted in the Table 6, the energy requirement increased as implement working width decreased.

Similar to the results of some previously discussed performance parameters, the minimum and maximum values of the energy requirement noted in the Table 16 were found in the lowest (forward speed = 2 km/h and plowing depth = 10 cm) and the highest (forward speed = 6 km/h and plowing depth = 30 cm) level of combination of the treatments, respectively, for the implements. The energy requirement results reported by Jr et al. (1985) and Celik et al. (2007) are similar compared to results of this research.

3.1.10. Overall energy efficiency

Table 17 shows values of statistical descriptor parameters determined for overall energy efficiency of the tractor-implement systems in plowing process. The mean value of the efficiency of disk plow implement in the Table 17 is higher than that of chisel plow followed by moldboard plow implement. This result occurred due to higher tractor tractive efficiency, when disk plow implement was attached to the tractor. Moreover, based on the Eq.(6), overall energy efficiency is inverse function of fuel consumption per tilled area. Therefore, the lower values of fuel consumption per tilled area for disk plow implement (Table 11) than those of other two implements were effective in obtained higher values of overall energy efficiency.

Similar to the results of some previously discussed performance parameters, the minimum and maximum values of the efficiency in plowing process documented in the Table 17 were found in the lowest (forward speed = 2 km/h and plowing depth = 10 cm) and the highest (forward speed = 6 km/h and plowing depth = 30 cm) level of combination of the treatments, respectively, for the implements. The obtained values for the efficiency in current research are similarly ranged with

Table 15
The values of statistical descriptor parameters determined for tractor tractive efficiency in plowing process.

Implement	Minimum (%)	Maximum (%)	Mean (%)	SD (%)	CV (%)	CNU (%)
Chisel plow	43.69	89.23	68.99	13.23	19.18	66.01
Disk plow	65.65	91.26	75.72	11.25	14.86	33.82
Moldboard plow	49.43	87.54	71.06	10.18	41.33	53.63

Table 16
The values of statistical descriptor parameters determined for energy requirement for the implements in plowing process.

Implement	Minimum (MJ/ha)	Maximum (MJ/ha)	Mean (MJ/ha)	SD (MJ/ha)	CV (%)	CNU (%)
Chisel plow	11.45	54.92	31.77	15.33	48.25	136.83
Disk plow	14.26	54.17	34.77	12.08	34.74	114.78
Moldboard plow	12.45	74.85	37.40	19.46	52.03	166.85

those described by Jr (1985), Sumer and Sabanci (2005), and Far et al. (2015b).

Overall view on the Tables 8–17 demonstrated high values obtained for the CV and CNU of the performance parameters. These high values imply drastic changes of the performance parameters as affected by level changes of the treatments (plowing depth and forward speed). According to the ranges obtained for the performance parameters of tractor-implement systems in plowing process in clay loam soil, it can be claimed that these results are complementary for the research study results which were comprehensively conducted by Kheiralla et al. (2004) in sandy clay loam soil of Malaysia in case of moldboard, disk plow, disk harrow, and rotary tiller implements. Hence, it is practically desired that the experts who work in respective realms focus their attention to these two published research results in order to optimize the management of machinery in plowing process in the similar conditions like these researches.

3.2. Performance appraisal of soft computing simulation workplaces

3.2.1. ANN

The parameters of the several structural arrangements in accordance with corresponding R^2, RMSE, and MRDM of selected twenty ANN soft computing simulation workplaces executed to prognosticate performance parameters of the tractor-implement systems in plowing process are provided in Tables 18–27. As it can be seen in the Tables 18–27, the prominent ANN soft computing simulation workplace was recognized with 6 nodes in hidden layer, 113 training cycles, and exponential and tangent transfer function in input and output layer, respectively. The corresponding values of R^2 for the prominent simulation workplace ranged from 0.683 to 0.890 for ten performance parameters. Graphical presentation of this improper range is illustrated in Fig. 6. With reference to the Fig. 6, the simulated and actual values of performance parameters are not clustered perfectly around 1:1 line which indicates poor agreement between the simulated and actual values. Additionally, scattered distribution of simulation residual error as shown in Fig. 7 clearly depicts that there was no pattern in the errors for the prominent simulation workplace. However, distribution of the error values was centralized in wide ranges. Fig. 8 displays frequency of simulation residual error that indicates scattered distribution of percentage of the errors. On the discussion about these observations, it can be stated that simulation residual errors of the prominent simulation workplace were sensitive to actual data and consequently, it is inferred that the simulation workplace was not matched well to actual data. It is related to the fact that the effect of a variable on performance parameter values was not appropriately simulated by the prominent simulation workplace. In contrast to this result, some previous investigators (Taghavifar et al., 2013; Taghavifar and Mardani, 2014a; Taghavifar and Mardani, 2014b; Taghavifar et al., 2015) pronounced excellent prognostication accuracy of well-developed ANN soft computing simulation workplaces for estimation of unit output target on the basis of numeral multiple input variables.

3.2.2. MANFIS

The parameters of the several structural arrangements in accordance with corresponding R^2, RMSE, and MRDM of selected twenty MANFIS soft computing simulation workplaces executed to prognosticate performance parameters of the tractor-implement systems in plowing process are presented in Tables 28–37. As it has been emphasized in the Tables 28–37, the structural arrangements of each prominent ANFIS sub-environment are not identical in comparison with those of other sub-environments.

The Table 28 implies that prominent ANFIS soft computing simulation sub-environment for prognostication of required draft force of the implements in plowing process was the one with structural arrangements of 125 training cycles, 3 input membership functions for forward speed, plowing depth, and implement type, trapezium and linear function for input and output, respectively, and weighted sum defuzzification method.

The Table 29 presents that prominent ANFIS soft computing simulation sub-environment for prognostication of tractor rear wheel slip in plowing process was the one with structural arrangements of 79 training cycles, 2 input membership functions for forward speed, and 3 input membership functions for plowing depth and implement type, sigmoid and constant function for input and output, respectively, and weighted sum defuzzification method.

The Table 30 indicates that prominent ANFIS soft computing simulation sub-environment for prognostication of fuel consumption per working hour in plowing process was the one with structural arrangements of 124 training cycles, 4 input membership functions for plowing depth, and 3 input membership functions for forward speed and implement type, sigmoid and linear function for input and output, respectively, and weighted sum defuzzification method.

The Table 31 address that prominent ANFIS soft computing simulation sub-environment for prognostication of fuel consumption per tilled area in plowing process was the one with structural arrangements of 157 training cycles, 4 input membership functions for forward speed and plowing depth, and 3 input membership functions for implement type, trapezium and constant function for input and output, respectively, and weighted average defuzzification method.

The Table 32 reports that prominent ANFIS soft computing simulation sub-environment for prognostication of specific volumetric fuel consumption in plowing process was the one with structural arrangements of 138 training cycles, 3 input membership functions for forward speed and implement type, and 4 input membership functions for plowing depth, triangular and linear function for input and output, respectively, and weighted sum defuzzification method.

The Table 33 highlights that prominent ANFIS soft computing simulation sub-environment for prognostication of specific draft force of the implements in plowing process was the one with structural

Table 17
The values of statistical descriptor parameters determined for overall energy efficiency of the tractor-implement systems in plowing process.

Implement	Minimum (%)	Maximum (%)	Mean (%)	SD (%)	CV (%)	CNU (%)
Chisel plow	5.61	25.89	14.58	6.91	47.39	139.10
Disk plow	6.85	27.69	16.29	6.46	39.66	127.93
Moldboard plow	5.64	21.63	11.54	4.82	41.77	138.56

Table 18
The parameters of the several structural arrangements in accordance with corresponding R^2, RMSE, and MRDM of selected twenty ANN soft computing simulation workplaces executed to prognosticate required draft force of the implements in plowing process.

The number of nodes in hidden layer	The number of training cycles	Transfer function		R^2	RMSE (kN)	MRDM (%)
		Input	Output			
2	107	Tangent	Tangent	0.790	5.011	9.414
4	85	Logistic	Exponential	0.709	5.541	10.125
5	145	Tangent	Sine	0.805	3.514	9.059
9	161	Tangent	Logistic	0.814	4.574	9.037
10	183	Logistic	Logistic	0.628	5.763	11.002
10	96	Exponential	Gaussian	0.698	5.587	10.589
10	112	Tangent	Gaussian	0.623	5.897	11.020
2	174	Gaussian	Tangent	0.777	4.568	9.645
3	135	Sine	Logistic	0.781	4.460	9.541
2	142	Exponential	Gaussian	0.629	5.064	10.124
3	119	Logistic	Tangent	0.755	4.521	9.974
7	157	Tangent	Logistic	0.804	4.026	9.412
8	164	Logistic	Logistic	0.798	4.578	9.568
2	105	Sine	Logistic	0.811	3.596	9.025
6	**113**	**Exponential**	**Tangent**	**0.825**	**3.116**	**8.979**
5	136	Logistic	Tangent	0.820	3.158	9.107
6	154	Tangent	Logistic	0.785	3.546	9.620
7	97	Tangent	Sine	0.780	3.600	9.691
9	189	Logistic	Sine	0.769	3.845	9.785
5	140	Logistic	Tangent	0.792	3.597	10.004

The boldfaced line represents prominent simulation workplace.

arrangements of 124 training cycles, 3 input membership functions for forward speed plowing depth, and implement type, Gbell and linear function for input and output, respectively, and weighted average defuzzification method.

The Table 34 describes that prominent ANFIS soft computing simulation sub-environment for prognostication of tractor drawbar power in plowing process was the one with structural arrangements of 115 training cycles, 2, 4 and 3 input membership functions for forward speed, plowing depth, and implement type, respectively, sigmoid and constant function for input and output, respectively, and weighted sum defuzzification method.

The Table 36 indicates that prominent ANFIS soft computing simulation sub-environment for prognostication of tractor energy requirement for tillage implements was the one with structural arrangements of 146 training cycles, 4 input membership functions for forward speed and plowing depth, 3 input membership functions for implement type, triangular and constant function for input and output, respectively, and weighted average defuzzification method.

The Table 37 presents that prominent ANFIS soft computing simulation sub-environment for prognostication of overall energy efficiency of the tractor-tillage implements was the one with structural arrangements of 144 training cycles, 3 input membership functions for forward speed, plowing depth, and implement type, Gbell and linear function for input and output, respectively, and weighted average defuzzification method.

An overview on the Tables 28–37 issues that the corresponding values of R^2 for the prominent sub-environment ranged from 0.971 to 0.997 for ten performance parameters. Graphical presentation of this superior range is depicted in Fig. 9. As it can be seen in the Fig. 9, the simulated and actual values of performance parameters were

Table 19
The parameters of the several structural arrangements in accordance with corresponding R^2, RMSE, and MRDM of selected twenty ANN soft computing simulation workplaces executed to prognosticate tractor rear wheel slip in plowing process.

The number of nodes in hidden layer	The number of training cycles	Transfer function		R^2	RMSE (%)	MRDM (%)
		Input	Output			
2	107	Tangent	Tangent	0.809	4.001	10.975
4	85	Logistic	Exponential	0.770	5.068	11.220
5	145	Tangent	Sine	0.819	3.871	10.447
9	161	Tangent	Logistic	0.847	3.547	10.158
10	183	Logistic	Logistic	0.794	4.847	11.024
10	96	Exponential	Gaussian	0.833	3.714	10.167
10	112	Tangent	Gaussian	0.818	3.899	10.810
2	174	Gaussian	Tangent	0.816	3.905	10.814
3	135	Sine	Logistic	0.838	3.875	9.912
2	142	Exponential	Gaussian	0.880	3.410	9.851
3	119	Logistic	Tangent	0.804	4.024	10.985
7	157	Tangent	Logistic	0.767	5.669	11.268
8	164	Logistic	Logistic	0.783	5.425	11.102
2	105	Sine	Logistic	0.773	5.517	11.161
6	**113**	**Exponential**	**Tangent**	**0.890**	**3.319**	**9.646**
5	136	Logistic	Tangent	0.760	5.126	11.215
6	154	Tangent	Logistic	0.848	3.895	9.785
7	97	Tangent	Sine	0.836	3.911	9.694
9	189	Logistic	Sine	0.811	4.006	10.012
5	140	Logistic	Tangent	0.773	5.547	11.120

The boldfaced line represents prominent simulation workplace.

Table 20
The parameters of the several structural arrangements in accordance with corresponding R^2, RMSE, and MRDM of selected twenty ANN soft computing simulation workplaces executed to prognosticate fuel consumption per working hour in plowing process.

The number of nodes in hidden layer	The number of training cycles	Transfer function		R^2	RMSE (L/h)	MRDM (%)
		Input	Output			
2	107	Tangent	Tangent	0.764	2.464	12.160
4	85	Logistic	Exponential	0.869	1.540	9.815
5	145	Tangent	Sine	0.772	2.651	11.895
9	161	Tangent	Logistic	0.857	1.884	10.007
10	183	Logistic	Logistic	0.838	1.965	9.984
10	96	Exponential	Gaussian	0.789	2.506	12.055
10	112	Tangent	Gaussian	0.865	1.823	10.129
2	174	Gaussian	Tangent	0.797	2.621	11.984
3	135	Sine	Logistic	0.751	2.776	12.113
2	142	Exponential	Gaussian	0.868	1.874	9.717
3	119	Logistic	Tangent	0.831	1.974	10.007
7	157	Tangent	Logistic	0.756	2.774	12.115
8	164	Logistic	Logistic	0.870	1.742	10.014
2	105	Sine	Logistic	0.789	2.336	12.060
6	**113**	**Exponential**	**Tangent**	**0.872**	**1.472**	**9.660**
5	136	Logistic	Tangent	0.782	2.512	12.057
6	154	Tangent	Logistic	0.788	2.498	12.064
7	97	Tangent	Sine	0.838	1.985	9.997
9	189	Logistic	Sine	0.750	2.781	12.117
5	140	Logistic	Tangent	0.757	2.779	12.104

The boldfaced line represents prominent simulation workplace.

appropriately clustered close to 1:1 line which specifies excellent correlation between the simulated and actual values. Furthermore, distribution of simulation residual error is scattered in Fig. 10. The Fig. 10 clearly illustrates that specific pattern was not recognized in the errors for the prominent sub-environments and distribution of the error values was scattered around zero value. Fig. 11 exhibitions frequency of simulation residual error revealing low ranges of percentage of the errors. Accordingly, it can be pointed out that simulation residual error of the prominent simulation workplace was not sensitive to actual data and therefore, it is inferred that the simulation workplace was matched well to actual data.

According to the observed results, it is found that the performance parameters of the tractor-implement systems in plowing process were satisfactorily prognosticated by the prominent MANFIS soft computing simulation workplace executed in this research. This means that the effect of nominal and numeral variables on the performance parameter values was appropriately simulated by the prominent simulation workplace.

The previous authors (Taghavifar and Mardani, 2014c; Taghavifar and Mardani, 2015; Taghavifar et al., 2016; Taghavifar and Mardani, 2017) who employed the ANFIS simulation workplace in their Agricultural and Biosystems Engineering studies have similarly found proper adequacy of the workplace for nonlinear prognostications of desired variables.

3.2.3. MANFIS+MNE

The parameters of the several structural arrangements in accordance with corresponding R^2, RMSE, and MRDM of selected twenty ANFIS soft computing simulation sub-environment executed to prognosticate gross traction force of the tractor-implement systems in plowing process are listed in Table 38. As it can be seen in the Table 38, the prominent ANFIS soft sub-environment is highlighted with structural

Table 21
The parameters of the several structural arrangements in accordance with corresponding R^2, RMSE, and MRDM of selected twenty ANN soft computing simulation workplaces executed to prognosticate fuel consumption per tilled area in plowing process.

The number of nodes in hidden layer	The number of training cycles	Transfer function		R^2	RMSE (L/ha)	MRDM (%)
		Input	Output			
2	107	Tangent	Tangent	0.646	4.120	11.515
4	85	Logistic	Exponential	0.657	4.020	11.856
5	145	Tangent	Sine	0.656	3.895	11.874
9	161	Tangent	Logistic	0.614	4.195	12.154
10	183	Logistic	Logistic	0.671	3.822	10.940
10	96	Exponential	Gaussian	0.649	4.013	11.807
10	112	Tangent	Gaussian	0.623	3.991	12.074
2	174	Gaussian	Tangent	0.615	4.198	12.127
3	135	Sine	Logistic	0.632	4.070	11.954
2	142	Exponential	Gaussian	0.658	3.641	11.748
3	119	Logistic	Tangent	0.642	4.075	11.852
7	157	Tangent	Logistic	0.631	4.076	12.017
8	164	Logistic	Logistic	0.637	4.069	11.994
2	105	Sine	Logistic	0.631	4.077	11.957
6	**113**	**Exponential**	**Tangent**	**0.701**	**3.480**	**9.074**
5	136	Logistic	Tangent	0.623	4.125	12.058
6	154	Tangent	Logistic	0.666	3.954	11.954
7	97	Tangent	Sine	0.678	3.812	11.895
9	189	Logistic	Sine	0.643	3.710	11.990
5	140	Logistic	Tangent	0.654	3.784	11.826

The boldfaced line represents prominent simulation workplace.

Table 22
The parameters of the several structural arrangements in accordance with corresponding R^2, RMSE, and MRDM of selected twenty ANN soft computing simulation workplaces executed to prognosticate specific volumetric fuel consumption in plowing process.

The number of nodes in hidden layer	The number of training cycles	Transfer function		R^2	RMSE (L/kW h)	MRDM (%)
		Input	Output			
2	107	Tangent	Tangent	0.831	0.174	8.376
4	85	Logistic	Exponential	0.782	0.301	9.174
5	145	Tangent	Sine	0.797	0.284	9.162
9	161	Tangent	Logistic	0.779	0.312	9.184
10	183	Logistic	Logistic	0.785	0.294	9.181
10	96	Exponential	Gaussian	0.850	0.172	8.315
10	112	Tangent	Gaussian	0.754	0.380	9.234
2	174	Gaussian	Tangent	0.778	0.315	9.192
3	135	Sine	Logistic	0.751	0.389	9.241
2	142	Exponential	Gaussian	0.837	0.191	8.624
3	119	Logistic	Tangent	0.793	0.321	9.111
7	157	Tangent	Logistic	0.797	0.324	9.125
8	164	Logistic	Logistic	0.825	0.184	8.547
2	105	Sine	Logistic	0.803	0.215	9.016
6	**113**	**Exponential**	**Tangent**	**0.859**	**0.169**	**8.292**
5	136	Logistic	Tangent	0.779	0.304	9.201
6	154	Tangent	Logistic	0.815	0.198	8.541
7	97	Tangent	Sine	0.775	0.311	9.198
9	189	Logistic	Sine	0.847	0.178	8.317
5	140	Logistic	Tangent	0.775	0.310	9.205

The boldfaced line represents prominent simulation workplace.

arrangements of 126 training cycles, 4 input membership functions for forward speed and plowing depth, 3 input membership functions for implement type, Gbell and linear function for input and output, respectively, and weighted average defuzzification method. Meanwhile, its statistical performance criteria is $R^2 = 0.984$, RMSE $= 0.985$ kN and MRDM $= 2.167\%$. It should be noted that the structural arrangements of the prominent ANFIS soft computing simulation sub-environments for the three master performance parameters of required draft force of implements, tractor rear wheel slip, and fuel consumption per working hour obtained in the MANFIS soft computing simulation workplace were also employed in the MANFIS+MNE simulation workplace. Consequently, it is expected that the statistical performance criteria related to the three master performance parameters in two simulation scenarios were the same.

Table 39 presents statistical performance criteria for three master as well as seven slave performance parameters prognosticated in the MANFIS+MNE simulation workplace. As it has been documented in the Table 39, the corresponding values of R^2 for prognostication of ten performance parameters ranged from 0.971 to 0.996. Graphical presentation of this excellent range as shown in Fig. 12 reveals that the simulated and actual values of performance parameters were properly clustered close to 1:1 line which implied outstanding correlation between the simulated and actual values. Additionally, distribution of simulation residual error is scattered in Fig. 13. The Fig. 13 clearly exhibits that no specific pattern was recognized in the errors for the simulation workplace and distribution of the error values was scattered around zero value. Fig. 14 displays frequency of simulation residual error revealing low ranges of percentage of the errors. Accordingly, it can be stated that simulation residual error of the simulation workplace was not sensitive to actual data and consequently, it is inferred that the workplace was matched well to actual data.

Table 23
The parameters of the several structural arrangements in accordance with corresponding R^2, RMSE, and MRDM of selected twenty ANN soft computing simulation workplaces executed to prognosticate specific draft force of the implements in plowing process.

The number of nodes in hidden layer	The number of training cycles	Transfer function		R^2	RMSE (kN/m^2)	MRDM (%)
		Input	Output			
2	107	Tangent	Tangent	0.724	8.142	9.136
4	85	Logistic	Exponential	0.727	7.900	9.130
5	145	Tangent	Sine	0.707	8.810	9.424
9	161	Tangent	Logistic	0.720	7.990	9.132
10	183	Logistic	Logistic	0.728	7.911	9.119
10	96	Exponential	Gaussian	0.704	9.045	9.541
10	112	Tangent	Gaussian	0.721	7.889	9.120
2	174	Gaussian	Tangent	0.723	7.902	9.124
3	135	Sine	Logistic	0.714	7.905	9.326
2	142	Exponential	Gaussian	0.728	8.006	9.148
3	119	Logistic	Tangent	0.727	7.914	9.143
7	157	Tangent	Logistic	0.700	8.987	9.551
8	164	Logistic	Logistic	0.723	7.994	9.098
2	105	Sine	Logistic	0.723	7.954	9.102
6	**113**	**Exponential**	**Tangent**	**0.731**	**7.835**	**8.490**
5	136	Logistic	Tangent	0.708	8.815	9.492
6	154	Tangent	Logistic	0.727	8.125	9.121
7	97	Tangent	Sine	0.707	8.812	9.432
9	189	Logistic	Sine	0.701	8.914	9.403
5	140	Logistic	Tangent	0.714	7.984	9.326

The boldfaced line represents prominent simulation workplace.

Table 24
The parameters of the several structural arrangements in accordance with corresponding R^2, RMSE, and MRDM of selected twenty ANN soft computing simulation workplaces executed to prognosticate tractor drawbar power in plowing process.

The number of nodes in hidden layer	The number of training cycles	Transfer function		R^2	RMSE (kW)	MRDM (%)
		Input	Output			
2	107	Tangent	Tangent	0.797	5.226	9.912
4	85	Logistic	Exponential	0.767	5.294	10.005
5	145	Tangent	Sine	0.742	5.312	10.019
9	161	Tangent	Logistic	0.838	5.042	9.551
10	183	Logistic	Logistic	0.817	5.159	9.609
10	96	Exponential	Gaussian	0.788	5.352	9.958
10	112	Tangent	Gaussian	0.763	5.315	10.012
2	174	Gaussian	Tangent	0.745	5.328	10.017
3	135	Sine	Logistic	0.780	5.249	9.962
2	142	Exponential	Gaussian	0.812	5.151	9.634
3	119	Logistic	Tangent	0.778	5.245	9.962
7	157	Tangent	Logistic	0.760	5.304	9.914
8	164	Logistic	Logistic	0.800	5.213	9.647
2	105	Sine	Logistic	0.831	5.042	9.502
6	**113**	**Exponential**	**Tangent**	**0.841**	**5.005**	**9.482**
5	136	Logistic	Tangent	0.808	5.203	9.623
6	154	Tangent	Logistic	0.836	5.096	9.586
7	97	Tangent	Sine	0.771	5.297	9.957
9	189	Logistic	Sine	0.838	5.012	9.584
5	140	Logistic	Tangent	0.810	5.169	9.625

The boldfaced line represents prominent simulation workplace.

3.3. Performance benchmark of prominent soft computing simulation workplaces

The statistical performance criteria of prominent soft computing simulation workplaces executed based on three simulation scenarios (ANN, MANFIS, and MANFIS+MNE) for prognostication of performance parameters of the tractor-implement systems in plowing process are compared in Fig. 15. According to the Fig. 15, the coefficient of determination varied as $0.683 < R^2 < 0.890$, $0.971 < R^2 < 0.997$ and $0.971 < R^2 < 0.996$ for the prominent ANN, MANFIS, and MANFIS+MNE workplace, respectively. Additionally, the relative error of prognostication varied as 7.91% < MRDM < 9.66%, 0.91% < MRDM < 4.79% and 1.48% < MRDM < 4.97% for the prominent ANN, MANFIS, and MANFIS+MNE workplace, respectively. Meanwhile, the RMSE and MAVSRE for the MANFIS and MANFIS+MNE simulation scenarios ranged in a lower bond than those of the ANN simulation scenario. Hence, robustness of prognostication accuracy of the MANFIS and MANFIS+MNE simulation scenario than that of the ANN simulation scenario was approved.

In this research, there was no precise relationship between performance parameters and implement type (nominal variable). Hence, weakness of several trained ANN simulation scenario based on neural strategy, to sufficiently prognosticate performance parameters resulted in uncovering this imprecise relationship. The neuro-fuzzy strategy can extract sophisticated relationship between output and input parameters using both neural and fuzzy benefits. The fuzzy strategy can prognosticate output based on multiple input variables using defined rules which are ascertained by expert knowledge. Unlike the neural strategy, the fuzzy strategy cannot find relationship between input and output

Table 25
The parameters of the several structural arrangements in accordance with corresponding R^2, RMSE, and MRDM of selected twenty ANN soft computing simulation workplaces executed to prognosticate tractor tractive efficiency in plowing process.

The number of nodes in hidden layer	The number of training cycles	Transfer function		R^2	RMSE (%)	MRDM (%)
		Input	Output			
2	107	Tangent	Tangent	0.676	4.198	8.410
4	85	Logistic	Exponential	0.669	4.230	8.569
5	145	Tangent	Sine	0.611	5.025	8.799
9	161	Tangent	Logistic	0.680	4.123	7.956
10	183	Logistic	Logistic	0.635	4.852	8.847
10	96	Exponential	Gaussian	0.625	4.956	8.927
10	112	Tangent	Gaussian	0.678	4.145	8.417
2	174	Gaussian	Tangent	0.658	4.789	8.869
3	135	Sine	Logistic	0.664	4.119	8.812
2	142	Exponential	Gaussian	0.635	4.927	9.024
3	119	Logistic	Tangent	0.610	5.123	9.011
7	157	Tangent	Logistic	0.634	4.911	9.016
8	164	Logistic	Logistic	0.618	5.195	8.902
2	105	Sine	Logistic	0.603	5.114	8.875
6	**113**	**Exponential**	**Tangent**	**0.683**	**4.046**	**7.912**
5	136	Logistic	Tangent	0.646	4.751	8.741
6	154	Tangent	Logistic	0.669	4.239	8.563
7	97	Tangent	Sine	0.666	4.236	8.560
9	189	Logistic	Sine	0.651	4.536	8.667
5	140	Logistic	Tangent	0.625	5.007	8.915

The boldfaced line represents prominent simulation workplace.

Table 26
The parameters of the several structural arrangements in accordance with corresponding R^2, RMSE, and MRDM of selected twenty ANN soft computing simulation workplaces executed to prognosticate energy requirement for the implements in plowing process.

The number of nodes in hidden layer	The number of training cycles	Transfer function		R^2	RMSE (MJ/ha)	MRDM (%)
		Input	Output			
2	107	Tangent	Tangent	0.728	6.148	10.201
4	85	Logistic	Exponential	0.792	5.691	9.707
5	145	Tangent	Sine	0.756	6.009	10.025
9	161	Tangent	Logistic	0.758	5.998	9.991
10	183	Logistic	Logistic	0.717	6.211	10.281
10	96	Exponential	Gaussian	0.756	6.004	10.017
10	112	Tangent	Gaussian	0.798	5.675	9.697
2	174	Gaussian	Tangent	0.757	6.004	10.021
3	135	Sine	Logistic	0.807	5.584	9.657
2	142	Exponential	Gaussian	0.796	5.681	9.710
3	119	Logistic	Tangent	0.747	6.094	10.53
7	157	Tangent	Logistic	0.710	6.352	10.301
8	164	Logistic	Logistic	0.807	5.571	9.650
2	105	Sine	Logistic	0.724	6.157	10.212
6	**113**	**Exponential**	**Tangent**	**0.813**	**5.484**	**9.582**
5	136	Logistic	Tangent	0.737	6.097	10.053
6	154	Tangent	Logistic	0.742	6.102	10.107
7	97	Tangent	Sine	0.734	6.102	10.075
9	189	Logistic	Sine	0.725	6.150	10.212
5	140	Logistic	Tangent	0.708	6.340	10.325

The boldfaced line represents prominent simulation workplace.

parameters by training itself. On the other hand, to appropriately prognosticate target, the neural strategy based simulation workplace trains itself and the fuzzy strategy based simulation workplace uses defined fuzzy rules. The neuro-fuzzy strategy finds proper fuzzy rules based on training itself. Hence, an outstanding ability of the neuro-fuzzy strategy based simulation scenario is to find compound and uncertain relationships between output and input parameters. In this research, it was found that the prominent MANFIS and MANFIS+MNE simulation workplaces could detect exhaustive relationships between performance parameters (dependent variables) and independent numeral variables of plowing depth and forward speed, and nominal variable of implement type. These relationships were ruled in fuzzy form and then trained to attain minimum value of simulation residual errors.

In parallel with this obtained result, satisfactory prognostication accuracy of the ANFIS simulation workplace versus the ANN simulation workplace in several previous Biosystems Engineering researches has been covered by Khoshnevisan et al. (2014) and Khoshnevisan et al. (2015).

Profound appraisal of structural arrangements of the prominent MANFIS and MANFIS+MNE simulation workplaces in the Figs. 3 and 4, and Tables 28–38 confirms that the statistical performance criteria of two simulation workplaces were approximately identical. However, in the MANFIS simulation workplace, ten different ANFIS simulation sub-environments with various structural arrangements must be run to acceptably prognosticate the performance parameters of the tractor-implement systems in plowing process. While, in the MANFIS +MNE simulation workplace, four different ANFIS simulation sub-environments must be run. In other words, the ten performance parameters could be adequately prognosticated with the lower simulation time and more user-friendly configuration in the MANFIS+MNE simulation workplace than MANFIS simulation workplace. Hence, it can be stated that the MANFIS+MNE simulation workplace is trustworthy

Table 27
The parameters of the several structural arrangements in accordance with corresponding R^2, RMSE, and MRDM of selected twenty ANN soft computing simulation workplaces executed to prognosticate overall energy efficiency of the tractor-implement systems in plowing process.

The number of nodes in hidden layer	The number of training cycles	Transfer function		R^2	RMSE (%)	MRDM (%)
		Input	Output			
2	107	Tangent	Tangent	0.825	2.851	9.256
4	85	Logistic	Exponential	0.848	2.610	9.117
5	145	Tangent	Sine	0.803	3.181	9.704
9	161	Tangent	Logistic	0.852	2.591	9.125
10	183	Logistic	Logistic	0.848	2.527	9.019
10	96	Exponential	Gaussian	0.821	3.007	9.410
10	112	Tangent	Gaussian	0.804	3.179	9.611
2	174	Gaussian	Tangent	0.839	2.819	9.367
3	135	Sine	Logistic	0.811	3.124	9.527
2	142	Exponential	Gaussian	0.839	2.682	9.303
3	119	Logistic	Tangent	0.852	2.548	9.073
7	157	Tangent	Logistic	0.831	2.911	9.417
8	164	Logistic	Logistic	0.831	2.917	9.426
2	105	Sine	Logistic	0.803	3.180	9.715
6	**113**	**Exponential**	**Tangent**	**0.878**	**2.142**	**8.666**
5	136	Logistic	Tangent	0.827	2.806	9.220
6	154	Tangent	Logistic	0.836	2.709	9.174
7	97	Tangent	Sine	0.830	2.711	9.210
9	189	Logistic	Sine	0.859	2.523	9.006
5	140	Logistic	Tangent	0.865	2.421	8.954

The boldfaced line represents prominent simulation workplace.

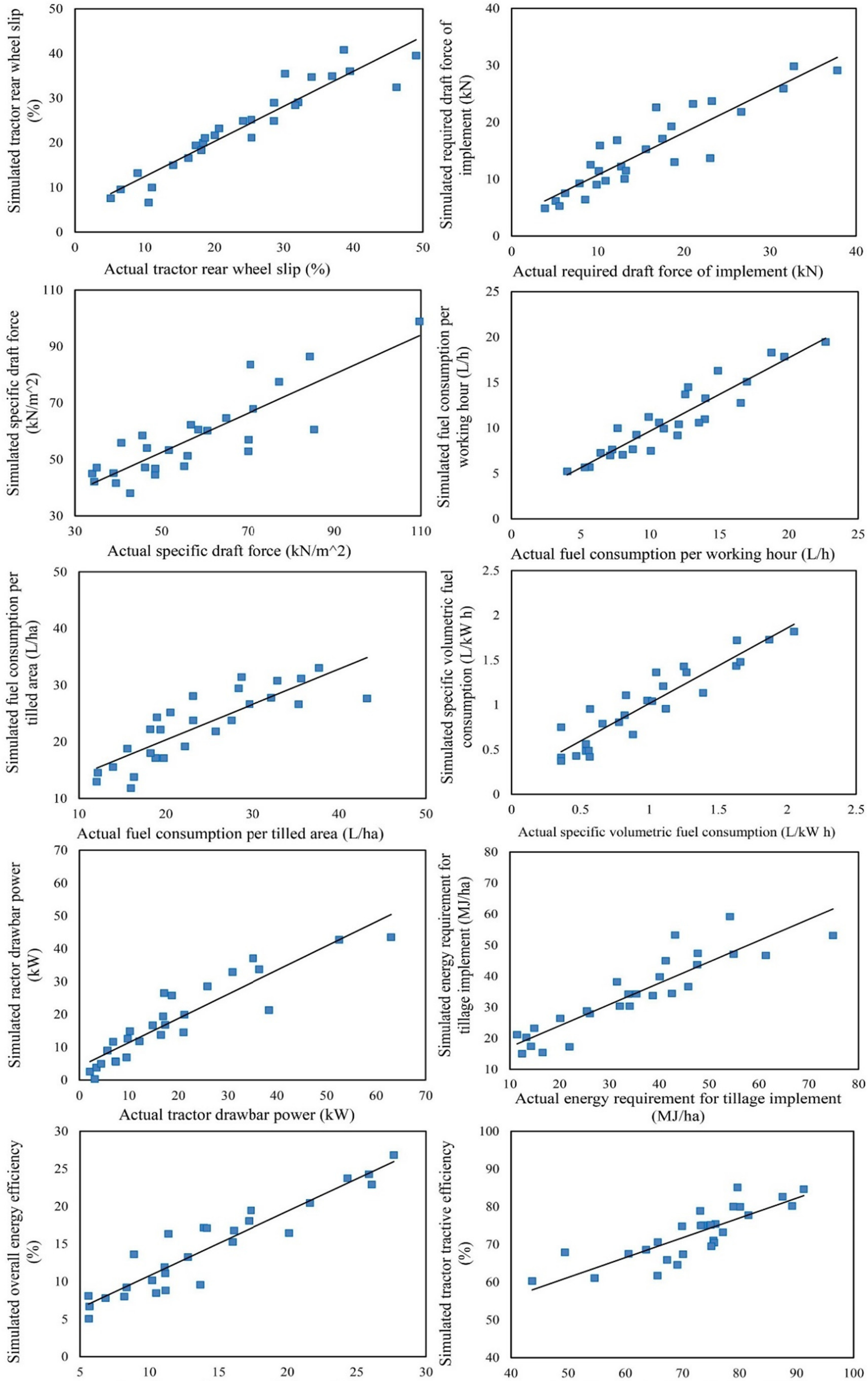

Fig. 6. Graphical presentation of correlation between the simulated values by the prominent ANN simulation workplace and actual values of performance parameters of tractor-implement systems in plowing process.

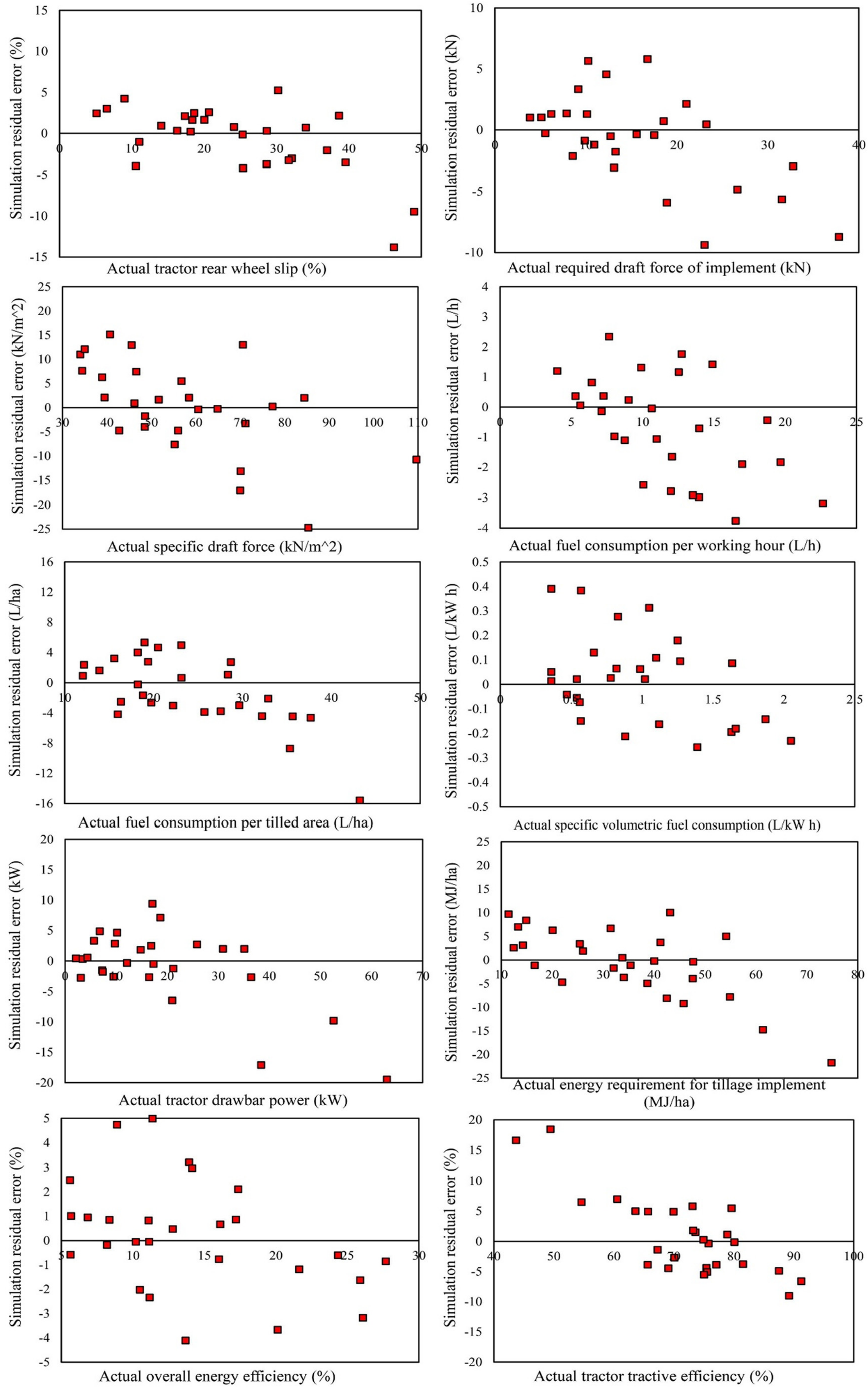

Fig. 7. Simulation residual error plots for the simulated values by the prominent ANN simulation workplace for performance parameters of tractor-implement systems in plowing process.

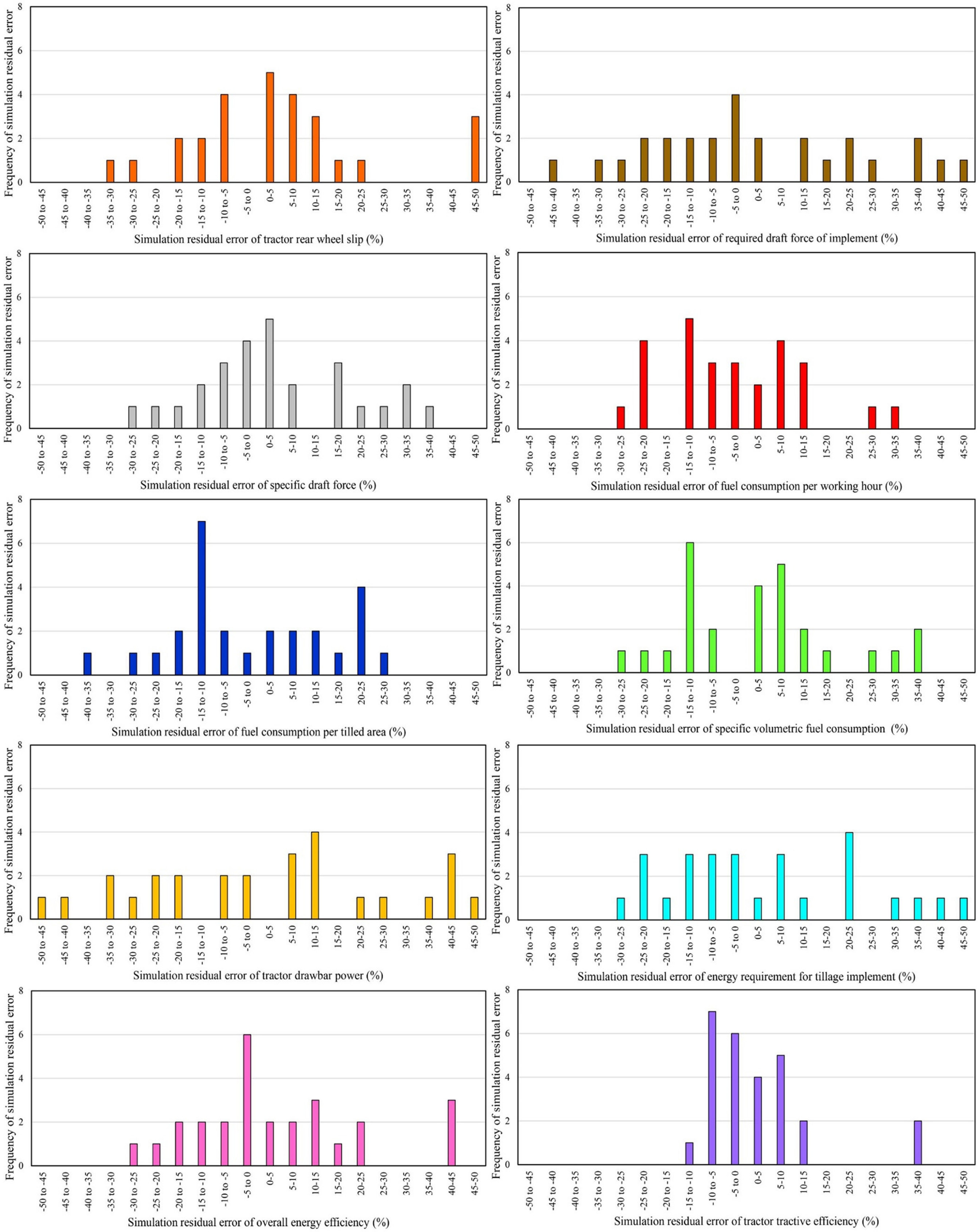

Fig. 8. Frequency plots of simulation residual error for the simulated values by the prominent ANN simulation workplace for performance parameters of tractor-implement systems in plowing process.

Table 28
The parameters of the several structural arrangements in accordance with corresponding R^2, RMSE, and MRDM of selected twenty ANFIS soft computing simulation sub-environment executed to prognosticate required draft force of the implements in plowing process.

The number of training cycles	The number of input membership functions	Membership function		Defuzzification method	R^2	RMSE (kN)	MRDM (%)
		Input	Output				
125	3,2,3	Gaussian	Linear	Weighted sum	0.893	2.006	3.019
93	4,4,3	Sigmoid	Constant	Weighted sum	0.882	2.058	3.084
80	4,2,3	Gaussian	Linear	Weighted sum	0.914	1.422	2.601
83	3,3,3	Sigmoid	Linear	Weighted average	0.934	1.416	2.623
96	2,2,3	Gaussian	Linear	Weighted average	0.914	1.420	2.615
111	2,4,3	Triangular	Constant	Weighted average	0.905	1.653	2.729
134	4,4,3	Gbell	Constant	Weighted average	0.949	1.330	2.511
125	**3,3,3**	**Trapezium**	**Linear**	**Weighted sum**	**0.985**	**1.117**	**2.267**
72	2,2,3	Gbell	Constant	Weighted average	0.947	1.337	2.519
108	3,4,3	Gaussian	Linear	Weighted sum	0.969	1.221	2.325
114	4,3,3	Triangular	Constant	Weighted sum	0.892	2.011	3.028
75	2,2,3	Pi	Linear	Weighted average	0.971	1.198	2.312
106	3,3,3	Gbell	Constant	Weighted average	0.899	1.952	2.913
121	3,4,3	Gaussian	Linear	Weighted sum	0.890	1.984	2.910
88	2,3,3	Gaussian	Linear	Weighted sum	0.958	1.296	2.410
95	3,2,3	Trapezium	Linear	Weighted sum	0.971	1.192	2.296
138	4,4,3	Trapezium	Constant	Weighted sum	0.903	1.782	2.756
120	4,2,3	Triangular	Constant	Weighted sum	0.971	1.188	2.294
138	3,3,3	Pi	Constant	Weighted average	0.910	1.477	2.665
79	3,3,3	Gbell	Constant	Weighted average	0.915	1.418	2.591

The boldfaced line represents distinguished simulation framework.

and simple enough to be employed by the users for direct prognostication of the ten performance parameters based on forward speed, plowing depth, and implement type. Therefore, for presentation of clear physical perceptions of performance parameters of the tractor-implement systems in plowing process in this research, the MANFIS +MNE simulation workplace was employed.

3.4. Prognostication of performance parameters of tractor-implement systems

3.4.1. Required draft force of implement

Fig. 16 displays surface and contour plots obtained from the MANFIS +MNE simulation workplace for prognostication of required draft force of the implements in plowing process. As it is obvious in the surface plots of the Fig. 16, the draft force for each implement increased nonlinearly as plowing depth and forward speed increased. Moreover, the contour plots of the Fig. 16 clarify that the dual interaction effect of forward speed and plowing depth on the draft force was increasingly synergistic. It is clear in the contour plots of the Fig. 16 that the draft force increased from the lowest bound (<4 kN) to the highest bound (>35 kN) when plowing depth along with forward speed increased from 10 to 30 cm and 2 to 6 km/h, respectively.

To interpret this obtained result, various physical perception have been indicated by previous investigators. Zhang et al. (2001) have stated that at higher plowing depth, the soil might become denser, and density, cohesion and the tensile strength of the soil would increase further and results in higher draft force requirement. Additionally, Al-Suhaibani and Ghaly (2013) indicated that with plowing depth increment, the soil volume which should be cut, dispersed and moved increases and whereby, higher draft force is required for plowing higher

Table 29
The parameters of the several structural arrangements in accordance with corresponding R^2, RMSE, and MRDM of selected twenty ANFIS soft computing simulation sub-environment executed to prognosticate tractor rear wheel slip in plowing process.

The number of training cycles	The number of input membership functions	Membership function		Defuzzification method	R^2	RMSE (%)	MRDM (%)
		Input	Output				
60	2,2,3	Triangular	Linear	Weighted average	0.946	1.911	4.123
64	3,4,3	Pi	Constant	Weighted average	0.943	1.946	4.169
123	4,3,3	Gbell	Linear	Weighted sum	0.913	2.113	4.369
83	2,2,3	Sigmoid	Constant	Weighted sum	0.953	1.903	4.058
94	3,3,3	Gaussian	Linear	Weighted sum	0.937	2.103	4.355
120	2,2,3	Triangular	Linear	Weighted sum	0.948	1.910	4.119
76	2,3,3	Sigmoid	Linear	Weighted average	0.927	2.004	4.264
131	3,2,3	Trapezium	Constant	Weighted sum	0.957	1.894	4.014
94	4,4,3	Gbell	Constant	Weighted sum	0.876	2.412	4.703
119	4,2,3	Gaussian	Constant	Weighted average	0.922	2.078	4.239
72	3,3,3	Triangular	Linear	Weighted average	0.909	2.213	4.404
61	3,4,3	Sigmoid	Linear	Weighted sum	0.970	1.812	3.993
65	2,3,3	Gbell	Linear	Weighted average	0.917	2.096	4.313
118	3,3,3	Gbell	Constant	Weighted average	0.960	1.869	4.007
82	3,3,3	Gbell	Constant	Weighted average	0.912	2.103	4.364
79	**2,3,3**	**Sigmoid**	**Constant**	**Weighted sum**	**0.979**	**1.716**	**3.906**
63	2,2,3	Gaussian	Linear	Weighted sum	0.900	2.259	4.510
109	3,3,3	Sigmoid	Linear	Weighted sum	0.915	2.023	4.298
116	3,4,3	Gaussian	Constant	Weighted sum	0.890	2.310	4.594
73	2,3,3	Sigmoid	Constant	Weighted sum	0.889	2.398	4.652

The boldfaced line represents prominent simulation workplace.

Table 30
The parameters of the several structural arrangements in accordance with corresponding R^2, RMSE, and MRDM of selected twenty ANFIS soft computing simulation sub-environment executed to prognosticate fuel consumption per working hour in plowing process.

The number of training cycles	The number of input membership functions	Membership function		Defuzzification method	R^2	RMSE (L/h)	MRDM (%)
		Input	Output				
140	2,3,3	Trapezium	Constant	Weighted sum	0.927	1.112	3.785
99	3,2,3	Trapezium	Linear Constant Constant	Weighted average	0.911	1.203	4.007
141	4,4,3	Trapezium	Linear	Weighted average	0.942	1.007	3.512
158	4,2,3	Gbell	Linear	Weighted sum	0.938	1.010	3.687
119	3,3,3	Sigmoid	Linear	Weighted average	0.888	1.302	4.107
106	2,2,3	Gaussian	Linear	Weighted average	0.919	1.159	3.918
119	3,4,3	Triangular	Constant	Weighted average	0.899	1.259	4.056
151	4,3,3	Sigmoid	Linear	Weighted average	0.928	1.078	3.594
110	2,2,3	Trapezium	Constant	Weighted average	0.958	0.956	3.311
133	3,3,3	Trapezium	Linear	Weighted average	0.899	1.263	4.077
124	2,2,3	Gaussian	Linear	Weighted sum	0.881	1.387	4.342
144	2,3,3	Triangular	Linear	Weighted sum	0.872	1.523	4.523
114	3,2,3	Sigmoid	Constant	Weighted average	0.953	0.910	3.298
153	3,2,3	Gaussian	Constant	Weighted average	0.969	0.896	3.259
91	4,4,3	Triangular	Constant	Weighted sum	0.950	0.922	3.303
136	2,2,3	Sigmoid	Constant	Weighted sum	0.962	0.918	3.290
124	**3,4,3**	**Sigmoid**	**Linear**	**Weighted sum**	**0.971**	**0.803**	**3.204**
116	3,3,3	Sigmoid	Constant	Weighted sum	0.876	1.475	4.400
142	2,2,3	Sigmoid	Constant	Weighted sum	0.887	1.314	4.210
128	3,4,3	Sigmoid	Constant	Weighted sum	0.947	0.963	3.456

The boldfaced line represents prominent simulation workplace.

soil volume. Moreover, increment of soil mass gathered around shank, disk or bottom of the implement causes higher normal stress on the shank, disk or bottom and consequently, friction force between shank, disk or bottom surface and soil increases. To overcome higher produced friction force, higher draft force is required (Almaliki, 2018; Upadhyay and Raheman, 2019a).

On the other side, with increment of forward speed, soil particles are subjected to higher acceleration. The higher acceleration forces result in increase of normal loads which are acted on shanks, disks or bottoms of the implement. Higher normal loads lead to higher frictional forces and thereby, higher draft force is required (Kepner et al., 2005). Meanwhile, it is comprehensible that higher forward speed leads to higher shear rate and greater throw of the soil and therefore, higher draft force is expected (Upadhyay and Raheman, 2019a).

The results of increasing effect of plowing depth on the draft force of the implements in a clay loam soil (current research) were similar to those announced by Mouazen and Ramon (2002) and Naderloo et al. (2009) for subsoiler implement in a sandy loam soil and moldboard plow implement in a clay loam soil, respectively. Besides, the increasing effect of forward speed on the draft force has been addressed for one-way disk with seeder (Cullum et al., 1989) and cultivator (Novak et al., 2014), which is paralleled to the results of the present research.

3.4.2. Tractor rear wheel slip

Fig. 17 shows surface and contour plots obtained from the MANFIS +MNE simulation workplace for prognostication of tractor rear wheel slip in plowing process. As it can be seen in the surface plots of the Fig. 17, the wheel slip increased nonlinearly as plowing depth and forward speed increased. Additionally, the contour plots of the Fig. 17 elucidate that the dual interaction effect of forward speed and plowing depth on the wheel slip was increasingly synergistic. It is observable in the contour plots of the Fig. 17 that the wheel slip increased from

Table 31
The parameters of the several structural arrangements in accordance with corresponding R^2, RMSE, and MRDM of selected twenty ANFIS soft computing simulation sub-environment executed to prognosticate fuel consumption per tilled area in plowing process.

The number of training cycles	The number of input membership functions	Membership function		Defuzzification method	R^2	RMSE (L/ha)	MRDM (%)
		Input	Output				
152	2,2,3	Gbell	Constant	Weighted average	0.916	1.603	5.571
134	3,4,3	Sigmoid	Constant	Weighted average	0.895	1.723	5.519
168	4,3,3	Gaussian	Constant	Weighted average	0.961	1.412	5.114
168	2,2,3	Triangular	Constant	Weighted average	0.955	1.358	5.012
163	2,3,3	Sigmoid	Constant	Weighted average	0.929	1.525	5.367
169	3,2,3	Trapezium	Linear	Weighted sum	0.898	1.720	5.523
128	3,2,3	Trapezium	Linear	Weighted sum	0.923	1.574	5.406
148	4,4,3	Trapezium	Linear	Weighted average	0.963	1.392	5.007
158	2,3,3	Trapezium	Constant	Weighted sum	0.896	1.750	5.222
157	**4,4,3**	**Trapezium**	**Constant**	**Weighted average**	**0.979**	**1.258**	**4.792**
127	2,2,3	Sigmoid	Linear	Weighted sum	0.949	1.492	5.190
106	3,3,3	Gaussian	Constant	Weighted sum	0.915	1.611	5.585
148	2,2,3	Triangular	Linear	Weighted sum	0.884	1.589	5.613
114	4,4,3	Pi	Linear	Weighted sum	0.879	1.692	5.721
150	4,2,3	Sigmoid	Linear	Weighted sum	0.879	1.690	5.843
119	3,3,3	Sigmoid	Linear	Weighted sum	0.870	1.775	6.121
168	2,2,3	Trapezium	Constant	Weighted sum	0.875	1.701	5.916
162	3,4,3	Trapezium	Linear	Weighted sum	0.873	1.746	6.014
98	3,3,3	Gbell	Constant	Weighted sum	0.952	1.450	5.106
114	3,3,3	Gbell	Linear	Weighted sum	0.959	1.311	4.859

Table 32
The parameters of the several structural arrangements in accordance with corresponding R^2, RMSE, and MRDM of selected twenty ANFIS soft computing simulation sub-environment executed to prognosticate specific volumetric fuel consumption in plowing process.

The number of training cycles	The number of input membership functions	Membership function		Defuzzification method	R^2	RMSE (L/kW h)	MRDM (%)
		Input	Output				
134	3,3,3	Pi	Linear	Weighted sum	0.964	0.084	3.926
147	2,2,3	Pi	Linear	Weighted sum	0.912	0.159	4.412
117	2,2,3	Gaussian	Constant	Weighted sum	0.908	0.178	4.536
54	2,3,3	Triangular	Constant	Weighted sum	0.922	0.113	4.198
65	3,2,3	Triangular	Linear	Weighted average	0.877	0.225	4.917
95	2,2,3	Triangular	Constant	Weighted average	0.965	0.085	3.911
138	**3,4,3**	**Triangular**	**Linear**	**Weighted average**	**0.977**	**0.075**	**3.885**
123	3,2,3	Triangular	Constant	Weighted average	0.960	0.089	3.916
59	4,4,3	Sigmoid	Constant	Weighted average	0.855	0.231	5.213
80	4,4,3	Gaussian	Linear	Weighted average	0.918	0.118	4.250
110	4,2,3	Triangular	Linear	Weighted average	0.917	0.111	4.256
80	3,3,3	Pi	Linear	Weighted average	0.904	0.182	4.591
92	2,2,3	Sigmoid	Constant	Weighted sum	0.886	0.214	4.807
137	3,4,3	Trapezium	Constant	Weighted sum	0.876	0.233	4.912
138	4,4,3	Gaussian	Constant	Weighted average	0.859	0.276	5.103
122	3,2,3	Gaussian	Linear	Weighted sum	0.891	0.196	4.698
81	2,2,3	Trapezium	Linear	Weighted sum	0.926	0.097	4.117
71	3,4,3	Trapezium	Linear	Weighted sum	0.885	0.211	4.884
65	3,3,3	Gbell	Linear	Weighted sum	0.898	0.189	4.634
113	3,3,3	Gaussian	Linear	Weighted sum	0.869	0.249	5.009

The boldfaced line represents prominent simulation workplace.

the lowest bound (<10%) to the highest bound (>35%) when plowing depth along with forward speed increased from 10 to 30 cm and 2 to 6 km/h, respectively.

The possible explanation for this observation is associated with higher draft force required to pull the implement at higher plowing depth. As a result of lack of adequate traction force produced by the tractor rear driving wheels, at higher plowing depth, the wheel slip increases. It was also revealed by previous researchers that required draft force for pulling the implement grows with increase of forward speed. Consequently, the traction force generated by the tractor might be inadequate and accordingly, the wheel slip increases (Raheman and Jha, 2007).

Similar to this observed result, the increasing effect of plowing depth and forward speed on the wheel slip in plowing process has been documented in previous published papers (Raheman and Jha, 2007; Kumar et al., 2017b).

3.4.3. Fuel consumption per working hour

Fig. 18 illustrates surface and contour plots obtained from the MANFIS+MNE simulation workplace for prognostication of fuel consumption per working hour in plowing process. As it can be seen in the surface plots of the Fig. 18, the fuel consumption increased nonlinearly as plowing depth and forward speed increased. Furthermore, the contour plots of the Fig. 18 reveal that the dual interaction effect of forward speed and plowing depth on the fuel consumption was increasingly synergistic. It is visible in the contour plots of the Fig. 18 that the fuel consumption increased from the lowest bound (<6 L/h) to the highest bound (>22 L/h) as plowing depth along with forward speed increased from 10 to 30 cm and 2 to 6 km/h, respectively.

As forward speed increases, the time required for movement of an assumed distance becomes smaller and therefore, time decrement will result in increment of the fuel consumption rate. Moreover, higher

Table 33
The parameters of the several structural arrangements in accordance with corresponding R^2, RMSE, and MRDM of selected twenty ANFIS soft computing simulation sub-environment executed to prognosticate specific draft force of the implements in plowing process.

The number of training cycles	The number of input membership functions	Membership function		Defuzzification method	R^2	RMSE (kN/m^2)	MRDM (%)
		Input	Output				
117	3,3,3	Trapezium	Linear	Weighted average	0.901	3.526	5.019
124	**3,3,3**	**Gbell**	**Linear**	**Weighted average**	**0.980**	**2.651**	**4.253**
114	2,2,3	Gbell	Constant	Weighted average	0.971	2.968	4.380
108	2,3,3	Triangular	Constant	Weighted average	0.954	3.090	4.680
73	3,3,3	Triangular	Linear	Weighted average	0.957	3.102	4.661
72	3,2,3	Pi	Linear	Weighted sum	0.968	3.041	4.512
36	4,4,3	Gaussian	Linear	Weighted sum	0.945	3.170	4.721
105	4,4,3	Gaussian	Linear	Weighted average	0.975	2.914	4.313
47	4,2,3	Gaussian	Constant	Weighted sum	0.924	3.357	4.832
121	3,3,3	Trapezium	Constant	Weighted sum	0.946	3.173	4.716
35	3,3,3	Trapezium	Linear	Weighted sum	0.921	3.392	4.894
120	2,2,3	Gbell	Linear	Weighted sum	0.906	3.517	5.003
102	2,2,3	Gaussian	Constant	Weighted average	0.933	3.330	4.811
57	3,4,3	Gbell	Constant	Weighted average	0.937	3.267	4.756
39	4,4,3	Gbell	Constant	Weighted average	0.953	3.156	4.655
109	3,2,3	Triangular	Linear	Weighted average	0.977	2.886	4.298
56	2,2,3	Sigmoid	Linear	Weighted average	0.912	3.416	4.916
73	3,4,3	Gaussian	Constant	Weighted average	0.901	3.517	5.025
66	3,3,3	Triangular	Constant	Weighted average	0.901	3.569	5.063
128	3,3,3	Pi	Constant	Weighted average	0.901	3.525	5.034

Table 34
The parameters of the several structural arrangements in accordance with corresponding R^2, RMSE, and MRDM of selected twenty ANFIS soft computing simulation sub-environment executed to prognosticate tractor drawbar power in plowing process.

The number of training cycles	The number of input membership functions	Membership function		Defuzzification method	R^2	RMSE (kW)	MRDM (%)
		Input	Output				
99	3,3,3	Gaussian	Constant	Weighted sum	0.900	1.587	3.207
78	3,3,3	Gaussian	Constant	Weighted sum	0.953	1.195	2.648
115	**2,4,3**	**Sigmoid**	**Constant**	**Weighted sum**	**0.997**	**0.821**	**2.101**
75	2,3,3	Trapezium	Constant	Weighted average	0.953	1.103	2.412
129	3,3,3	Trapezium	Constant	Weighted sum	0.921	1.370	2.944
130	3,2,3	Trapezium	Constant	Weighted sum	0.945	1.017	2.369
34	4,4,3	Gaussian	Constant	Weighted sum	0.965	0.954	2.298
84	4,4,3	Triangular	Linear	Weighted average	0.934	1.216	2.704
71	4,4,3	Gbell	Linear	Weighted sum	0.988	0.897	2.156
86	3,2,3	Gaussian	Linear	Weighted average	0.916	1.455	3.004
49	2,3,3	Gaussian	Linear	Weighted average	0.956	1.025	2.388
96	3,3,3	Triangular	Linear	Weighted average	0.904	1.511	3.118
109	3,2,3	Triangular	Constant	Weighted average	0.956	1.188	2.598
61	4,4,3	Pi	Linear	Weighted sum	0.951	1.185	2.652
89	4,4,3	Gaussian	Linear	Weighted sum	0.975	0.916	2.217
73	4,2,3	Gaussian	Constant	Weighted average	0.926	1.354	2.884
49	3,3,3	Gaussian	Constant	Weighted average	0.950	1.196	2.742
80	2,2,3	Trapezium	Constant	Weighted average	0.928	1.356	2.818
80	3,4,3	Trapezium	Linear	Weighted average	0.922	1.371	2.935
73	4,4,3	Trapezium	Linear	Weighted average	0.927	1.312	2.750

The boldfaced line represents prominent simulation workplace.

draft force at higher plowing depth results in higher required fuel energy and subsequently, the fuel consumption increment.

The same results for increase of the fuel consumption as a result of plowing depth increment have been found by Sarauskis et al. (2017) for strip tillage machine.

3.4.4. Fuel consumption per tilled area

Fig. 19 exhibits surface and contour plots obtained from the MANFIS +MNE simulation workplace for prognostication of fuel consumption per tilled area in plowing process. As it can be seen in the surface plots of the Fig. 19, the fuel consumption changed nonlinearly as plowing depth and forward speed increased. Besides, the contour plots of the Fig. 19 reveal that the dual interaction effect of forward speed and plowing depth on the fuel consumption was nonlinearly antagonism. It is obvious in the contour plots of the Fig. 19 that the fuel consumption changed from the lowest bound (<14 L/ha) to the highest bound (>40 L/ha) as plowing depth along with forward speed increased from 10 to 30 cm and 2 to 6 km/h, respectively.

Table 35
The parameters of the several structural arrangements in accordance with corresponding R^2, RMSE, and MRDM of selected twenty ANFIS soft computing simulation sub-environment executed to prognosticate tractor tractive efficiency in plowing process.

The number of training cycles	The number of input membership functions	Membership function		Defuzzification method	R^2	RMSE (%)	MRDM (%)
		Input	Output				
90	4,4,3	Triangular	Constant	Weighted sum	0.954	1.213	1.303
150	4,4,3	Gbell	Linear	Weighted sum	0.963	1.159	1.243
79	3,2,3	Gaussian	Constant	Weighted sum	0.943	1.312	1.512
61	2,3,3	Gaussian	Constant	Weighted average	0.942	1.315	1.503
92	3,3,3	Pi	Linear	Weighted average	0.910	1.562	1.912
128	4,4,3	Gaussian	Linear	Weighted average	0.917	1.512	1.867
85	4,2,3	Gaussian	Constant	Weighted average	0.955	1.311	1.458
142	3,3,3	Trapezium	Linear	Weighted sum	0.918	1.487	1.852
142	2,2,3	Gaussian	Constant	Weighted sum	0.930	1.467	1.617
130	3,4,3	Triangular	Constant	Weighted average	0.930	1.450	1.623
125	3,3,3	Triangular	Constant	Weighted sum	0.972	1.016	1.051
146	3,3,3	Triangular	Linear	Weighted sum	0.962	1.124	1.187
107	**3,4,3**	**Trapezium**	**Constant**	**Weighted sum**	**0.994**	**0.871**	**0.913**
109	3,3,3	Triangular	Constant	Weighted average	0.990	0.914	0.994
57	4,4,3	Triangular	Linear	Weighted average	0.973	1.011	1.088
60	3,2,3	Trapezium	Linear	Weighted average	0.943	1.290	1.369
52	2,3,3	Trapezium	Constant	Weighted average	0.952	1.215	1.310
84	3,3,3	Gaussian	Constant	Weighted sum	0.912	1.554	1.903
101	3,2,3	Triangular	Constant	Weighted sum	0.965	1.136	1.800
100	3,3,3	Triangular	Linear	Weighted sum	0.969	1.147	1.326

The boldfaced line represents prominent simulation workplace.

Table 36
The parameters of the several structural arrangements in accordance with corresponding R^2, RMSE, and MRDM of selected twenty ANFIS soft computing simulation sub-environment executed to prognosticate energy requirement for the implements in plowing process.

The number of training cycles	The number of input membership functions	Membership function		Defuzzification method	R^2	RMSE (MJ/ha)	MRDM (%)
		Input	Output				
170	3,3,3	Gbell	Constant	Weighted sum	0.985	1.013	2.086
53	3,2,3	Triangular	Linear	Weighted sum	0.995	0.885	1.823
107	2,3,3	Triangular	Constant	Weighted sum	0.969	1.152	2.313
95	3,3,3	Gaussian	Constant	Weighted sum	0.977	1.137	2.287
126	4,4,3	Gaussian	Constant	Weighted average	0.980	1.086	2.165
103	4,2,3	Gaussian	Linear	Weighted average	0.979	1.110	2.207
86	3,3,3	Gaussian	Linear	Weighted average	0.955	1.281	2.410
154	2,2,3	Trapezium	Constant	Weighted sum	0.944	1.311	2.710
122	3,3,3	Gaussian	Constant	Weighted sum	0.989	0.985	1.911
51	3,2,3	Gaussian	Constant	Weighted sum	0.966	1.181	2.315
128	3,2,3	Pi	Constant	Weighted average	0.940	1.387	2.852
167	2,3,3	Gaussian	Linear	Weighted average	0.958	1.198	2.357
95	4,4,3	Gaussian	Constant	Weighted average	0.974	1.139	2.272
95	2,3,3	Trapezium	Constant	Weighted sum	0.988	1.004	2.007
99	3,3,3	Gaussian	Constant	Weighted sum	0.970	1.145	2.301
161	4,4,3	Triangular	Constant	Weighted average	0.976	1.140	2.283
190	2,3,3	Gaussian	Linear	Weighted average	0.990	0.968	1.983
101	3,3,3	Gaussian	Linear	Weighted sum	0.993	0.894	1.915
146	**4,4,3**	**Triangular**	**Constant**	**Weighted average**	**0.997**	**0.873**	**1.809**
58	3,3,3	Gbell	Linear	Weighted sum	0.941	1.352	2.804

The boldfaced line represents prominent simulation workplace.

The physical perception for this observed result can be explained as an assumed distance is traveled in shorter time when forward speed increases. Thus, the fuel consumption decrease as caused by time decrement. Meanwhile, it should be considered that higher draft force required for higher plowing depth might result in higher required fuel energy in hectare scale and accordingly, the fuel consumption increment.

The same trend of fuel consumption increment as affected by plowing depth increment was previously described by Sirhan et al. (2002) and Ajav and Adewoyin (2012). This phenomenon was also found by Serrano et al. (2003) and Gulsoylu et al. (2012) for forward speed increment of offset disk harrow and chisel plow implement, respectively.

3.4.5. Specific volumetric fuel consumption

Fig. 20 presents surface and contour plots obtained from the MANFIS+MNE simulation workplace for prognostication of specific volumetric fuel consumption in plowing process. As it can be seen in the surface plots of the Fig. 20, the fuel consumption decreased nonlinearly as plowing depth and forward speed increased. Moreover, the contour plots of the Fig. 20 indicate that the dual interaction effect of forward speed and plowing depth on the fuel consumption was decreasingly synergistic. It is evident in the contour plots of the Fig. 20 that the fuel consumption decreased from the highest bound (>3 L/kW h) to the lowest bound (<0.4 L/kW h) as plowing depth along with forward speed increased from 10 to 30 cm and 2 to 6 km/h, respectively.

Table 37
The parameters of the several structural arrangements in accordance with corresponding R^2, RMSE, and MRDM of selected twenty ANFIS soft computing simulation sub-environment executed to prognosticate overall energy efficiency of the tractor-implement systems in plowing process.

The number of training cycles	The number of input membership functions	Membership function		Defuzzification method	R^2	RMSE (%)	MRDM (%)
		Input	Output				
142	4,2,3	Trapezium	Linear	Weighted average	0.917	1.303	4.455
88	3,3,3	Triangular	Linear	Weighted average	0.936	1.159	4.368
37	2,2,3	Gaussian	Constant	Weighted sum	0.945	1.123	4.230
53	3,3,3	Gaussian	Constant	Weighted sum	0.953	1.103	4.117
54	3,2,3	Gaussian	Constant	Weighted sum	0.930	1.211	4.401
149	3,2,3	Gaussian	Constant	Weighted average	0.960	0.986	4.103
120	2,3,3	Triangular	Constant	Weighted average	0.960	0.988	4.110
42	4,4,3	Triangular	Constant	Weighted average	0.957	1.051	4.092
144	**3,3,3**	**Sigmoid**	**Linear**	**Weighted average**	**0.984**	**0.817**	**3.809**
138	3,2,3	Trapezium	Constant	Weighted sum	0.966	0.977	4.076
52	3,3,3	Trapezium	Constant	Weighted sum	0.959	1.084	4.111
115	2,2,3	Gbell	Linear	Weighted sum	0.972	0.898	3.926
121	3,2,3	Triangular	Linear	Weighted sum	0.960	1.075	4.109
136	3,2,3	Triangular	Constant	Weighted sum	0.944	1.156	4.268
116	3,3,3	Gaussian	Constant	Weighted average	0.961	1.066	4.098
141	2,2,3	Trapezium	Constant	Weighted sum	0.963	0.958	4.028
99	3,3,3	Gaussian	Constant	Weighted sum	0.953	1.103	4.169
47	3,2,3	Gaussian	Constant	Weighted sum	0.927	1.269	4.498
79	3,2,3	Pi	Constant	Weighted sum	0.952	1.105	4.220
149	2,3,3	Triangular	Constant	Weighted average	0.933	1.202	4.387

The boldfaced line represents prominent simulation workplace.

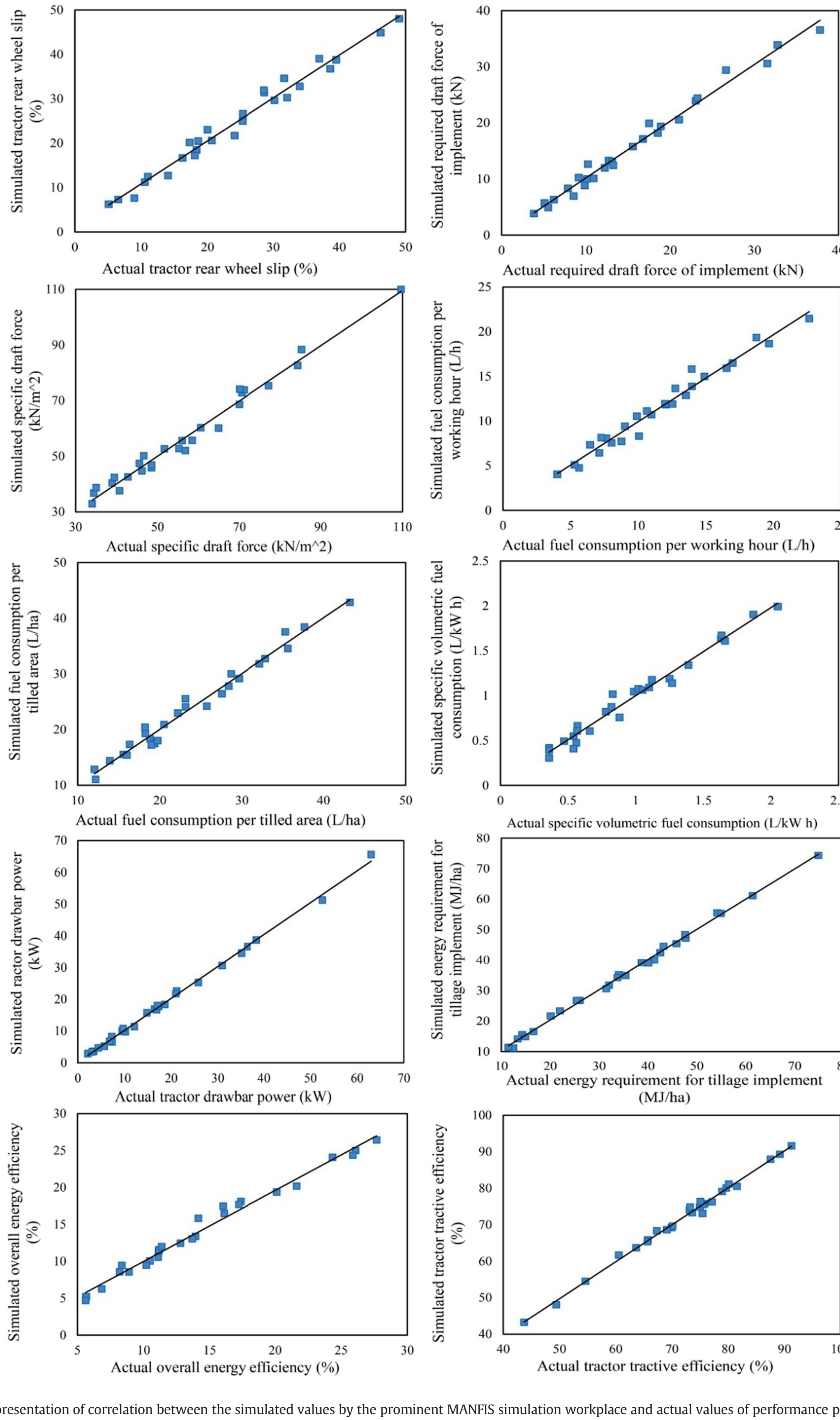

Fig. 9. Graphical presentation of correlation between the simulated values by the prominent MANFIS simulation workplace and actual values of performance parameters of tractor-implement systems in plowing process.

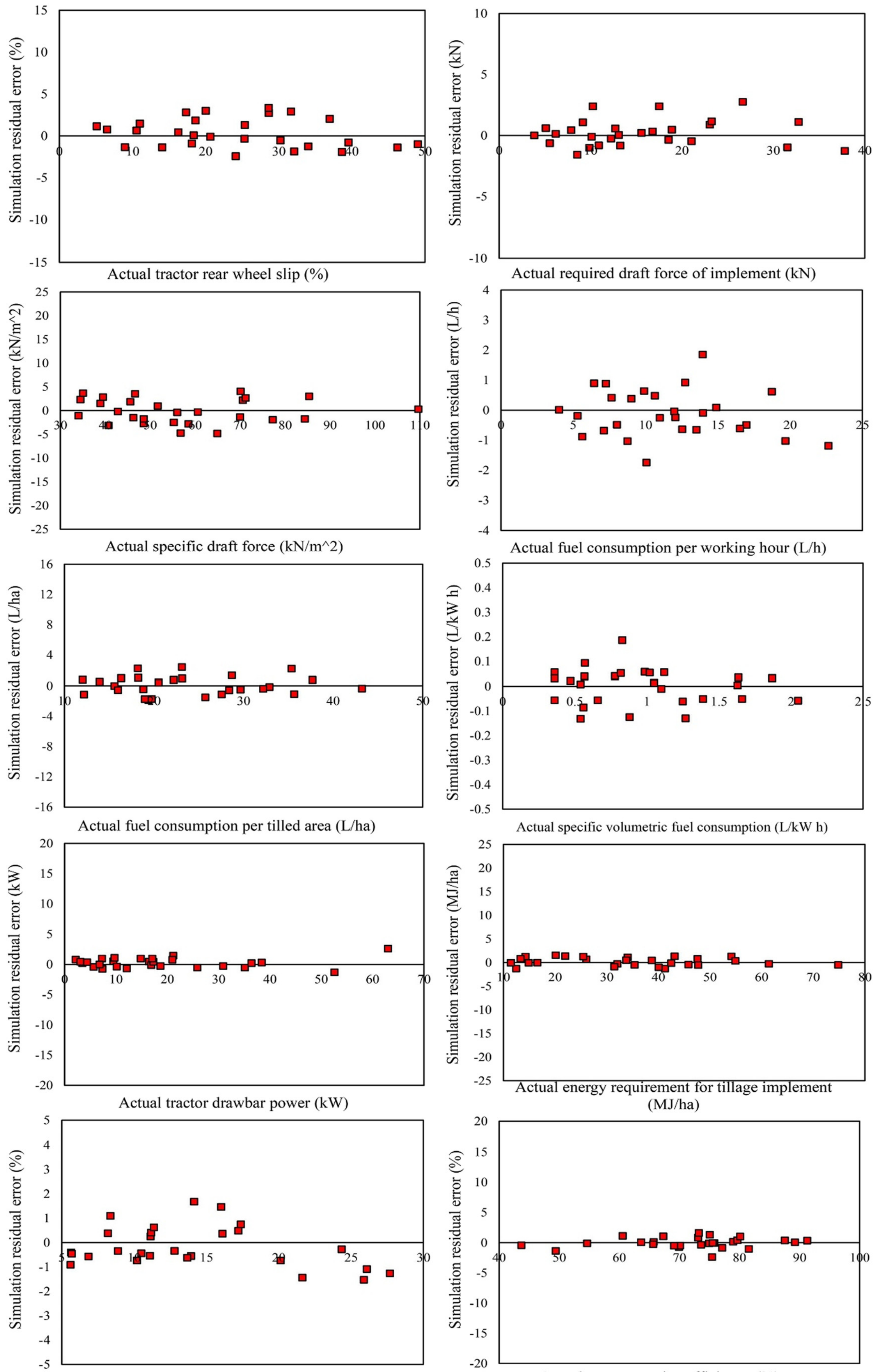

Fig. 10. Simulation residual error plots for the simulated values by the prominent MANFIS simulation workplace for performance parameters of tractor-implement systems in plowing process.

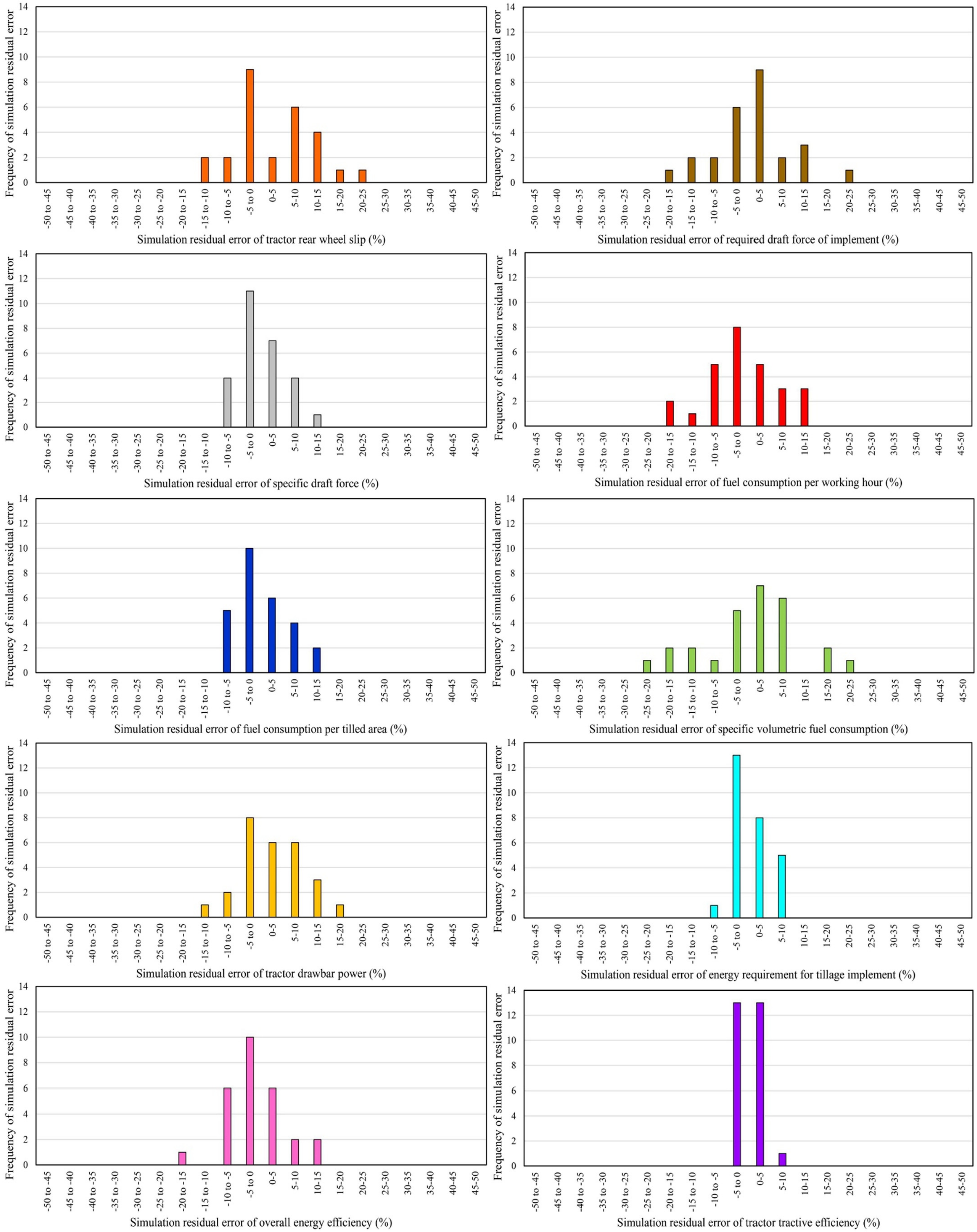

Fig. 11. Frequency plots of simulation residual error for the simulated values by the prominent MANFIS simulation workplace for performance parameters of tractor-implement systems in plowing process.

Table 38
The parameters of the several structural arrangements in accordance with corresponding R^2, RMSE, and MRDM of selected twenty ANFIS soft computing simulation sub-environment executed to prognosticate gross traction force of the tractor-implement systems in plowing process.

The number of training cycles	The number of input membership functions	Membership function		Defuzzification method	R^2	RMSE (kN)	MRDM (%)
		Input	Output				
91	2,2,3	Gaussian	Linear	Weighted sum	0.974	1.018	2.220
137	3,2,3	Triangular	Linear	Weighted average	0.953	1.120	2.352
144	3,2,3	Triangular	Linear	Weighted sum	0.911	1.552	2.689
165	3,3,3	Sigmoid	Linear	Weighted average	0.959	1.113	2.357
150	2,2,3	Trapezium	Linear	Weighted average	0.973	1.016	2.221
155	2,2,3	Trapezium	Constant	Weighted average	0.949	1.218	2.368
75	4,4,3	Gbell	Constant	Weighted sum	0.944	1.320	2.437
83	4,4,3	Gbell	Constant	Weighted average	0.904	1.601	2.712
126	**4,4,3**	**Gbell**	**Linear**	**Weighted average**	**0.984**	**0.985**	**2.167**
101	4,2,3	Gaussian	Constant	Weighted sum	0.973	1.021	2.118
167	3,3,3	Trapezium	Constant	Weighted sum	0.945	1.320	2.511
86	2,2,3	Gaussian	Linear	Weighted sum	0.900	1.615	2.714
75	3,3,3	Gaussian	Linear	Weighted average	0.901	1.626	2.756
138	3,2,3	Pi	Linear	Weighted sum	0.897	1.789	2.803
150	3,2,3	Gaussian	Linear	Weighted sum	0.914	1.465	2.551
99	2,3,3	Gbell	Linear	Weighted average	0.949	1.222	2.352
163	4,4,3	Triangular	Linear	Weighted average	0.901	1.612	2.659
164	4,4,3	Triangular	Linear	Weighted average	0.969	1.156	2.207
169	4,4,3	Gbell	Linear	Weighted average	0.975	0.991	2.194
145	4,4,3	Gbell	Constant	Weighted average	0.945	1.324	2.412

The boldfaced line represents prominent simulation workplace.

Specific volumetric fuel consumption indicates how much fuel is consumed per each unit of effective engine power output. According to the obtained results, the fuel consumption diminishes due to forward speed growth because the fuel consumption is an inverse function of forward speed (Eq.(3)). The fuel consumption decrease regarding plowing depth increment is due to increase of the draft force.

The observed trend in this research for the fuel consumption as affected by forward speed in plowing process is consistent with the trend found by Parvanloo et al. (2015) in previous research.

3.4.6. Specific draft force

Fig. 21 shows surface and contour plots obtained from the MANFIS +MNE simulation workplace for prognostication of specific draft force of the implements in plowing process. As it can be seen in the surface plots of the Fig. 21, specific draft force changed nonlinearly as plowing depth and forward speed increased. In addition, the contour plots of the Fig. 21 represent that the dual interaction effect of forward speed and plowing depth on specific draft force was nonlinearly antagonism. It is recognizable in the contour plots of the Fig. 21 that specific draft force changed from the lowest bound (<40 kN/m^2) to the highest bound (>100 kN/m^2) as plowing depth along with forward speed increased from 10 to 30 cm and 2 to 6 km/h, respectively.

According to the Eq.(8), specific draft force is direct function of draft force and invers function of plowing depth. Taking note that draft force is direct function of plowing depth and forward speed. Therefore, the component direct effect of plowing depth and forward speed, and inverse effect of plowing depth on specific draft force is effective. The surface plots in the Fig. 21 demonstrate that specific draft force increased as forward speed increased (the direct effect of forward speed). However, in case of moldboard plow implement, it firstly decreased and in the following increased nonlinearly as plowing depth increased. In case of disk and chisel plow implement, it firstly increased and then decreased nonlinearly as plowing depth increased. For the moldboard plow implement, in the first stage, it seems the inverse effect of plowing depth was more effective than direct effect of plowing depth and therefore, specific draft force decreased. In the second stage, the direct effect of plowing depth was more pronounced than the inverse effect of plowing depth. In case of disk and chisel plow implement, it seems the direct effect of plowing depth was predominant over the inverse effect of plowing depth in the first stage and therefore, specific draft force increased. In the second stage, the inverse effect of plowing depth was greater than the direct effect of plowing depth.

The direct positive effect of forward speed on specific draft force based on N/mm was similarly reported by Al-Suhaibani and Al-Janobi (1997), and Al-Janobi and Al-Suhaibani (1998) for chisel, offset disk harrow, moldboard plow, and disk plow implements.

3.4.7. Tractor drawbar power

Fig. 22 provides surface and contour plots obtained from the MANFIS +MNE simulation workplace for prognostication of tractor drawbar power in plowing process. As it can be seen in the surface plots of the Fig. 22, the drawbar power increased nonlinearly as plowing depth

Table 39
The values of the statistical performance criteria for prognostication of ten performance parameters of the tractor-implement systems in plowing process obtained from MANFIS+MNE simulation workplace.

Performance parameter	Unit	R^2	RMSE	MRDM (%)
Required draft force of the implements	kN	0.985	1.117	2.267
Tractor rear wheel slip	%	0.979	1.716	3.906
Fuel consumption per working hour	L/h	0.971	0.803	3.204
Fuel consumption per tilled area	L/ha	0.990	0.786	3.036
Specific volumetric fuel consumption	L/kW h	0.985	0.062	4.965
Specific draft force	kN/m^2	0.995	1.264	1.931
Tractor drawbar power	kW	0.996	1.031	4.175
Tractor tractive efficiency	%	0.984	1.416	1.479
Energy requirement for tillage implements	MJ/ha	0.996	1.095	2.918
Overall energy efficiency	%	0.985	0.808	4.202

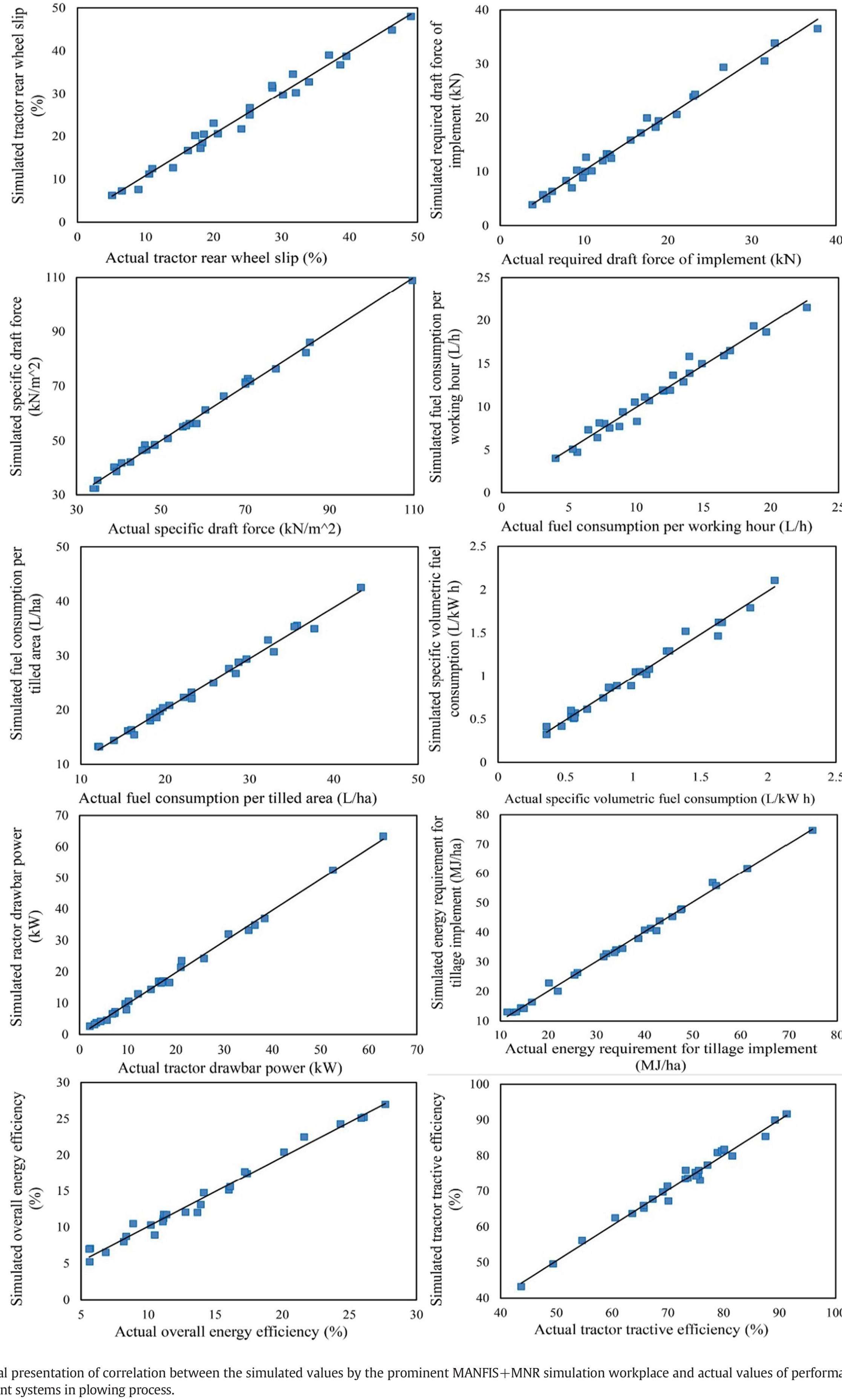

Fig. 12. Graphical presentation of correlation between the simulated values by the prominent MANFIS+MNR simulation workplace and actual values of performance parameters of tractor-implement systems in plowing process.

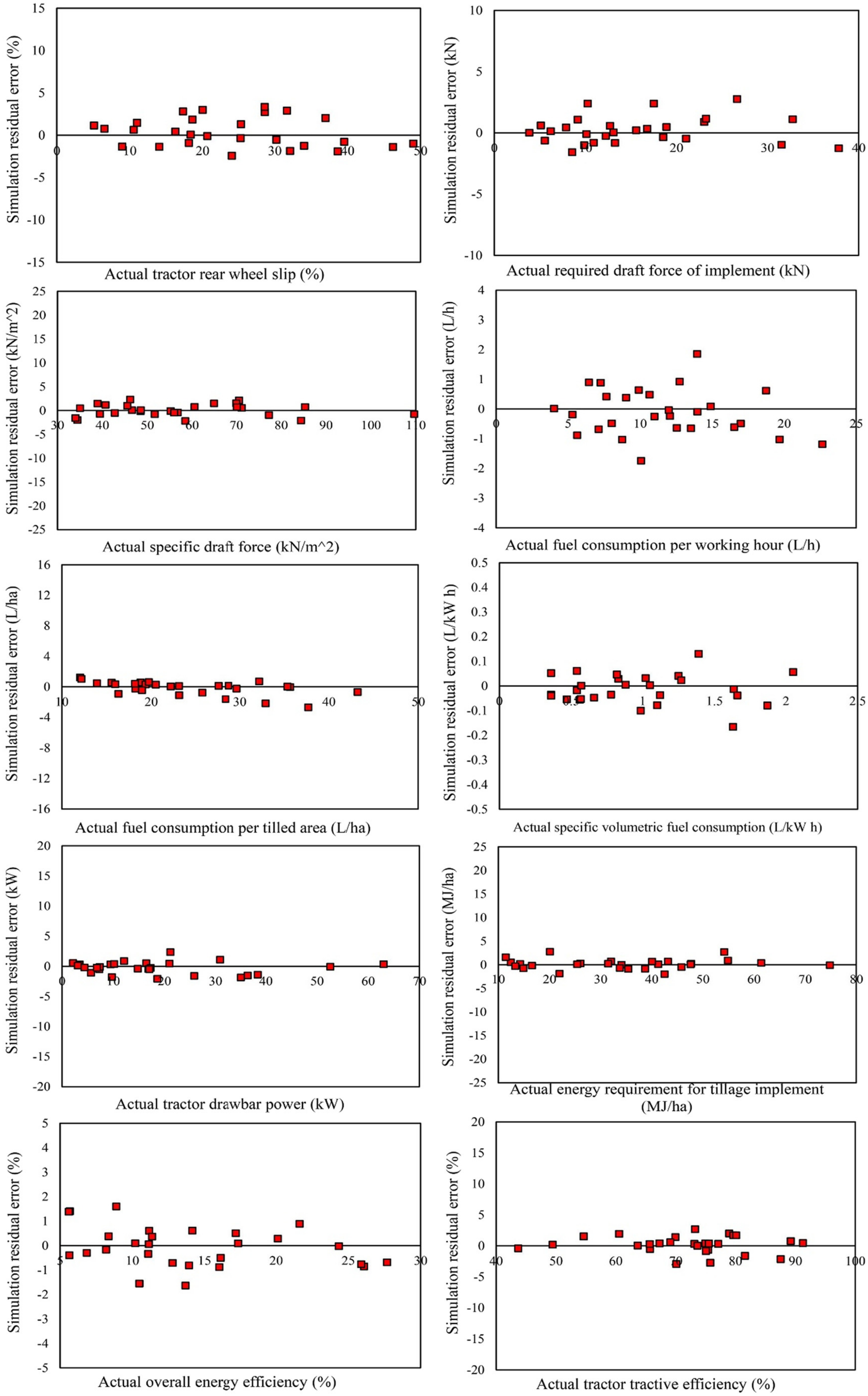

Fig. 13. Simulation residual error plots for the simulated values by the prominent MANFIS+MNR simulation workplace for performance parameters of tractor-implement systems in plowing process.

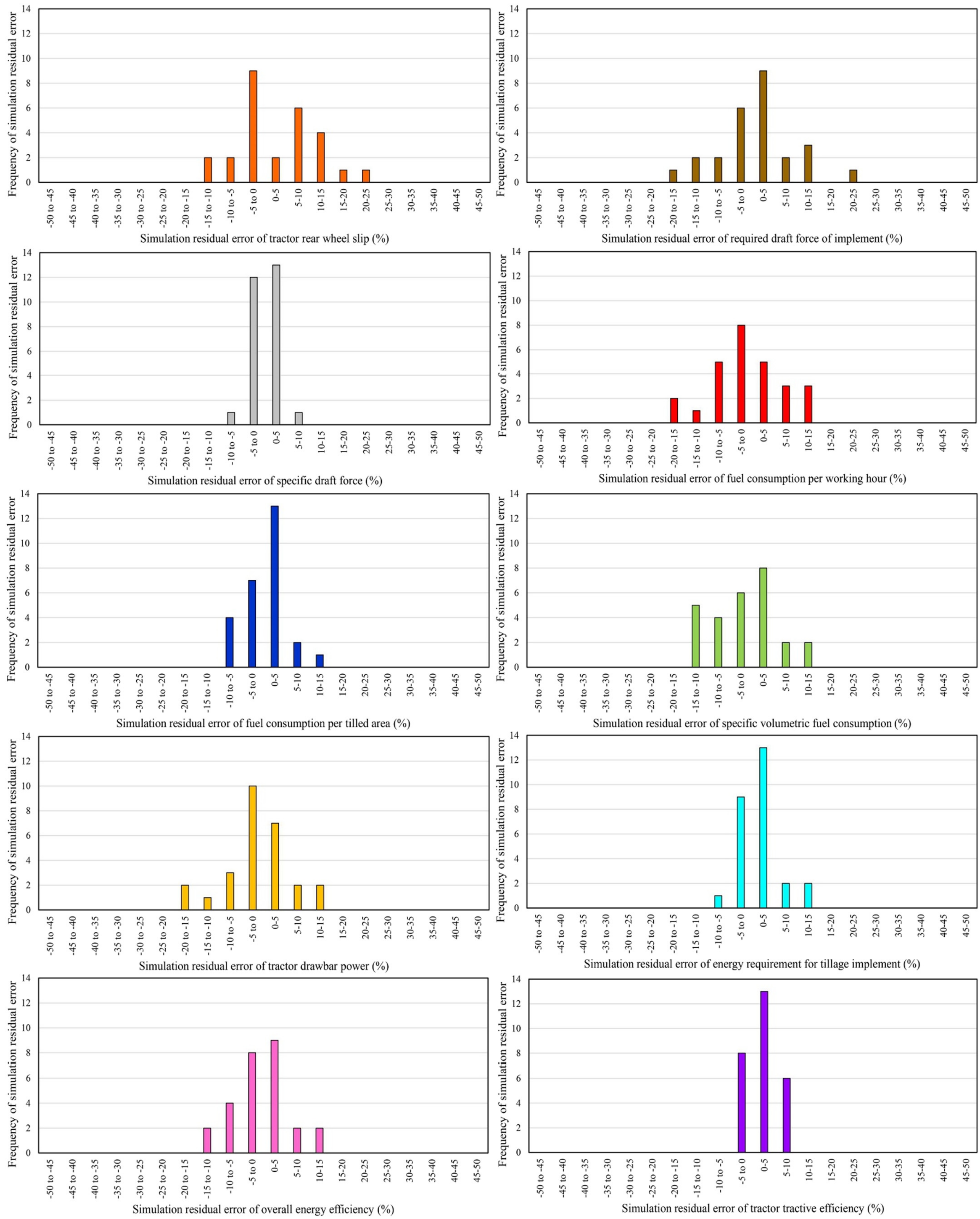

Fig. 14. Frequency plots of simulation residual error for the simulated values by the prominent MANFIS+MNE simulation workplace for performance parameters of tractor-implement systems in plowing process.

A

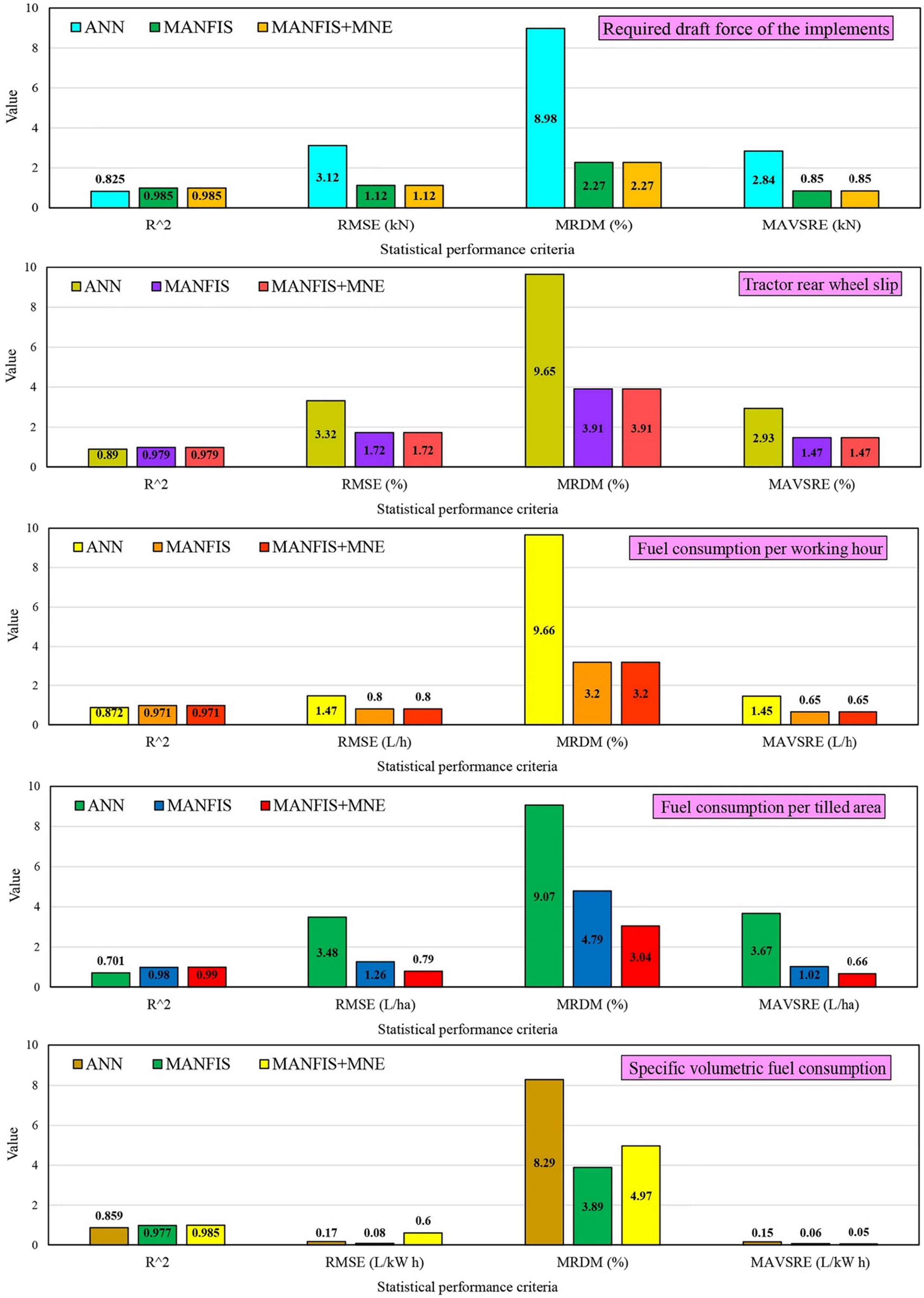
ANN
MANFIS
MANFIS+MNE
Required draft force of the implements
Value
0.825
0.985
0.985
3.12
1.12
1.12
8.98
2.27
2.27
2.84
0.85
0.85
R^2
RMSE (kN)
MRDM (%)
MAVSRE (kN)
Statistical performance criteria
ANN
MANFIS
MANFIS+MNE
Tractor rear wheel slip
Value
0.89
0.979
0.979
3.32
1.72
1.72
9.65
3.91
3.91
2.93
1.47
1.47
R^2
RMSE (%)
MRDM (%)
MAVSRE (%)
Statistical performance criteria
ANN
MANFIS
MANFIS+MNE
Fuel consumption per working hour
Value
0.872
0.971
0.971
1.47
0.8
0.8
9.66
3.2
3.2
1.45
0.65
0.65
R^2
RMSE (L/h)
MRDM (%)
MAVSRE (L/h)
Statistical performance criteria
ANN
MANFIS
MANFIS+MNE
Fuel consumption per tilled area
Value
0.701
0.98
0.99
3.48
1.26
0.79
9.07
4.79
3.04
3.67
1.02
0.66
R^2
RMSE (L/ha)
MRDM (%)
MAVSRE (L/ha)
Statistical performance criteria
ANN
MANFIS
MANFIS+MNE
Specific volumetric fuel consumption
Value
0.859
0.977
0.985
0.17
0.08
0.6
8.29
3.89
4.97
0.15
0.06
0.05
R^2
RMSE (L/kW h)
MRDM (%)
MAVSRE (L/kW h)
Statistical performance criteria

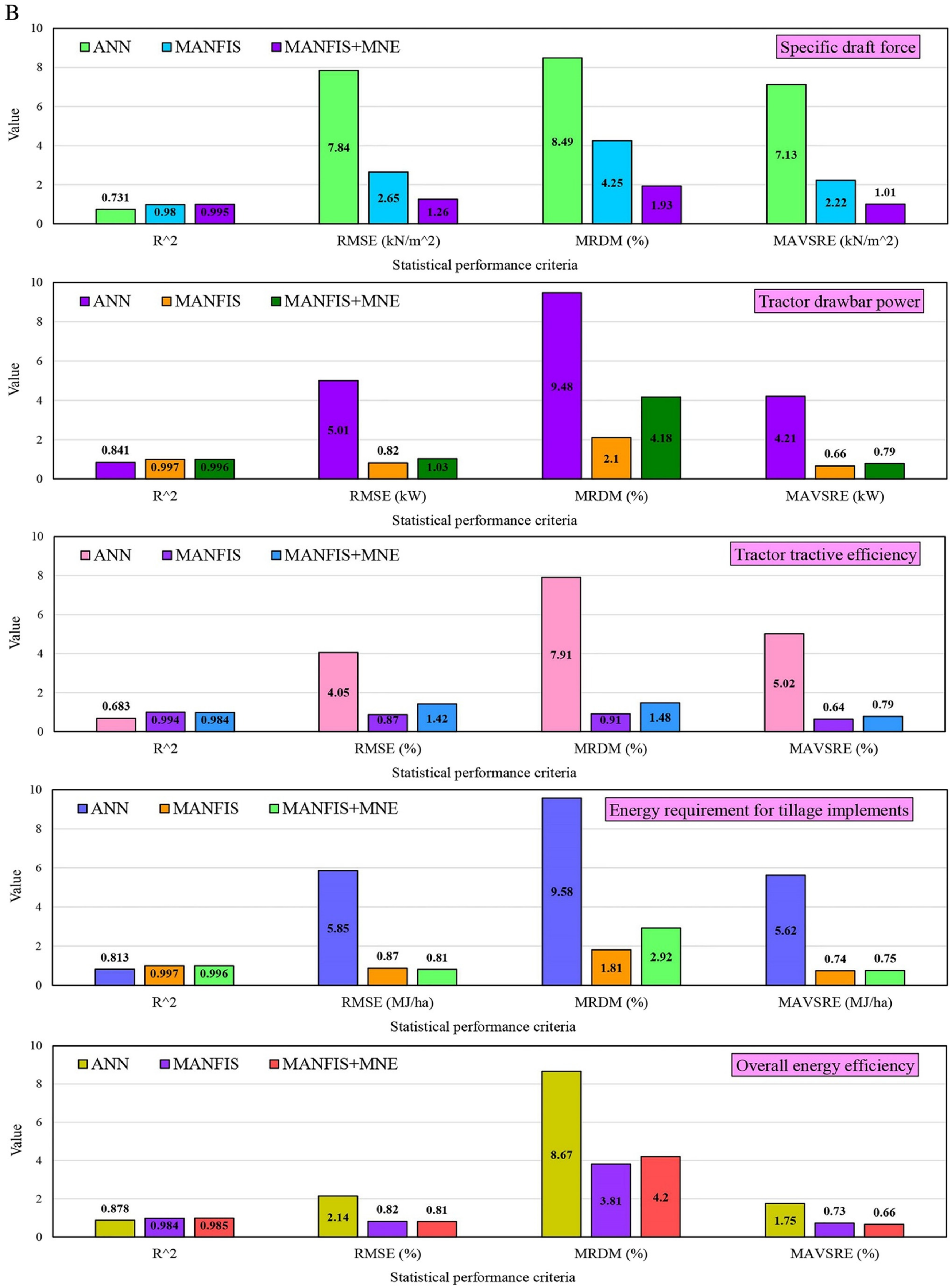

Fig. 15. a–b Comparison between the statistical performance criteria of three simulation scenarios for prognostication of performance parameters of tractor-implement systems in plowing process.

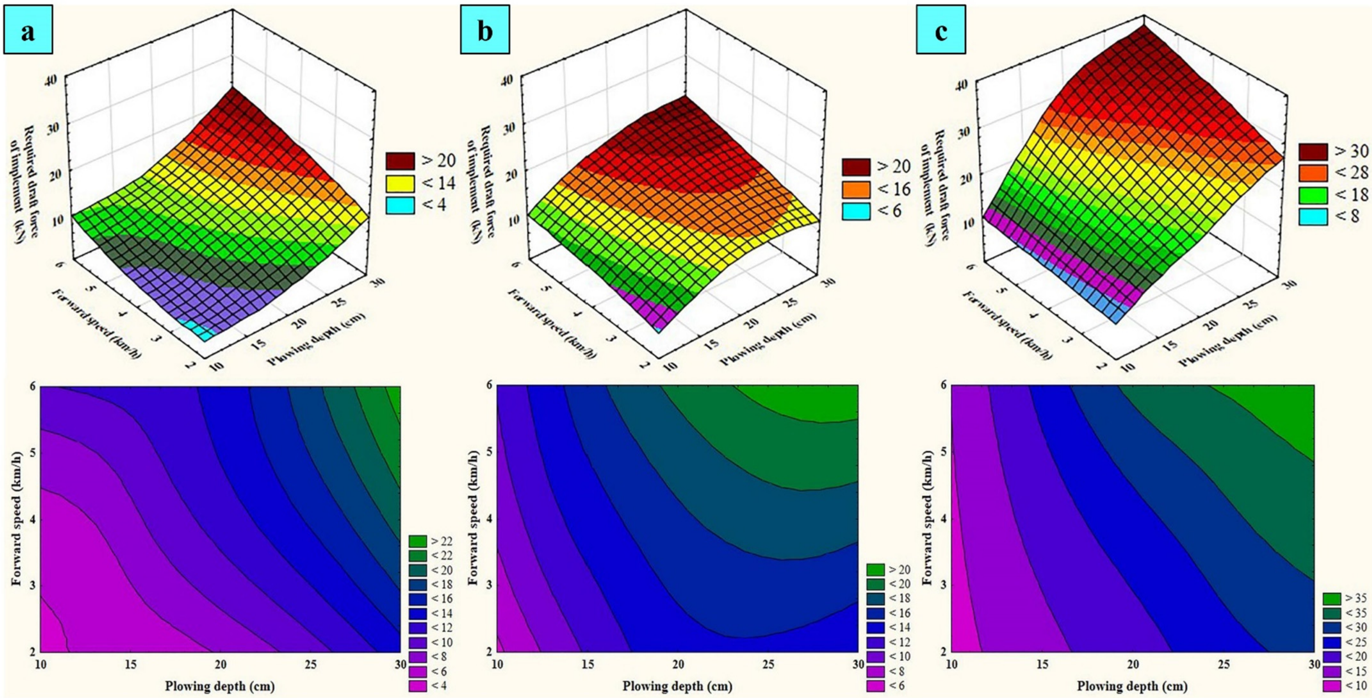

Fig. 16. Surface and contour plots obtained from the MANFIS+MNE simulation workplace for prognostication of required draft force of the implement in plowing process (a: moldboard, b: disk, and c: chisel plow implement).

and forward speed increased. Furthermore, the contour plots of the Fig. 22 clarify that the dual interaction effect of forward speed and plowing depth on the drawbar power was increasingly synergistic. It is plausible in the contour plots of the Fig. 22 that the drawbar power increased from the lowest bound (<5 kW) to the highest bound (>60 kW) as plowing depth along with forward speed increased from 10 to 30 cm and 2 to 6 km/h, respectively.

According to the Eq.(4), the drawbar power is direct function of forward speed and draft force. The draft force is direct function of plowing depth and forward speed. Therefore, it can be inferred that the drawbar

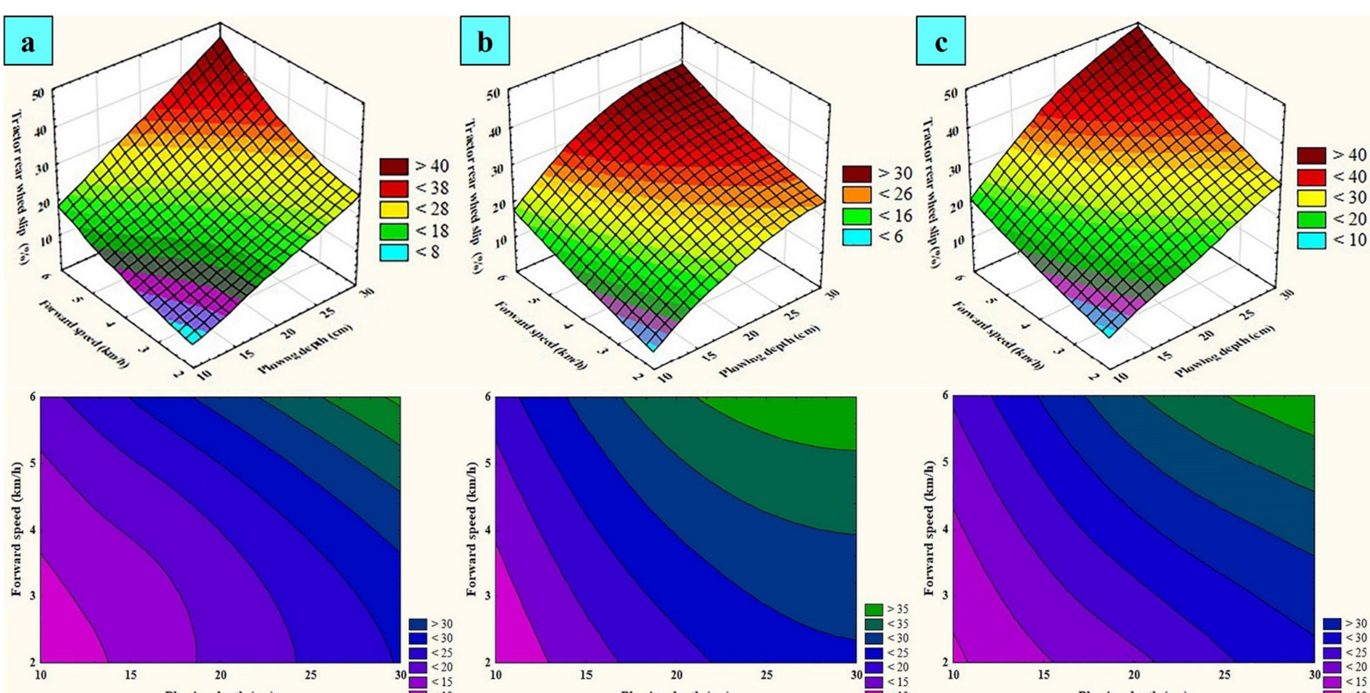

Fig. 17. Surface and contour plots obtained from the MANFIS+MNE simulation workplace for prognostication of tractor rear wheel slip in plowing process (a: moldboard, b: disk, and c: chisel plow implement).

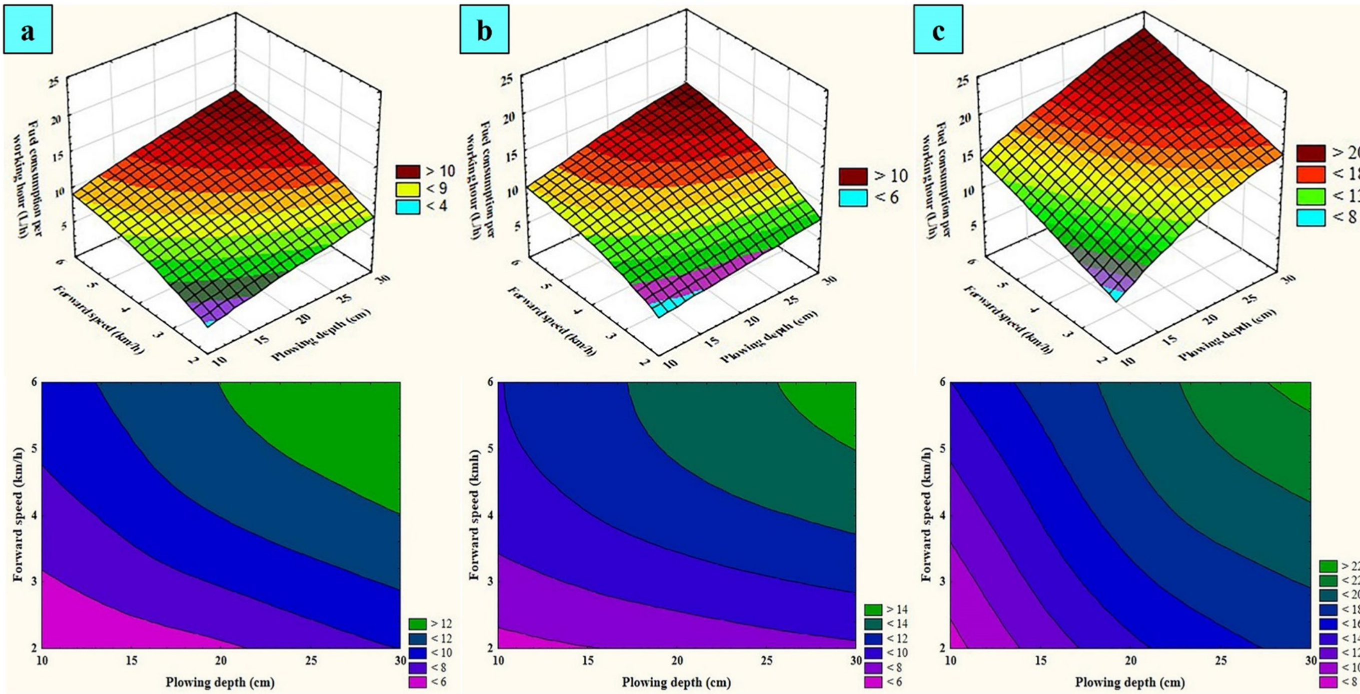

Fig. 18. Surface and contour plots obtained from the MANFIS+MNE simulation workplace for prognostication of fuel consumption per working hour in plowing process (a: moldboard, b: disk, and c: chisel plow implement).

power is direct function of forward speed and plowing depth. Accordingly, the drawbar power increases with increase of forward speed and plowing depth.

The increasing effect of plowing depth on the drawbar power in plowing process was also addressed by KarimiInchebron et al. (2012) which is associate with the result of this research.

3.4.8. Tractor tractive efficiency

Fig. 23 depicts surface and contour plots obtained from the MANFIS +MNE simulation workplace for prognostication of tractor tractive efficiency in plowing process. As it can be seen in the surface plots of the Fig. 23, the tractive efficiency decreased nonlinearly as plowing depth and forward speed increased. Moreover, the contour plots of the

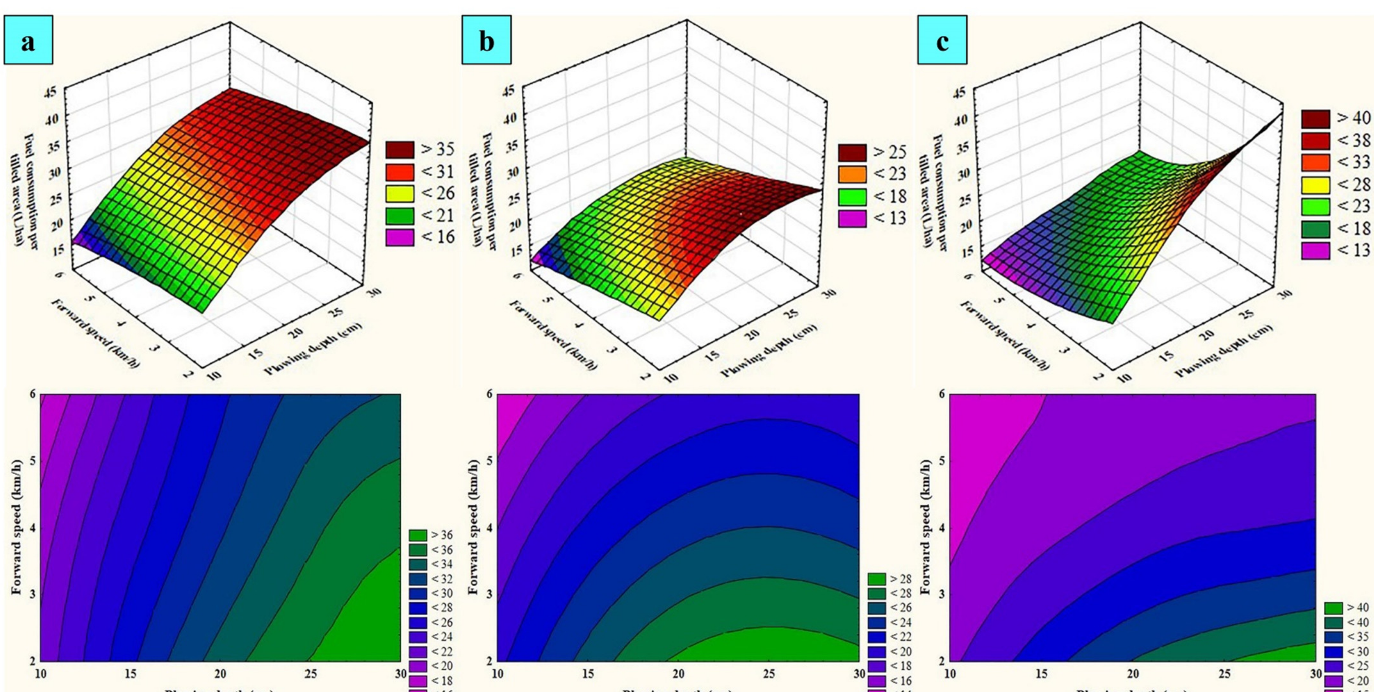

Fig. 19. Surface and contour plots obtained from the MANFIS+MNE simulation workplace for prognostication of fuel consumption per tilled area in plowing process (a: moldboard, b: disk, and c: chisel plow implement).

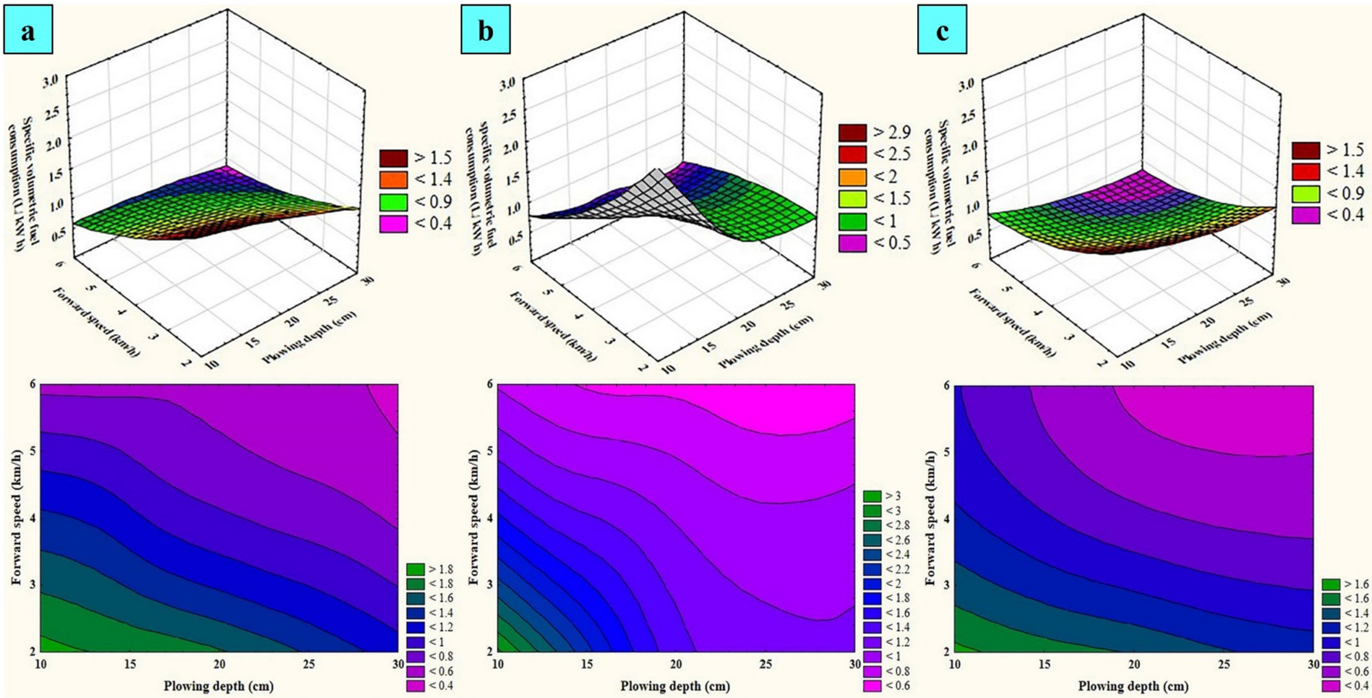

Fig. 20. Surface and contour plots obtained from the MANFIS+MNE simulation workplace for prognostication of specific volumetric fuel consumption in plowing process (a: moldboard, b: disk, and c: chisel plow implement).

Fig. 23 state that the dual interaction effect of forward speed and plowing depth on the tractive efficiency was decreasingly synergistic. It is observable in the contour plots of the Fig. 23 that the tractive efficiency decreased from the highest bound (>90%) to the lowest bound (<50%) as plowing depth along with forward speed increased from 10 to 30 cm and 2 to 6 km/h, respectively.

To interpret the obtained trend, it should be considered that with increase of plowing depth and forward speed, tractor rear wheel slip increases (Section 3.4.2). According to the Eq.(7), the tractive efficiency is negative direct function of the wheel slip. Therefore, as plowing depth or forward speed increases, the wheel slip increases and consequently, the tractive efficiency decreases. Another interpretation is

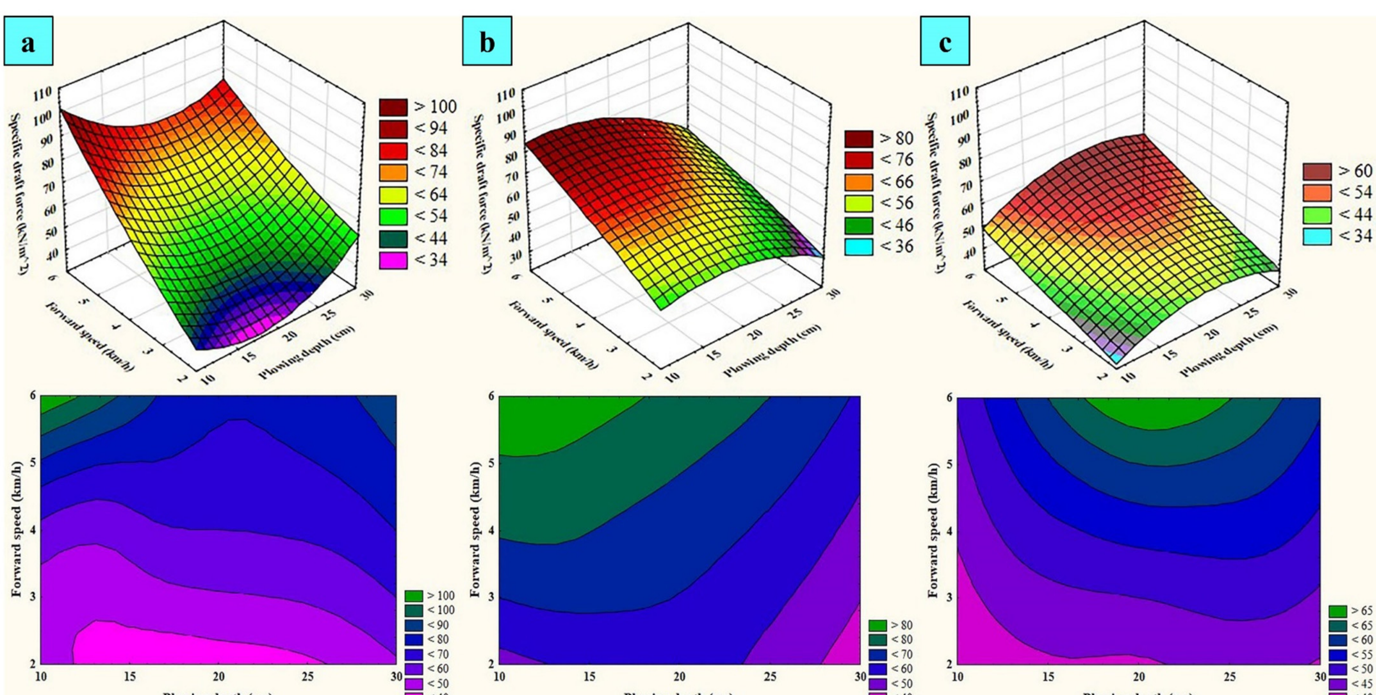

Fig. 21. Surface and contour plots obtained from the MANFIS+MNE simulation workplace for prognostication of specific draft force of the implements in plowing process (a: moldboard, b: disk, and c: chisel plow implement).

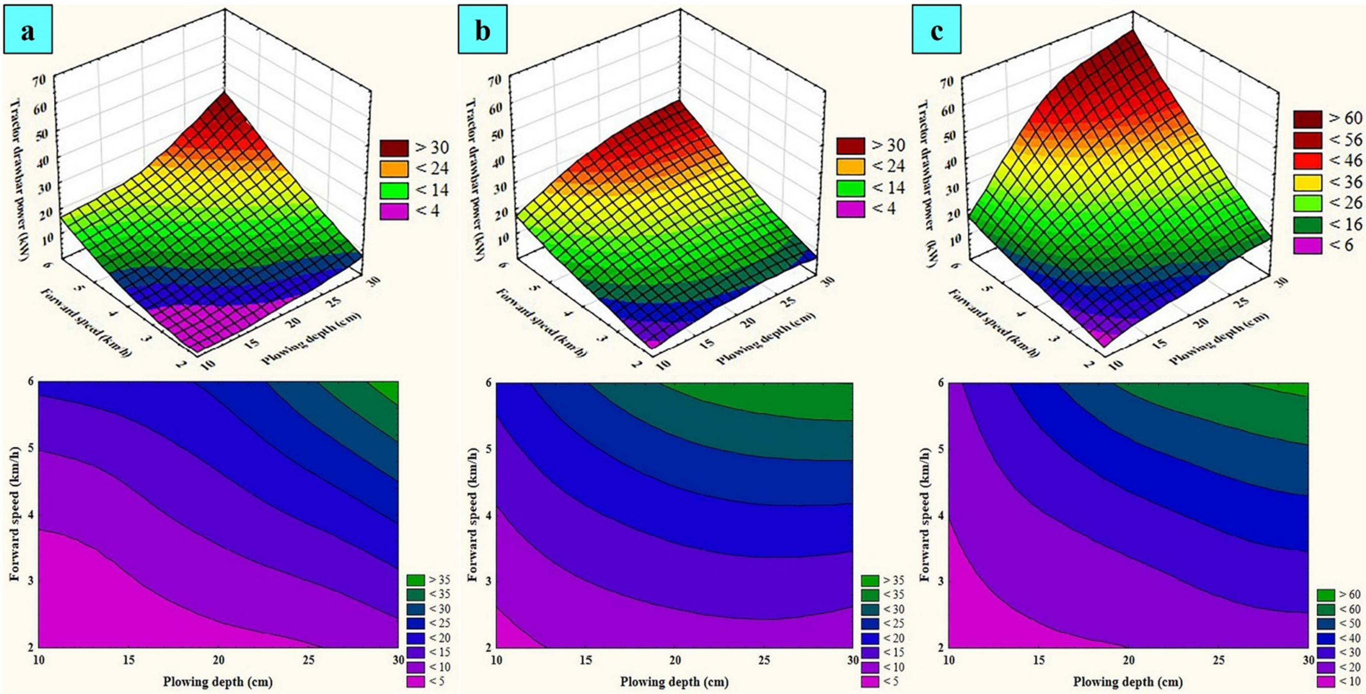

Fig. 22. Surface and contour plots obtained from the MANFIS+MNE simulation workplace for prognostication of tractor drawbar power in plowing process (a: moldboard, b: disk, and c: chisel plow implement).

attributed to gross traction force (draft force plus rolling resistance force). According to the Eq.(7), the tractive efficiency is inverse function of gross traction force. Increment of plowing depth or forward speed leads to draft force increment (Section 3.4.1). Increment of draft force results in the tractive efficiency decrease.

The observed decreasing trend of the tractive efficiency as influenced by increment of plowing depth and forward speed was in general agreement with the results of previous researches conducted by Inchebron et al. (2012) and Ranjbarian et al. (2017).

3.4.9. Energy requirement for tillage implement

Fig. 24 illustrates surface and contour plots obtained from the MANFIS+MNE simulation workplace for prognostication of energy requirement for tillage implements in plowing process. As it can be seen

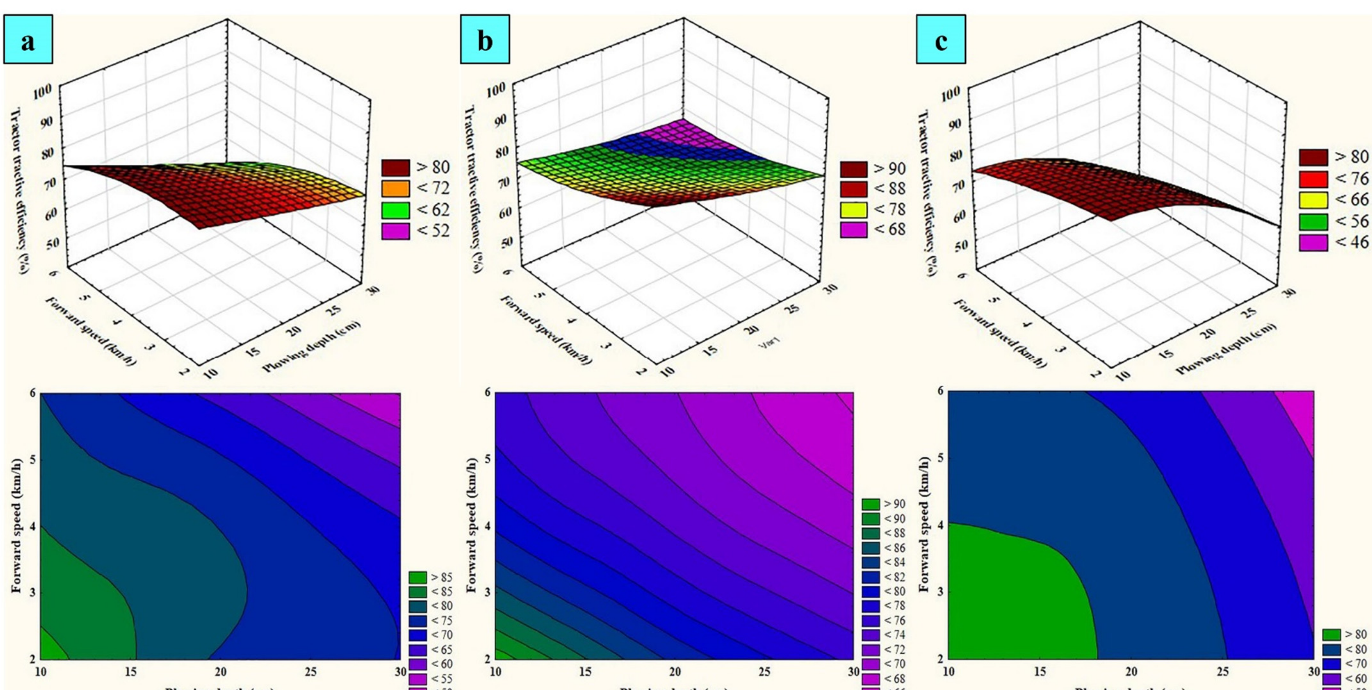

Fig. 23. Surface and contour plots obtained from the MANFIS+MNE simulation workplace for prognostication of tractor tractive efficiency in plowing process (a: moldboard, b: disk, and c: chisel plow implement).

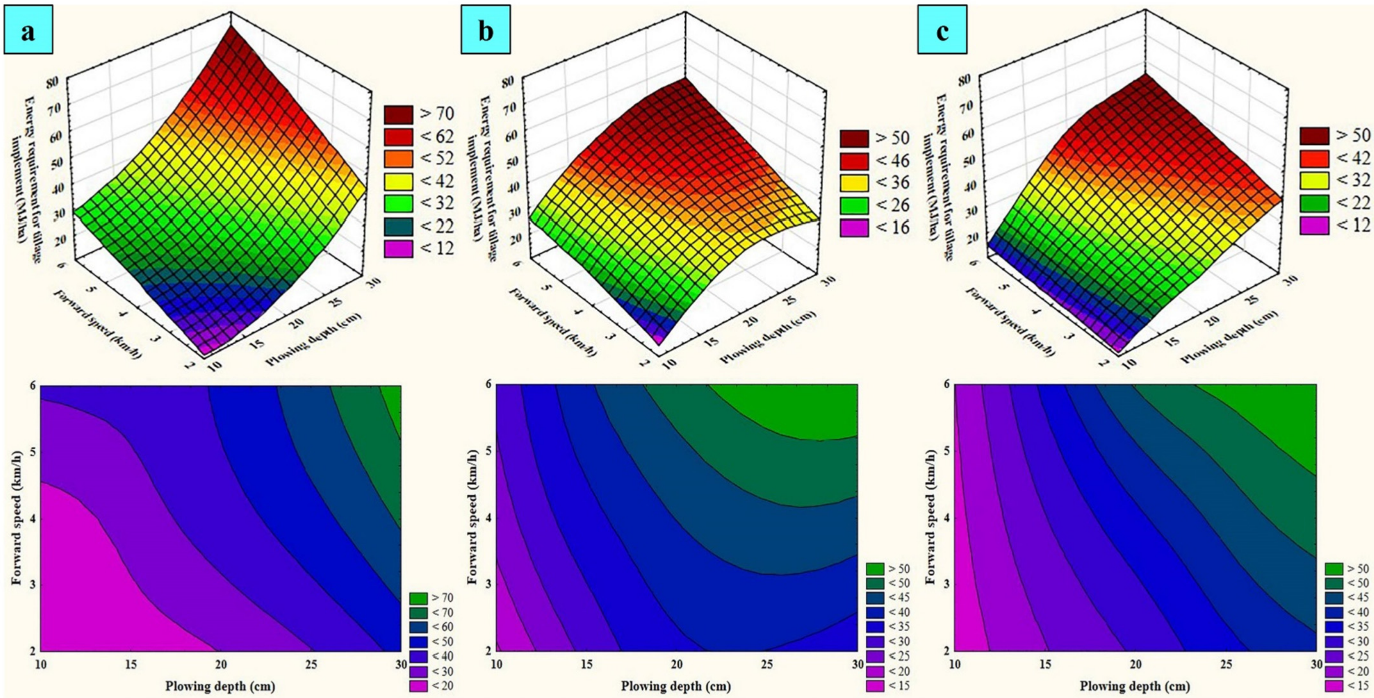

Fig. 24. Surface and contour plots obtained from the MANFIS+MNE simulation workplace for prognostication of energy requirement for the implements in plowing process (a: moldboard, b: disk, and c: chisel plow implement).

in the surface plots of the Fig. 24, the energy requirement increased nonlinearly as plowing depth and forward speed increased. Besides, the contour plots of the Fig. 24 display that the dual interaction effect of forward speed and plowing depth on the energy requirement was increasingly synergistic. It is perceptible in the contour plots of the Fig. 24 that the energy requirement increased from the lowest bound (<15 MJ/ha) to the highest bound (>70 MJ/ha) as plowing depth along with forward speed increased from 10 to 30 cm and 2 to 6 km/h, respectively.

According to the Eqs.(4) and (5), the energy requirement is directly related to the draft force. As it has been discussed in the Section 3.4.1, the draft force increases as increment of plowing depth and forward

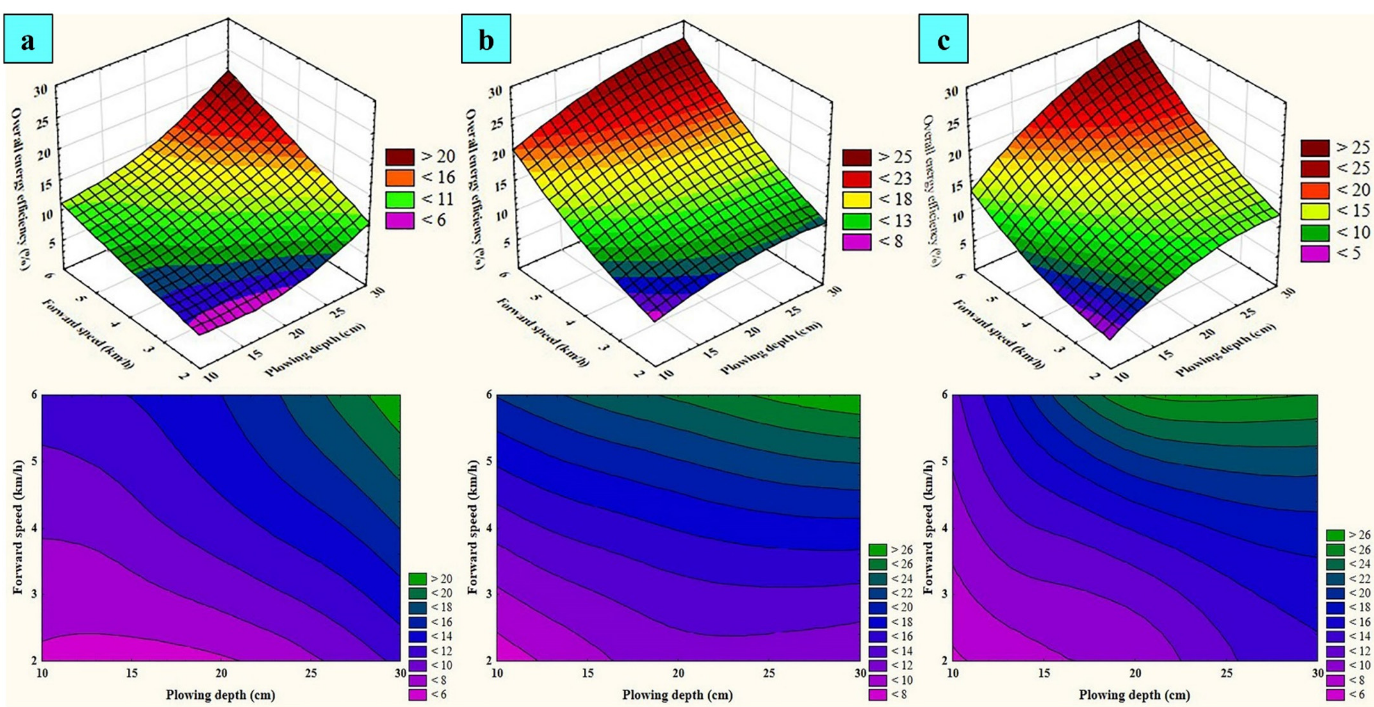

Fig. 25. Surface and contour plots obtained from the MANFIS+MNE simulation workplace for prognostication of overall energy efficiency of tractor-implement systems in plowing process (a: moldboard, b: disk, and c: chisel plow implement).

speed. Thus, the energy requirement rises due to increment of forward speed and plowing depth. The increasing effect of forward speed on the energy requirement was also mentioned in the published paper by Thomas and Singh (2002).

3.4.10. Overall energy efficiency

Fig. 25 shows surface and contour plots obtained from the MANFIS +MNE simulation workplace for prognostication of overall energy efficiency of the tractor-implement systems in plowing process. As it can be seen in the surface plots of the Fig. 25, the efficiency increased nonlinearly as plowing depth and forward speed increased. Moreover, the contour plots of the Fig. 25 indicate that the dual interaction effect of forward speed and plowing depth on the efficiency was increasingly synergistic. It is visible in the contour plots of the Fig. 25 that the efficiency increased from the lowest bound (<6%) to the highest bound (>26%) as plowing depth along with forward speed increased from 10 to 30 cm and 2 to 6 km/h, respectively.

According to the Eq.(6), overall energy efficiency is direct function of tractor drawbar power. The drawbar power is function of forward speed and the draft force (Eq.(4)). The draft force is direct function of plowing depth and forward speed (Section 3.4.1). Therefore, it can be stated that the efficiency is direct function of plowing depth and forward speed. Hence, it is anticipated that the efficiency increases with increment of plowing depth and forward speed.

Jr (1985) has pointed out that the range of 10–20% for overall energy efficiency should be considered as normal range. The efficiency <10% is known as poor tractive efficiency and/or load matching. It is also considered as good tractive efficiency and/or load match for the efficiency above 20%. In this research, the efficiency ranged from 5.61 to 27.69% for three tillage implements (Table 17). The efficiency <10% was related to treatment of plowing depth = 10 cm and forward speed = 2 km/h. With increment of plowing depth and forward speed, the efficiency ranged from 10 to 20% and finally, it reached above 20%. Therefore, it can be stated that in this research, proper tractive efficiency of the tractor and good load match between implement and the tractor were achieved at the upper levels of the plowing depth and forward speed.

The previous study results of Kheiralla et al. (2004) are similar to the range and trend of overall energy efficiency of tractor-implement systems in this research.

4. Summary and conclusion

This research focused on development of soft computing simulation workplaces for performance prognostication of tractor-implement systems in plowing process. Three simulation scenarios (ANN, MANFIS, and MANFIS+MNE) were executed in the workplace. The operational variables of plowing depth (10, 20 and 30 cm), forward speed (2, 4 and 6 km/h), and tillage implement type (moldboard, disk, and chisel plow) were taken as the workplace inputs and ten performance parameters (required draft force of implement, tractor rear wheel slip, fuel consumption per working hour, specific draft force, fuel consumption per tilled area, specific volumetric fuel consumption, tractor drawbar power, tractor tractive efficiency, energy requirement for tillage implement, and overall energy efficiency) were considered as the workplace outputs. According to aggregation of the results obtained in this research, it can be asserted that this research satisfied both quantity and quality aspects concerned in this realm, and the following conclusions were drawn from the results:

1- In case of chisel plow implement with higher working width than that of other implements, draft force, fuel energy, and drawbar power required to pull the implement within soil were higher than those of other implements.
2- Comparison of prognostication accuracy of two soft computing scenarios of the MANFIS and the ANN simulation workplace indicated higher performance of the MANFIS against the ANN, based on the obtained statistical performance criteria. Therefore, the hypotheses of higher performance of neuro-fuzzy strategy than neural strategy in prognostication of desired output targets based on the compound effect of nominal and numeral input variables was approved.
3- According to obtained prognostication accuracy based on statistical performance criteria, simulation time, and user-friendly configuration of two neuro-fuzzy strategies based on the MANFIS and MANFIS+MNE, the MANFIS+MNE simulation workplace was recognized as prominent simulation scenario. Therefore, the claim of applicability of new simulation scenario of the MANFIS+MNE as a simple neuro-fuzzy calculator was asserted. Accordingly, it can be mentioned that difficulties of utilization of puzzling tables and graphical charts for calculation of performance parameters are eliminated by means of neuro-fuzzy calculator.
4- In accordance with previous conclusions 2 and 3, the prominent simulation scenario among three simulation scenarios (ANN, MANFIS, and MANFIS+MNE), executed in the workplace, was the MANFIS +MNE simulation scenario.
5- The MANFIS+MNE simulation results revealed that simultaneous increase of forward speed and plowing depth led to nonlinear increment of required draft force of implement, tractor rear wheel slip, fuel consumption per working hour, tractor drawbar power, energy requirement for tillage implement, and overall energy efficiency for each tillage implement. Moreover, it demonstrated that simultaneous increase of forward speed and plowing depth led to nonlinear decrement of specific volumetric fuel consumption and tractor tractive efficiency.
6- The exhaustive physical perception obtained from the MANFIS +MNE simulation results presented that the dual interaction effect of forward speed and plowing depth on some performance parameters (required draft force of implement, tractor rear wheel slip, fuel consumption per working hour, specific volumetric fuel consumption, tractor drawbar power, energy requirement for tillage implement, overall energy efficiency, and tractor tractive efficiency) was nonlinearly synergetic. However, it was nonlinearly antagonism for specific draft force and fuel consumption per tilled area. Based on these interpretations, it can be advocated that the physical perception obtained from the MANFIS+MNE simulation results enrich state of the art in the domain of comprehending behavior of the performance of tractor-implement systems in plowing process.

These remarkable conclusions are in response to the fundamental questions presented in the Section 1.4. Hence, it is desired to apply the MANFIS+MNE simulation workplace and related physical perceptions by technical farmer associations involved in the decision-making of agricultural machinery management in plowing process.

5. Recommendations for future research requirements

- Deficiency of soil moisture content and tractor driving mode (2WD and 4WD) as input variables and tractor front wheel slip as output variable of robust soft computing simulation workplace found on the MANFIS+MNE scenario indicates requirement for further researches to extend capability of the workplace. Hence, the associated researchers in this realm are strongly encouraged to follow this extension in their future research works.
- Parametric analysis to ascertain the interaction effect of independent variables (forward speed, plowing depth, and implement type) on dependent variables (required draft force of implement, tractor rear wheel slip, fuel consumption per working hour, specific draft force, fuel consumption per tilled area, specific volumetric fuel consumption, tractor drawbar power, tractor tractive efficiency, energy requirement for tillage implement, and overall energy efficiency) was not considered in the framework of the present research. Hence, it should be investigated in more detail utilizing the MANOVA technique.

- Prior to recommendation of this MANFIS+MNE simulation scenario for practical applications, its employment is recommended as a resource for forthcoming commercial attempts to release an exhaustive user friendly graphical software package for prognostication of the performance parameters of tractor-implement systems in plowing process. The software package could be applied, as a new computational tool (neuro-fuzzy calculator), by the associated researchers, engineers, managements and students in order to familiarize fundamental concepts of variation trends of the performance parameters as influenced by field operational variables.

References

Aboukarima, A.E.W.M., 2007. Draft models of chisel plow based on simulation using artificial neural networks. Misr J. Ag. Eng. 24 (1), 42–61.
Aboukarima, A.E.W.M., Saad, A.F., 2006. Assessment of different indices depicting soil texture for predicting chisel plow draft using neural networks. ASEJ 27 (2), 170–180.
Adewoyin, A.O., 2013. Fuel consumption evaluation of some commonly used farm tractors for ploughing operations on the sandy-loam soil of Oyo state, Nigeria. Res. J. Appl. Sci. Eng. Technol. 6 (15), 2865–2871.
Adewoyin, A.O., Ajav, E.A., 2013. Fuel consumption of some tractor models for ploughing operations in the sandy-loam soil of Nigeria at various speeds and ploughing depths. Agric. Eng. Int. CIGR J. 15 (3), 67–74.
Ahmadi, I., 2016a. Development and evaluation of a draft force calculator for moldboard plow using the laws of classical mechanics. Soil Tillage Res. 161 (1), 129–134.
Ahmadi, I., 2016b. Development and assessment of a draft force calculator for disk plow using the laws of classical mechanics. Soil Tillage Res. 163 (1), 32–40.
Ahmadi, I., 2016c. Effect of soil, machine, and working state parameters on the required draft force of a subsoiler using a theoretical draft-calculating model. Soil Res. 55 (4), 389–400.
Ahmadi, I., 2017a. A torque calculator for rotary tiller using the laws of classical mechanics. Soil Tillage Res. 165 (1), 137–143.
Ahmadi, I., 2017b. A power estimator for an integrated active-passive tillage machine using the laws of classical mechanics. Soil Tillage Res. 171 (1), 1–8.
Ahmadi, I., 2018. A draught force estimator for disc harrow using the laws of classical soil mechanics. Biosyst. Eng. 171 (1), 52–62.
Al-Hamed, S.A., Grisso, R.D., Zoz, F.M., Bargen, K.V., 1994. Tractor performance spreadsheet for radial tires. Comput. Electron. Agric. 10 (1), 45–62.
Ajav, E.A., Adewoyin, A.O., 2012. Effect of ploughing depth and speed on tractor fuel consumption in a sandy-loam soil of Oyo State-Nigeria. J. Agric. Eng. Technol. 20 (2), 1–10.
Akbarnia, A., Mohammadi, A., Farhani, F., Alimardani, R., 2014. Simulation of draft force of winged share tillage tool using artificial neural network model. Agric. Eng. Int. CIGR J. 16 (4), 57–65.
Alele, J.O., Ngunjiri, G.M.N., Njue, M.R., 2018. Effects of depth and speed on power requirements for disc and mouldboard ploughs in silt loam soils. Int. J. Sci. Technol. Res. 7 (8), 167–174.
Al-Hamed, S.A., Al-Janobi, A.A., 2001. A program for predicting tractor performance in visual C++. Comput. Electron. Agric. 31 (2), 137–149.
Al-Hamed, S.A., Al-Suhaibani, S.A., Mohammad, F.S., Wahby, M.F.I., 2010. Development of a comprehensive computer program for predicting farm energy. Am. J. Agric. Biol. Sci. 5 (1), 89–101.
Al-Hamed, S.A., Wahby, M.F., Al-Saqer, S.M., Aboukarima, A.M., Sayedahmed, A.A., 2013. Artificial neural network model for predicting draft and energy requirements of disk plow. J. Anim. Plant Sci. 23 (6), 1714–1724.
Alimardani, R., Colvin, T.S., Marley, S.J., 1989. Verification of the "TERMS" traction prediction model. Trans. ASAE 32 (3), 817–821.
Alimardani, R., Abbaspour-Gilandeh, Y., Khalilian, A., Keyhani, A., Sadati, S.H., 2009. Prediction of draft force and energy of subsoiling operation using ANN model. J. Food Agric. Environ. 7 (3&4), 537–542.
Al-Janobi, A.A., Al-Suhaibani, S.A., 1998. Draft of primary tillage implements in sandy loam soil. Appl. Eng. Agric. 14 (4), 343–348.
Al-Janobi, A.A., Aboukarima, A.M., Ahmed, K.A., 2001. Prediction of specific draft of different tillage implements using neural networks. Misr J. Ag. Eng. 18 (3), 699–714.
Al-Janobi, A., Al-Hamed, S., Aboukarima, A.M., 2010. An excel spreadsheet to estimate performance parameters for chisel plow-tractor combination based on trained an artificial neural network. Bull. USAMV Agric. 67 (2), 1–9.
Almaliki, S., 2018. Simulation of draft force for three types of plow using response surface method under various field conditions. Iraqi J. Agri. Sci. 49 (6), 1123–1131.
Almaliki, S., Alimardani, R., Omid, M., 2016a. Fuel consumption models of MF285 tractor under various field conditions. Agric. Eng. Int. CIGR J. 18 (3), 147–158.
Almaliki, S., Alimardani, R., Omid, M., 2016b. Artificial neural network based modeling of tractor performance at different field conditions. Agric. Eng. Int. CIGR J. 18 (4), 262–274.
Al-Suhaibani, S.A., Al-Janobi, A.A., 1997. Draught requirements of tillage implements operating on sandy loam soil. J. Agric. Eng. Res. 66 (3), 177–182.
Al-Suhaibani, S.A., Ghaly, A.E., 2013. Comparative study of the kinetic parameters of three chisel plows operating at different depths and forward speed in a sandy soil. Int. J. Eng. Sci. 2 (7), 42–59.
Al-Suhaibani, S.A., Al-Janobi, A.A., Al-Majhadi, Y.N., 2010. Development and evaluation of tractors and tillage implements instrumentation system. Am. J. Eng. Appl. Sci. 3 (2), 363–371.
Al-Suhaibani, S.A., Wahby, M.F., Aboukarima, A.M., Tabash, I.S., 2015. Study on the effect of soil moisture content and plowing speed on draft requirements of a moldboard plow. J. Adv. Agric. 4 (3), 477–486.
Arvidsson, J., Keller, T., Gustafsson, K., 2004. Specific draught for mouldboard plough, chisel plough and disc harrow at different water contents. Soil Tillage Res. 79 (2), 221–231.
ASAE, 2003. ANSI/ASAE S296.5. General Terminology for Traction of Agricultural Traction and Transport Devices and Vehicles. ASAE, St. Joseph, MI, USA.
ASAE, 2011. ASAE D497.7. Agricultural Machinery Management Data. ASAE, St. Joseph, MI, USA.
Askari, M., Khalifahamzehghasem, S., 2013. Draft force inputs for primary and secondary tillage implements in a clay loam soil. World Appl. Sci. J. 21 (12), 1789–1794.
Askari, M., Shahgholi, G., Abbaspour-Gilandeh, Y., Tash-Shamsabadi, H., 2016. The effect of new wings on subsoiler performance. Appl. Eng. Agric. 32 (3), 353–362.
Askari, M., Shahgholi, G., Abbaspour-Gilandeh, Y., 2017. The effect of tine, wing, operating depth and speed on the draft requirement of subsoil tillage tines. Res. Agric. Eng. 63 (4), 160–167.
Bashford, L.L., Byerly, D.V., Grisso, R.D., 1991. Draft and energy requirements of agricultural implements in semi-arid regions of Morocco. Agric. Mech. Asia Afr. Lat. Am. 22 (3), 79–82.
Battiato, A., Diserens, E., 2017. Tractor traction performance simulation on differently textured soils and validation: a basic study to make traction and energy requirements accessible to the practice. Soil Tillage Res. 166 (1), 18–32.
Catalan, H., Linares, P., Mendez, V., 2008. Tractor PT: a traction prediction software for agricultural tractors. Comput. Electron. Agric. 60 (2), 289–295.
Celik, A., Boydas, M.G., Turgut, N., 2007. Comparison of the energy requirements of an experimental plow, a moldboard plow and a disk plow. Philipp. Agric. Sci. 9 (2), 173–178.
Chaplin, J., Jenane, C., Lueders, M., 1988. Drawbar energy use for tillage operations on loamy sand. Trans. ASAE 31 (6), 1692–1694.
Choi, Y.S., Lee, K.S., Park, W.Y., 2000. Application of a neural network to dynamic draft model. Agric. Biosyst. Eng. 1 (2), 67–72.
Coffman, B.A., Kocher, M.F., Adamchuk, V.I., Hoy, R.M., Blankenship, E.E., 2010. Testing fuel efficiency of a tractor with a continuously variable transmission. Appl. Eng. Agric. 26 (1), 31–36.
Colvin, T.S., McConnell, K.L., Catus, B.J., 1989. "TERMS": a computer model for field simulation. Trans. ASAE 32 (2), 391–396.
Cullum, R.F., Graham, W.D., Gaultney, L.D., 1989. Tillage energy requirements in interior Alaska. Soil Tillage Res. 13 (3), 317–327.
Dahab, M.H., Kheiry, A.N.O., Talha, T.H.A., 2016. A computer model of fuel consumption estimation for different agricultural farm operations. Int. J. Env. Agr. Res. 2 (3), 77–85.
Fakhraei, O., Karparvarfard, S.H., 2008. Development of a general equation for estimation of tractive efficiency by dimensional analysis. J. Agric. Machin. Sci. 4 (1), 19–26.
Far, S.A., Kazemi, N., Rahnama, M., Nejad, M.G., 2015a. Effect of ballasting and changing of angles disk offset on performance of tractors. Euro J. Acad. Ess. 2 (5), 5–9.
Far, S.A., Kazemi, N., Rahnama, M., Nejad, M.G., 2015b. Simultaneous comparison of the effects of shaft load and shaft positions on tractor OEE in two soil conditions (cultivated and uncultivated). Int. J. Farm Alli. Sci. 4 (3), 215–221.
Fathollahzadeh, H., Mobli, H., Tabatabaie, S.M.H., 2009. Effect of ploughing depth on average and instantaneous tractor fuel consumption with three-share disc plough. Int. Agrophys. 23 (4), 399–402.
Fathollahzadeh, H., Mobli, H., Rajabipour, A., Minaee, S., Jafari, A., Tabatabaie, S.M.H., 2010. Average and instantaneous fuel consumption of Iranian conventional tractor with moldboard plow in tillage. ARPN J. Eng. Appl. Sci. 5 (2), 30–35.
Gee-Clough, D., McAllister, M., Pearson, G., Evernden, D.W., 1978. The empirical prediction of tractor-implement field performance. J. Terrramech. 15 (2), 81–94.
Glancey, J.L., Upadhyaya, S.K., 1995. An improved technique for agricultural implement draught analysis. Soil Tillage Res. 35 (4), 175–182.
Glancey, J.L., Upadhyaya, S.K., Chancellor, W.J., Rumsey, J.W., 1996. Prediction of agricultural implement draft using an instrumented analog tillage tool. Soil Tillage Res. 37 (1), 47–65.
Godwin, R.J., O'Dogherty, M.J., Saunders, C., Balafoutis, A.T., 2007. A force prediction model for mouldboard ploughs incorporating the effects of soil characteristic properties, plough geometric factors and ploughing speed. Biosyst. Eng. 97 (1), 117–129.
Grisso, R.D., Yasin, M., Kocher, M.F., 1996. Tillage implement forces operating in silty clay loam. Trans. ASAE 39 (6), 977–1982.
Grisso, R.D., Kocher, M.F., Vaughan, D.H., 2004. Predicting tractor fuel consumption. Appl. Eng. Agric. 20 (5), 553–561.
Grisso, R.D., Perumpral, J.V., Zoz, F.M., 2007. Spreadsheet for matching tractors and drawn implements. Appl. Eng. Agric. 23 (3), 259–265.
Grisso, R.D., Vaughan, D.H., Roberson, G.T., 2008. Fuel prediction for specific tractor models. Appl. Eng. Agric. 24 (4), 423–428.
Gulsoylu, E., Cakir, E., Aykas, E., Yalcin, H., Cakmak, B., Cay, A., 2012. Determination of the field performances of different types of chisel legs. Bulgarian J. Agr. Sci. 18 (5), 794–800.
Hansson, P.A., Lindgren, M., Nordin, M., Pettersson, O., 2003. A methodology for measuring the effects of transient loads on the fuel efficiency of agricultural tractors. Appl. Eng. Agric. 19 (3), 251–257.
Harrigan, T.M., Rotz, C.A., 1995. Draft relationships for tillage and seeding equipment. Appl. Eng. Agric. 11 (6), 773–783.
Harrison, H.P., Reed, W.B., 1962. An analysis of draft, depth and speed of tillage equipment. Can. Agric. Eng. 4 (1), 20–23.
Hemmat, A., Khashoei, A.A., 1995. Fuel requirements and machine capacity for tillage and planting operations on a clay loam soil in Isfahan. Iran Agric. Res. 14 (2), 175–201.
Hughes, K.A., Baker, C.J., 1977. Tractor fuel requirements of two tillage systems and zero-tillage. N. Z. J. Exp. Agric. 5 (4), 370–388.

Inchebron, K., Seyedi, S.R.M., Tabatabaekoloor, R., 2012. Performance evaluation of a light tractor during plowing at different levels of depth and soil moisture content. Int. Res. J. Basic Appl. Sci. 3 (3), 626–631.

Ishola, T.A., Ogunlela, A.O., Abubakar, M.S., 2010. An object-oriented program for matching tractors and implements. Int. J. Eng. Tech. 10 (2), 1–4.

Ismail, W.I.W., Burkhardt, T.H., 1993. Draft and fuel requirements measurement using tractor on board data acquisition system. Pertanika J. Sci. Technol. 1 (1), 51–64.

Jr, C.G.B., 1985. Southeastern tillage energy data and recommended reporting. Trans. ASAE 28 (3), 731–737.

Jr, C.G.B., 1989. Tillage draft and energy measurements for twelve southeastern soil series. Trans. ASAE 32 (5), 1492–1502.

Jr, J.A.M., Fornstrom, K.J., Borrelli, J., 1985. Energy requirements of two tillage systems for irrigated sugarbeets, dry beans and corn. Trans. ASAE 28 (6), 1731–1735.

Juostas, A., Janulevicius, A., 2008. Investigation of tractor engine power and economical working conditions utilization during transport operation. Transport 23 (1), 37–43.

KarimiInchebron, A., Seyedi, S.R.M., Koloor, R.T., 2012. Investigating the effect of soil moisture content and depth on the draught, specific draught and drawbar power of a light tractor. Int. Res. J. Basic Appl. Sci. 3 (11), 2289–2293.

Karparvarfard, S.H., Rahmanian-Koushkaki, H., 2015. Development of a fuel consumption equation: test case for a tractor chisel-ploughing in a clay loam soil. Biosyst. Eng. 130 (1), 23–33.

Kepner, R.A., Bainer, R., Barger, E.L., 2005. Principles of Farm Machinery. 3rd edition. Published by CBS Publishers and Distributors Pvt. Ltd., New Delhi.

Khadr, K.A.A., 2008. Effect of some primary tillage implement on soil pulverization and specific energy. Misr J. Ag. Eng. 25 (3), 731–745.

Kheiralla, A.F., Yahya, A., Zohadie, M., Ishak, M., 2004. Modelling of power and energy requirements for tillage implements operating in Serdang sandy clay loam, Malaysia. Soil Tillage Res. 78 (1), 21–34.

Khoshnevisan, B., Rafiee, S., Omid, M., Mousazadeh, H., 2014. Development of an intelligent system based on ANFIS for predicting wheat grain yield on the basis of energy inputs. Info. Proc. Agri. 1 (1), 14–22.

Khoshnevisan, B., Rafiee, S., Igbal, J., Shamshirband, S., Omid, M., Anuar, N.B., Wahab, A.W.A., 2015. A comparative study between artificial neural networks and adaptive neuro-fuzzy inference systems for modeling energy consumption in greenhouse tomato production: a case study in Isfahan province. J. Agric. Sci. Technol. 17 (1), 49–62.

Kim, S.C., Kim, K.U., Kim, D.C., 2011. Prediction of fuel consumption of agricultural tractors. Appl. Eng. Agric. 27 (5), 705–709.

Kocher, M.F., Smith, B.J., Hoy, R.M., Woldstad, J.C., Pitla, S.K., 2017. Fuel consumption models for tractor test reports. Trans. ASABE 60 (3), 693–701.

Kolahloo, A.A.M., Loghavi, M., 1994. Evaluation and comparison of traction performance of two common tractors in Iran. Iran Agric. Res. 13 (2), 77–95.

Kolator, B., Bialobrzewski, I., 2011. A simulation model of 2WD tractor performance. Comput. Electron. Agric. 76 (2), 231–239.

Kumar, R., Pandey, K.P., 2009. A program in visual basic for predicting haulage and field performance of 2WD tractors. Comput. Electron. Agric. 67 (1–2), 18–26.

Kumar, N., Pandey, K.P., 2015. A visual basic program for predicting optimum gear and throttle position for best fuel economy for 32 kW tractor. Comput. Electron. Agric. 119 (1), 217–227.

Kumar, A.A., Tewari, V.K., Gupta, C., Kumar, N., 2017a. A visual basic program and instrumentation system for power and energy mapping of tractor implement. Eng. Agric. Env. Food 10 (2), 121–132.

Kumar, A.A., Tewari, V.K., Gupta, C., Pareek, C.M., 2017b. A device to measure wheel slip to improve the fuel efficiency of off road vehicles. J. Terrramech. 70 (1), 1–11.

Lee, J.W., Kim, J.S., Kim, K.U., 2016. Computer simulations to maximise fuel efficiency and work performance of agricultural tractors in rotovating and ploughing operations. Biosyst. Eng. 142 (1), 1–11.

Loghavi, M., Moradi, A., 1996. Draft and drawbar power equirement of moldboard plow in a clay loam soil. Iran Agric. Res. 15 (2), 203–214.

Machindra, A.R., Raheman, H., 2017. Investigations on power requirement of active-passive combination tillage implement. Eng. Agric. Env. Food 10 (1), 4–13.

Mamman, E., Oni, K.C., 2005. Draught performance of a range of model chisel furrowers. Agric. Eng. Int. CIGR EJ VII (Manuscript PM 05 003).

Manian, R., Kathirvel, K., 2001. Development and evaluation of an active-passive tillage machine. Agric. Mech. Asia Afr. Lat. Am. 32 (1), 9–18.

Marakoglu, T., Carman, K., 2010. Fuzzy knowledge-based model for prediction of soil loosening and draft efficiency in tillage. J. Terrramech. 47 (3), 173–178.

Mehta, C.R., Singh, K., Selvan, M.M., 2011. A decision support system for selection of tractor-implement system used on Indian farms. J. Terrramech. 48 (1), 65–73.

Moeenifar, A.M., Kalantari, D., Seyedi, S.R.M., 2013. Application of dimensional analysis in determination of traction force acting on a narrow blade. Int. J. Agric. Crop. Sci. 5 (9), 1034–1039.

Moeenifar, A., Mousavi-Seyedi, S.R., Kalantari, D., 2014. Influence of tillage depth, penetration angle and forward speed on the soil/thin-blade interaction force. Agric. Eng. Int. CIGR J. 16 (1), 69–74.

Mohammadi, A., Alimardani, R., Akbarnia, A., Akram, A., 2012. Modeling of draft force variation in a winged share tillage tool using fuzzy table look-up scheme. Agric. Eng. Int. CIGR J. 14 (4), 262–268.

Moinfar, A.M., Shahgholi, G., 2018. Dimensional analysis of the tractor tractive efficiency parameters. Acta Tech. Agri. 21 (3), 94–99.

Moitzi, G., Wagentristl, H., Refenner, K., Weingartmann, H., Piringer, G., Boxberger, J., Gronauer, A., 2014. Effects of working depth and wheel slip on fuel consumption of selected tillage implements. Agric. Eng. Int. CIGR J. 16 (1), 182–190.

Mouazen, A.M., Ramon, H., 2002. A numerical-statistical hybrid modelling scheme for evaluation of draught requirements of a subsoiler cutting a sandy loam soil, as affected by moisture content, bulk density and depth. Soil Tillage Res. 63 (3–4), 155–165.

Naderloo, L., Alimadani, R., Akram, A., Javadikia, P., Khanghah, H.Z., 2009. Tillage depth and forward speed effects on draft of three primary tillage implements in clay loam soil. J. Food Agric. Environ. 7 (3&4), 382–385.

Ndisya, J., Gitau, A., Mbuge, D., Hiuhu, A., 2016. The effect of the operational parameters on the draft requirement of ripping in a sandy clay soil. Open J. Optim. 5 (1), 1–13.

Nkakini, S.O., 2015a. Draught force requirements of a disc plough at various tractor forward speeds in loamy sand soil during ploughing. Int. J. Adv. Res. Sci. Eng. Technol. 6 (7), 52–68.

Nkakini, S.O., 2015b. Measuring the sensitivity of parameters estimates to evaluate the tractive force model. Agric. Eng. Int. CIGR J. 17 (3), 43–60.

Nkakini, S.O., Akor, A.J., 2012. Modeling tractive force requirements of wheel tractors for disc ploughing in sandy loam soil. Int. J. Eng. Technol. 2 (10), 1707–1716.

Novak, P., Chyba, J., Kumhala, F., Prochazk, P., 2014. Measurement of stubble cultivator draught force under different soil conditions. Agron. Res. 12 (1), 135–142.

Okoko, P., Ajav, E.A., Olosunde, W.A., 2018. Draft and power requirements for some tillage implements operating in clay loam soil. Agric. Eng. Int. CIGR J. 20 (1), 95–102.

Papendick, R., 2002. Managing Soil Cover and Farming With the Wind. Department of Crop and Soil Sciences, Washington State University, USA.

Parvanloo, M., Kazemi, N., Rahnama, M., Sheikhdavoodi, M.J., 2015. Assessment and equipment of parameters of MF399 tractor with synthetic fuel system of gasoline and liquid petroleum gas (LPG). Int. J. Farm Alli. Sci. 4 (5), 434–441.

Pitla, S.K., Lin, N., Shearer, S.A., Luck, J.D., 2014. Use of controller area network (CAN) data to determine field efficiencies of agricultural machinery. Appl. Eng. Agric. 30 (6), 829–839.

Plouffe, C., McLaughlin, N.B., Tessier, S., Lague, C., 1995. Energy requirements and depth stability of two different moldboard plow bottoms in a heavy clay soil. Can. Agric. Eng. 37 (4), 279–285.

Pranav, P.K., Pandey, K.P., 2008. Computer simulation of ballast management for agricultural tractors. J. Terrramech. 45 (6), 185–192.

Pranav, P.K., Pandey, K.P., Tewari, V.K., 2010. Digital wheel slipmeter for agricultural 2WD tractors. Comput. Electron. Agric. 73 (2), 188–193.

Pranav, P.K., Patel, T., Rathore, M., Sonowal, A.J., Tapang, T., Laji, S., 2012. Computer simulation for haulage performance of power tiller. Int. J. Comput. Appl. 58 (5), 19–25.

Raheman, H., Jha, S.K., 2007. Wheel slip measurement in 2WD tractor. J. Terrramech. 44 (1), 89–94.

Rahimi-Ajdadi, F., Abbaspour-Gilandeh, Y., 2011. Artificial neural network and stepwise multiple range regression methods for prediction of tractor fuel consumption. Measurement 44 (10), 2104–2111.

Rahmanian-Koushkaki, H., Karparvarfard, S.H., Mortezaei, A., 2015. The effect of the operational characteristics of the tractor composite electronic measurement system by the standards of emotion on the performance of chisel plows in a clay loam soil. Agric. Eng. Int. CIGR J. 17 (1), 44–49.

Ranjbar, I., Rashidi, M., Najjarzadeh, I., Niazkhani, A., Niyazadeh, M., 2013. Modeling of moldboard plow draft force based on tillage depth and operation speed. Middle-East J. Sci. Res. 17 (7), 891–897.

Ranjbarian, S., Askari, M., Jannatkhah, J., 2017. Performance of tractor and tillage implements in clay soil. J. Saudi Soc. Agric. Sci. 16 (2), 154–162.

RNAM, 1995. RNAM test codes and procedures for farm machinery/Economic and Social Commission for Asia and the Pacific, Regional Network for Agricultural Machinery. RNAM Technical Publications: 12. Thailand, Bangkok.

Roul, A.K., Raheman, H., Pansare, M.S., Machavaram, R., 2009. Predicting the draught requirement of tillage implements in sandy clay loam soil using an artificial neural network. Biosyst. Eng. 104 (4), 476–485.

SAA, 1977. Standards Association of Australia. AS 1289 B1.1. Determination of the Moisture Content of a Soil: Oven Drying Method.

Sahay, C.S., Thomas, E.V., Satapathy, K.K., 2009. Performance evaluation of a novel power-tiller-operated oscillatory tillage implement for dry land tillage. Biosyst. Eng. 102 (4), 385–391.

Sahu, R.K., Raheman, H., 2006. An approach for draft prediction of combination tillage implements in sandy clay loam soil. Soil Tillage Res. 90 (1–2), 145–155.

Sahu, R.K., Raheman, H., 2008. A decision support system on matching and field performance prediction of tractor-implement system. Comput. Electron. Agric. 60 (1), 76–86.

Saleh, B., Aly, A.A., 2013. Artificial neural network model for evaluation of the plowing process performance. Int. J. Control. Autom. Syst. 2 (2), 1–11.

Santos, F.L., Queiroz, D.M.D., 2016. Simtrac-an application for simulation of traction efficiency of agricultural tractors with front wheel assist. Acta Sci. Tech. 38 (4), 423–430.

Sarauskis, E., Vaitauskiene, K., Romaneckas, K., Jasinskas, A., Butkus, V., Kriauciuniene, Z., 2017. Fuel consumption and CO_2 emission analysis in different strip tillage scenarios. Energy 118 (1), 957–968.

Serrano, J.M., Peca, J.O., 2008. The forward speed effect on draught force required to pull trailed disc harrows. Span. J. Agric. Res. 6 (2), 182–188.

Serrano, J.M., Peca, J.O., Pinheiro, A., Carvalho, M., Nunes, M., Ribeiro, L., Santos, F., 2003. The effect of gang angle of offset disc harrows on soil tilth, work rate and fuel consumption. Biosyst. Eng. 84 (2), 171–176.

Serrano, J.M., Peca, J.O., Silva, J.M.D., Pinheiro, A., Carvalho, M., 2007. Tractor energy requirements in disc harrow systems. Biosyst. Eng. 98 (3), 286–296.

Shafaei, S.M., Kamgar, S., 2017. A comprehensive investigation on static and dynamic friction coefficients of wheat grain with the adoption of statistical analysis. J. Adv. Res. 8 (4), 351–361.

Shafaei, S.M., Heydari, A.R., Masoumi, A.A., Sadeghi, M., 2015. Determining and modeling of static friction coefficient of some agricultural seeds. Jordan J. Agric. Sci. 11 (4), 1007–1019.

Shafaei, S.M., Nourmohamadi-Moghadami, A., Kamgar, S., 2016a. Development of artificial intelligence based systems for prediction of hydration characteristics of wheat. Comput. Electron. Agric. 128 (1), 34–45.

Shafaei, S.M., Masoumi, A.A., Roshan, H., 2016b. Analysis of water absorption of bean and chickpea during soaking using Peleg model. J. Saudi Soc. Agric. Sci. 15 (2), 135–144.

Shafaei, S.M., Loghavi, M., Kamgar, S., 2017a. Appraisal of Takagi-Sugeno-Kang type of adaptive neuro-fuzzy inference system for draft force prediction of chisel plow implement. Comput. Electron. Agric. 142 (1), 406–415.

Shafaei, S.M., Nourmohamadi-Moghadami, A., Kamgar, S., 2017b. Experimental analysis and modeling of frictional behavior of lavender flowers (*Lavandula stoechas* L.). J. Appl. Res. Med. Aromat. Plants 4 (1), 5–11.

Shafaei, S.M., Loghavi, M., Kamgar, S., 2018a. On the neurocomputing based intelligent simulation of tractor fuel efficiency parameters. Info. Proc. Agri. 5 (2), 205–223.

Shafaei, S.M., Loghavi, M., Kamgar, S., 2018b. A comparative study between mathematical models and the ANN data mining technique in draft force prediction of disk plow implement in clay loam soil. Agric. Eng. Int. CIGR J. 20 (2), 71–79.

Shafaei, S.M., Loghavi, M., Kamgar, S., Raoufat, M.H., 2018c. Potential assessment of neuro-fuzzy strategy in prognostication of draft parameters of primary tillage implement. Ann. Agric. Sci. 16 (3), 257–266.

Shafaei, S.M., Loghavi, M., Kamgar, S., 2018d. An extensive validation of computer simulation frameworks for neural prognostication of tractor tractive efficiency. Comput. Electron. Agric. 155 (1), 283–297.

Shafaei, S.M., Loghavi, M., Kamgar, S., 2019a. Development and implementation of a human machine interface-assisted digital instrumentation system for high precision measurement of tractor performance parameters. Eng. Agric. Env. Food 12 (1), 11–23.

Shafaei, S.M., Nourmohamadi-Moghadami, A., Rahmanian-Koushkaki, H., Kamgar, S., 2019b. Neural computing efforts for integrated simulation of ultrasound-assisted hydration kinetics of wheat. Info. Proc. Agri. (in Press).

Shafaei, S.M., Loghavi, M., Kamgar, S., 2019c. Prognostication of energy indices of tractor-implement utilizing soft computing techniques. Info. Proc. Agri. 6 (1), 132–149.

Shafaei, S.M., Loghavi, M., Kamgar, S., 2019d. A practical effort to equip tractor-implement with fuzzy depth and draft control system. Eng. Agric. Env. Food 12 (2), 191–203.

Shafaei, S.M., Loghavi, M., Kamgar, S., 2019e. Feasibility of implementation of intelligent simulation configurations based on data mining methodologies for prediction of tractor wheel slip. Info. Proc. Agri. 6 (2), 183–199.

Shah, A.R., Mirjat, M.S., Mughal, A.Q., Rajper, I., Mirani, A.A., 2015. Performance evaluation of different tillage systems in a clay loam soil. Pak. J. Agric. Res. 28 (4), 369–376.

Sirhan, A.A., Battikhi, A., Snobar, B., 2002. Management of primary tillage operation to reduce tractor fuel consumption. Agric. Mech. Asia Afr. Lat. Am. 33 (4), 9–11.

Smith, L.A., 1993. Energy requirements for selected crop production implements. Soil Tillage Res. 25 (4), 281–299.

Smith, L.A., Williford, J.R., 1988. Power requirements of conventional, triplex, and parabolic subsoilers. Trans. ASAE 31 (6), 1685–1688.

Stajnko, D., Lakota, M., Vucajnk, F., Bernik, R., 2009. Effects of different tillage systems on fuel savings and reduction of CO_2 emissions in production of silage corn in eastern Slovenia. Pol. J. Environ. Stud. 18 (4), 711–716.

Sumer, S.K., Sabanci, A., 2005. Effects of different tire configurations on tractor performance. Turk. J. Agric. For. 29 (6), 461–468.

Summers, J.D., Khalilian, A., Batchelder, D.G., 1986. Draft relationships for primary tillage in Oklahoma soils. Trans. ASAE 29 (1), 37–39.

Tafesse, M., Intaravichai, S., Saitthiti, B., Kiatiwat, T., 2007. Regression modeling of fuel consumption optimization of rotary blades of power tiller under sandy clay loam condition. Kasetsart J. (Nat. Sci.) 41 (3), 586–600.

Taghavifar, H., Mardani, A., 2014a. Application of artificial neural networks for the prediction of traction performance parameters. J. Saudi Soc. Agric. Sci. 13 (1), 35–43.

Taghavifar, H., Mardani, A., 2014b. Wavelet neural network applied for prognostication of contact pressure between soil and driving wheel. Info. Proc. Agri. 1 (1), 51–56.

Taghavifar, H., Mardani, A., 2014c. On the modeling of energy efficiency indices of agricultural tractor driving wheels applying adaptive neuro-fuzzy inference system. J. Terrramech. 56 (1), 37–47.

Taghavifar, H., Mardani, A., 2015. Evaluating the effect of tire parameters on required drawbar pull energy model using adaptive neuro-fuzzy inference system. Energy 85 (1), 586–593.

Taghavifar, H., Mardani, A., 2017. Off-road Vehicle Dynamics. Springer, USA.

Taghavifar, H., Mardani, A., Karim-Maslak, H., Kalbkhani, H., 2013. Artificial neural network estimation of wheel rolling resistance in clay loam soil. Appl. Soft Comput. 13 (8), 3544–3551.

Taghavifar, H., Mardani, A., Hosseinloo, A.H., 2015. Appraisal of artificial neural network-genetic algorithm based model for prediction of the power provided by the agricultural tractors. Energy 93 (2), 1704–1710.

Taghavifar, H., Motlagh, A.M., Mardani, A., Hassanpour, A., Hosseinloo, A.H., Taghavifar, L., Wei, C., 2016. Appraisal of Takagi-Sugeno type neuro-fuzzy network system with a modified differential evolution method to predict nonlinear wheel dynamics caused by road irregularities. Transport 31 (2), 211–220.

Taiwo, A., Owusu-Sekyere, J.D., 2015. Slippage study of a two-wheel drive tractor during tillage operations on different soil surface conditions of the Atabadzi soil series of Ghana. Int. Res. J. Eng. Tech. 2 (6), 870–875.

Tayel, M.Y., Shaaban, S.M., Mansour, H.A., 2015. Effect of plowing conditions on the tractor wheel slippage and fuel consumption in sandy soil. Int. J. Chem. Res. 8 (12), 151–159.

Thansandote, A., Stuchly, S.S., Mladek, J., Townsend, J.S., Shlosser, H., 1977. A new slip monitor for traction equipment. Trans. ASAE 20 (5), 851–856.

Thomas, E.V., Singh, B., 2002. Performance of tractor implement combination. Agric. Mech. Asia Afr. Lat. Am. 33 (2), 25–28.

Udompetaikul, V., Upadhyaya, S.K., Vannucci, B., 2011. The effect of tire inflation pressure on fuel consumption of an agricultural tractor operating on paved roads. Trans. ASABE 54 (1), 25–30.

Upadhyay, G., Raheman, H., 2019a. Comparative analysis of tillage in sandy clay loam soil by free rolling and powered disc harrow. Eng. Agric. Env. Food 12 (1), 118–125.

Upadhyay, G., Raheman, H., 2019b. Specific draft estimation model for offset disc harrows. Soil Tillage Res. 191 (1), 75–84.

Upadhyaya, S.K., Williams, T.H., Kemble, L.J., Collins, N.E., 1984. Energy requirements for chiseling in coastal plain soils. Trans. ASAE 27 (6), 1643–1649.

Zhang, C., Araya, K., Kudoh, M., Liu, F., Jia, H., Zhang, H., Yang, S., 2001. A three-stage soil layer mixing plough for the improvement of meadow soil, part 3: field evaluation. J. Agric. Eng. Res. 79 (1), 47–53.